Hydrogen Fuel Cell Cold Operation

A THESIS

SUBMITTED TO THE FACULTY OF THE

UNIVERSITY OF MINNESOTA

BY

CHRISTINA BELL

IN PARTIAL FULFILLMENT OF THE REQUIREMENTS

FOR THE DEGREE OF

MASTER OF SCIENCE IN CHEMICAL ENGINEERING

Dr. STEVEN STERNBERG

SEPTEMBER 2019

Copyright 2019

Christina Bell

ALL RIGHTS RESERVED

Acknowledgement

The completion of this thesis would not have been possible without the help and guidance of my advisor, Dr. Steven Sternberg, who made sure to always push and humble me while supporting me in every way he could. Further, this thesis could not have come to fruition without the funding and support provided by the Chemical Engineering department at the University of Minnesota Duluth.

I would like to thank my committee members Dr. Sternberg and Dr. Venkatram Mereddy that laid the groundwork for this project and were my inspiration for this thesis. I would like to further thank my committee members Dr. Paul Siders and Dr. Zhihua Xu for their help and guidance both during this thesis and my undergraduate years.

I owe my deepest gratitude to my mother for her undying confidence in my abilities and never-ending support. Additionally, I am grateful to all my friends and family for their support and willingness to hear me vent, help me edit and redraft, and their loving kindness.

Abstract

The purpose of this project is to model the operation of a proton exchange membrane (PEM) fuel cell during operation in weather as cold as -40 °C. The fuel cell must be kept above the freezing point of water, and it is hypothesized this can be done by utilizing the heat produced in the system. The system is being designed to provide off-grid power for operation of various scientific sensors requiring power output of 20 W at a potential of 12 V. A fuel cell combines hydrogen and oxygen to form water, heat, and electricity. Process steps include generating hydrogen from the alcoholysis and/or hydrolysis of sodium borohydride, creating electricity from the fuel cell to charge a battery, and preheating feed air to provide oxygen to the fuel cell. The project explores 1) modeling of the reaction kinetics for hydrogen production, 2) modeling the efficiency and kinetics of the catalytic reaction between the generated hydrogen and oxygen from air within the fuel cell, and 3) modeling heat flow within the system to preheat the incoming air and maintain good fuel cell temperature. The reaction kinetics show sufficient hydrogen production to keep the fuel cell running as specified. The modeled efficiency gives an average efficiency just above 50% for the conversion of chemical potential energy to usable power. The heat flow, assumed to be 1-dimensional, shows sufficient heat transfer to keep the area around the fuel cell above the freezing point of water as modeled.

Table of Contents

List of Tables

List of Figures

Appendix C

List of Abbreviations

AFC	Apparatus fuel cell
EG	Ethylene glycol
EPA	Environmental Protection Agency
GE	General Electric
HFC	Horizon fuel cell
IVP	Initial value problem
PEM	Proton exchange membrane
PEMFC	Proton Exchange Membrane Fuel Cell
PG	Propylene glycol
SBH	Sodium Borohydride
SDS	Safety data sheets

Chapter 1
Background

Approximately 80% of the world's energy is supplied through the combustion of fossil fuels. These fuels are nonrenewable, thus finite, and create extensive pollution that has caused immense damage to the planet. By definition, having the majority of the world's energy fueled by a finite resource means we are in a global energy crisis. Thus, finding alternative energy sources that are renewable and do not harm our planet is imperative. When seeking these alternatives, it is necessary to utilize as many energy sources as possible to avoid any one issue with a source creating another energy crisis in the future. The last few decades have seen a strong drive in the scientific community to find these sources and put them into widespread use. One source that has been targeted, the one being addressed in this project, is the fuel cell. More specifically, a hydrogen, or proton exchange membrane fuel cell.

1.1 Proton Exchange Membrane Fuel Cell Design

A Proton Exchange Membrane Fuel Cell, (PEMFC, or PEM for short), is a device used to generate power. This power is produced by converting chemical energy into electrical energy. The overall process is shown in Figure 1-1. The hydrogen is first decomposed into protons and electrons and sent through a selective membrane that allows the protons to pass through but not the electrons. The electrons instead go around the membrane, through a circuit that connects the anode and the cathode. This path is where the load is connected and work done, as indicated by the resistance symbol in Figure 1-1. Once the electrons reach the other side of the membrane, they react with the protons that have crossed the membrane and the oxygen in the air that flows through the other side, to form water. The water leaves with the inert nitrogen and any unused reactants in the exhaust. The anode and the cathode have a noble metal, usually platinum, in them to act as a catalyst to both the water formation and hydrogen decomposition reactions. The continuous flow of product and the reactions create a hydrogen concentration gradient across the membrane. So long as hydrogen and oxygen are fed to the system, the fuel cell will continue to produce electricity. The balanced reactions at the anode and cathode are shown as equations 1.1 and 1.2, respectively, with equation 1.3 showing the overall balanced reaction:

$$2H_2 \rightarrow 4H^+ + 4e^- \quad (1.1)$$

$$O_2 + 4H^+ + 4e^- \rightarrow 2H_2O \quad (1.2)$$

$$2H_2 + O_2 \rightarrow 2H_2O \quad (1.3)$$

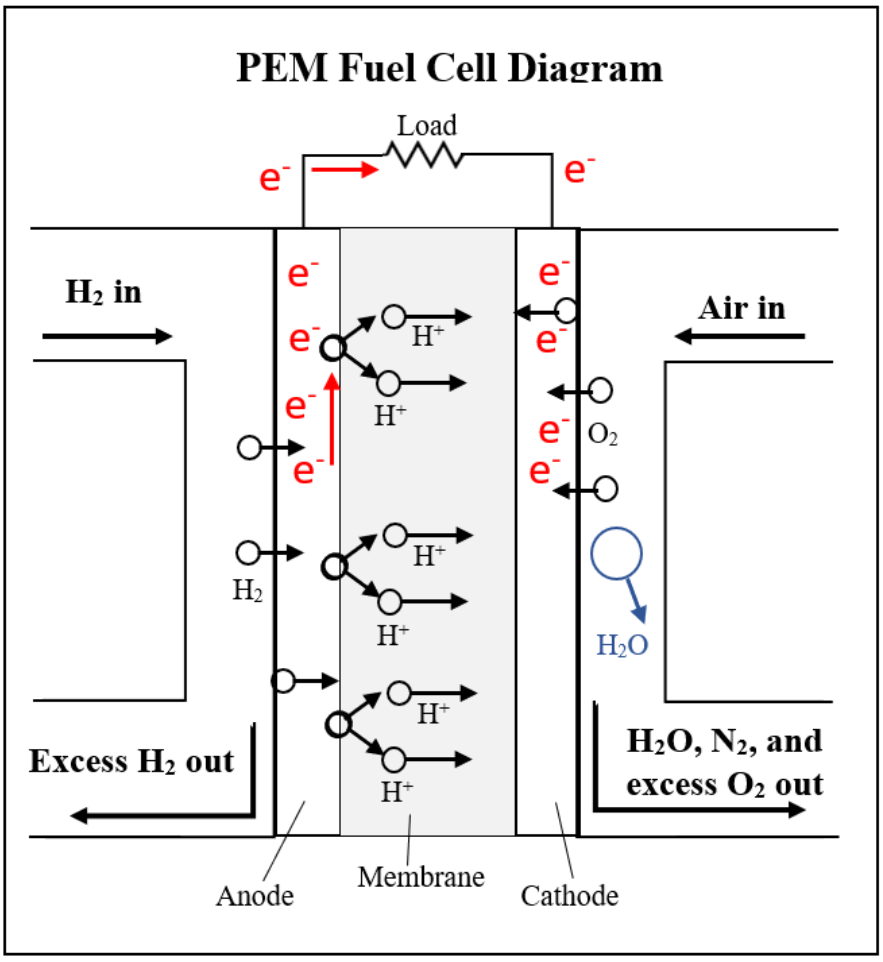

Figure 1-1 Diagram of a fuel cell with flow of reactants and products

The water formation reaction, shown in equation 1.3, has a heat of formation of 285.83 kJ/mol if the water produced is liquid, else 241.82 kJ/mol if the water produced is in vapor form [1]. The chemical energy of the reaction is converted directly into electricity (potential of a single cell at room temperature = 1.23 V) and heat. This is a direct advantage over our current energy system. Fossil fuels supply usable energy indirectly by having their chemical energy converted into heat. The heat can be used to generate electricity, although the efficiency is limited by thermodynamics to approximately 35% usable energy. The fuel cell generates electricity directly, so it does not have the same thermodynamic limits and has been shown to have electrical production efficiencies over 50% [2].

1.2 History of the PEMFC

The invention of the hydrogen fuel cell is rich in history. A version of the fuel cell was experimented with, though not put into widespread use, over a decade prior to the discovery of petroleum wells in 1853 [3]. The first fuel cell, or gas battery as it was called, was created in 1839 by William Grove, roughly 14 years earlier. All information regarding his findings was gathered from a paper he wrote and sent to the Royal Society [4]. Like most great inventions, the fuel cell working as it did was not intentional nor predicted. Grove had been meaning to show that oxygen and nitrogen on their own would not produce voltaic action, i.e. would not produce a current. Most experiments he performed confirmed this theory. However, one of the trials he ran did produce a current, likely due to phosphorus contamination since the nitrogen he was using was produced by burning phosphorus in the atmosphere. Grove sought to figure out what the cause of the current was. He hypothesized that phosphorus could be used as a "voltaic excitant," acting similar to the oxidizable metals found in voltaic cells used at the time.

To test his hypothesis, Grove designed an experiment to determine the voltaic action of phosphorus, sulphur, and hydrocarbons. He used a few different experimental setups. The main experimental setup was closed off from the atmosphere and the respective substances he was testing were kept separate from one another in inverted glass tubes submerged in the same water bath on the open side of the tube as shown in Figure 1-2, part a. The bath and a platinum wire were the only connection between the substances. His main experiment had solid phosphorus and gaseous nitrogen together with a platinum sponge in one glass capsule and oxygen with a platinum sponge in the other. This provided voltaic action, but the cause and reason were unknown to Grove. He then created a similar experiment with sulphur, but it did not give him reaction nor voltaic action until the sulphur was heated. This was interesting but did not aid in finding the cause or reason for the voltaic action of either substance.

Grove next sought to find additional substances that would produce voltaic action, so he experimented with camphor. He concluded that camphor decomposed into methane and carbon monoxide when exposed to a wire subjected to enough voltage to ignite. He further concluded that these gases were created with the phosphorus and sulphur experiments. Neither experiment had a source of carbon explicitly stated, so this seems unlikely. Despite this discrepancy, Grove seemed to have a firm grasp on the idea behind a hydrogen-oxygen electrochemical cell. In his concluding statements he describes a hypothetical self-charging battery that continuously produced hydrogen from a piece of zinc, presumably in a hydrochloric water bath. He explains how this battery would theoretically get oxygen continuously from the atmosphere and continue

to produce hydrogen so long as the zinc is replaced as soon as it stops moving, thus indicating it is no longer reacting. Figure 1-2, part b, shows the setup Grove designed for the battery. His description of the self-charging battery and the setup can be found in Appendix A. The full explanation is not necessary here, but the theoretical battery he designed makes it clear he was the first to design a version of the hydrogen-air fuel cell.

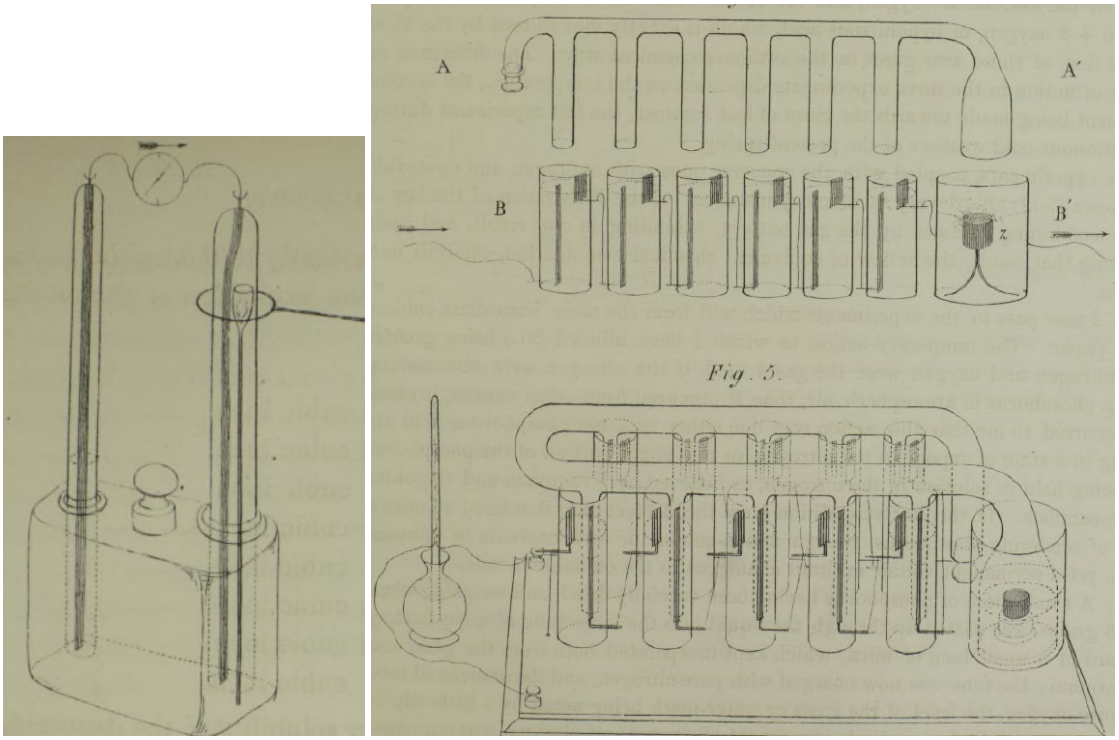

(a) Phosphorus setup (b) Hypothetical Zinc setup

Figure 1-2 Setup of voltaic action experiments created by William Grove [4]

William Grove's gas battery was the base model fuel cells were developed from. Several scientists took interest in the gas battery and developed it further during the following century. Most scientists of the time were thwarted by low power density, cost, electrolytes that were unsustainable, or a mixture thereof. It wasn't until the Gemini and Apollo missions that fuel cells were created and used successfully. The PEMFC was created by Thomas Grubb and Leonard Niedrach for the Gemini program. Both Grubb and Niedrach were chemists working for General Electric Company (GE). Grubb was the first of the two to work with the fuel cell. He created a membrane made of sulfonated polystyrene as an electrolyte in 1955. In 1958, Leonard Niedrach found a way to deposit platinum on the membrane, and thus the PEMFC was born. The hydrogen used to power this cell during the Gemini program was produced by mixing water and lithium hydride on site, as shown in equation 1.4. Their testing was successful and showed that the PEMFC could be used successfully under the requested conditions [5]. However, those in charge

of the Apollo missions chose to go with the alkaline fuel cell instead. Despite this set back, the PEMFC is used in many different applications today, including vehicles in temperate climates. Unlike the Gemini fuel cells, however, the fuel cells produced and used today use nafion as the membrane electrolyte. [6], [7]

$$LiH + H_2O \rightarrow LiOH + H_2 \quad (1.4)$$

1.3 Cold Operation of the PEMFC

One of the greatest benefits of the PEMFC is its ability to be run remotely. This benefit is greatly limited, however. Despite the many technological advances in material science, fuel cells are unable to be run in climates that have temperatures below the freezing point of water. This is due to the membrane needing to stay hydrated in order to maintain its conductivity. The fuel cell will cease to work and may be damaged irreparably if the membrane is allowed to freeze. Thus, any area of the world that experiences winter cannot utilize this technology in areas that are not climate controlled. This restriction has prevented the use of fuel cells for remote applications for a large portion of the globe. Strategies to combat this restriction have two available pathways. One is to alter the membrane such that the freezing point of the water produced is lower than that of the ambient temperature. The other is to alter the fuel cell's environment such that the ambient temperature is not allowed to fall below the freezing point of water. Altering the membrane is likely going to alter either its conductivity or permeability, potentially reducing the efficacy of the fuel cell. Altering the environment would be less likely to alter the function of the fuel cell and thus seems to be the better potential solution.

It is unlikely that there will be a solution that works for all scenarios the fuel cell may be used in. This project will focus on finding a cold weather solution for a specific application of a PEMFC. Specifically, it will focus on using the fuel cell remotely to power small devices such as research equipment out in the field for days to weeks at a time. Finding a potential solution for this project will also include designing a prototype setup for running research equipment. This was a natural addition to the project if altering the environment was the chosen solution. The environment needs to be modeled to determine the feasibility of the solution, so the necessary equipment such as sensors will be modeled as well. A prototype for the fuel cell in such a setup was already created but failed to address how the fuel cell would be kept from freezing. Rather, it seemed to be included as an assumption.

1.4 Prototype and Hydrogen Sources

The aforementioned prototype will be used as the beginning model and altered as deemed necessary. Figure 1-3 shows the original prototype [8]. The equipment is housed in a movable cabinet that protects it from the external environment. This is important for remote use where there may be plants, animals, and inclement weather. The equipment in the cabinet consists of the fuel cell, a battery, liquid storage, reactor, two valves, and a controller. To ensure the power provided is consistent, the fuel cell is used to charge a battery rather than having the device pull the power directly from the cell. The battery then powers the research equipment, assumed to be housed outside the cabinet. The battery can be used to power the controller as well if necessary. The controller is the brain of the operation. It controls the valves based on readings of voltage, current, temperature, and pressure. This control may either be preprogrammed into the controller or sent remotely depending on how the software is designed. One valve that is activated by the controller is used to determine flow of reactants into the reactor. This reactor's purpose is to produce the hydrogen used to run the fuel cell. If the current is low, the controller may open the valve to get more power to be produced in the fuel cell, for instance. The other valve controls the flow of the hydrogen into the fuel cell. Since hydrogen will dissipate if left to sit after it's produced, this is a safety control to protect the fuel cell rather than the means to determine how much/when hydrogen is pushed into the fuel cell. There is a connection of tubing between the fuel cell and the liquid storage for the water produced in the reaction within the fuel cell to be recycled to the liquid storage tank. There it will be a reactant as part of the hydrogen formation reaction. The hydrogen carrying reactant used to produce the hydrogen in this setup is sodium borohydride (SBH). The reasoning for this hydrogen source will be further explored and explained in the solution discussion. Appendix A has the original article for further information on the original project.

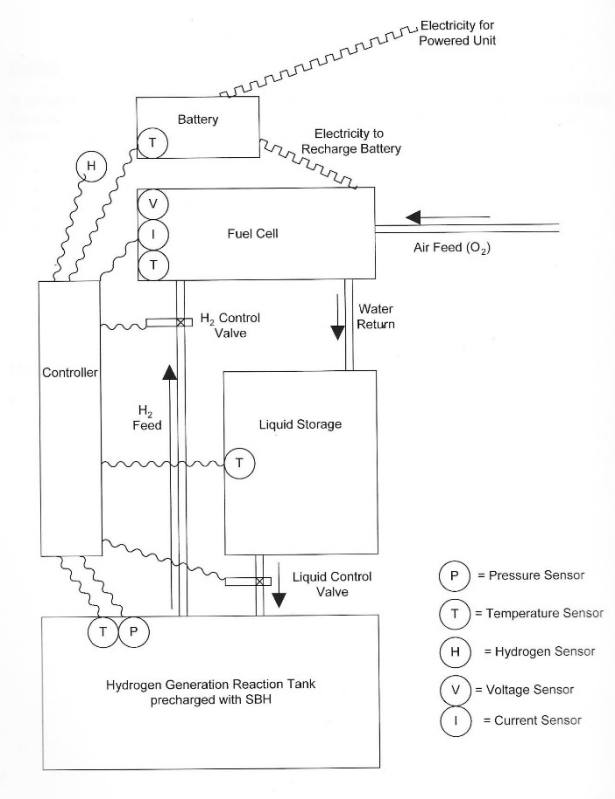

Figure 1-3 Fuel Cell Prototype [8]

One of the main variables to be considered when determining a solution to allow the fuel cell to be run in cold climates is the hydrogen source. Hydrogen can either be created or stored on site. To store hydrogen on site requires a heavy hydrogen tank that poses a safety risk were it to leak or be punctured. This is an especially large concern if the research equipment is near a roadway. Hydrogen being created on site also has a significant benefit. The reactions to produce the hydrogen are exothermic, meaning they give off heat. This is significant since the cold solution proposed is to increase the temperature of the environment around the fuel cell and the obvious solution to do so is to add heat to it. As such, creating hydrogen on site will be the source utilized. There are several reactions that can produce hydrogen. Metal hydrides are the optimum choice for reactants due to cost, high energy density, low weight, and safety of storing the materials on site [8]. See the article in Appendix A for further details on these considerations. The reason for choosing SBH as the hydride of choice is not explicitly stated in the original report. Due to this, the metal hydrides were further explored in this paper. Table 1-1 shows the comparisons of the most commonly used hydrides. The comparisons include cost per gram of substance and per gram of hydrogen since this is the desired product. It also lists the safety level as listed for the hydrides' safety data sheets (SDS). Environmental concerns were also considered. Aluminum (Al) was the only metal of those listed that is closely monitored by the

Environmental Protection Agency (EPA) for metal contamination [9]. Neither lithium nor sodium were listed. Considering only the hydrides that don't contain aluminum, SBH is 4 times cheaper than the next expensive metal hydride, costing 12 dollars per gram hydrogen compared to just under 54 dollars per gram hydrogen for lithium hydride. Given the price difference, the similarity in safety risks, and the lack of significant environmental concern, SBH will be the hydride used for hydrogen production.

Table 1-1 Metal Hydride Comparisons

Metal Hydride	Health Risk	Flammability Risk	Instability Risk	Physical Restraints	Cost ($/g)	Weight % H	Cost ($/g H)
$LiAlH_4$	2	4	2	W	3.40	10.5	32.38
$LiBH_4$	3	3	2	W	17.32	18.4	94.13
LiH	3	2	0	W	7.76	14.4	53.89
$NaAlH_4$	3	4	2	W	7.90	7.4	106.76
$NaBH_4$	3	3	2	W	1.27	10.6	12.00

Several reactants can be used with the metal hydrides to produce hydrogen. Alcohols and water are the most common. Water, methanol, ethanol, propylene glycol (PG), tert-Butanol, and ethylene glycol (EG) were the reactants considered in the original setup. Ethylene glycol and water in a fifty percent (50%) weight combination was selected as the reaction system. No explicit reason was given so these were investigated further. Tert-Butanol had negligible hydrogen reaction [8], so it will be omitted in further considerations. Table 1-2 shows the safety and cost comparisons of the remaining reactants. The cost was determined on a molar basis by using molecular weight and density of the substances in addition to the small volume price [1], [10]. The far-right column of the table shows the weighted cost per mole, taking into account how much of the substance is required per mol of hydrogen gas produced [8], [11], [12]. Water is the best reactant in both safety and cost, but the reaction rate leaves much to be desired. Where the alcohols achieved > 95% reaction within 30 minutes or less at room temperature, water achieved approximately 50% conversion within 24 hours [8]. Ethylene glycol is the best of the alcohols in terms of both safety and cost, as shown in the table. Both ethanol and methanol have significant flammability safety concerns and propylene glycol is significantly more expensive than ethylene glycol. Given that cost will be important for eventually utilizing these fuel cells in such an application, this was a deciding factor. While ethylene glycol would be a good choice on its own, water and ethylene glycol combined would be safer and more economically feasible.

Ethylene glycol mixed with water depresses the freezing point of water alone. This will be beneficial for startup when the reactants could reach temperatures lower than the freezing point of water. Further, adding water lessens the risk of a runaway reaction occurring. This analysis supports the use of the ethylene glycol and water mixture, so this is what will be used for the model.

Table 1-2 Alcoholysis Reactant Comparisons

Reactant	Health Risk	Flammability Risk	Instability Risk	Cost (/mol)	Ratio Produced	Cost (/mol H)
Methanol	1	3	0	$ 18.11	1	$ 18.11
Ethanol	2	3	0	$ 7.59	1	$ 7.59
EG	2	1	0	$ 7.97	0.5	$ 3.99
PG	2	1	1	$ 17.85	1	$ 17.85
H_2O	0	0	0	$ 0.24	1	$ 0.24

1.5 Model Prototype Setup

Several options, in addition to the hydrogen source, can be used to add heat to the environment around the fuel cell. The means of adding heat can significantly alter the overall energy efficiency. If the heat must be provided by a separate device that requires power, then the production of usable power is reduced. Due to this and keeping cost down, it's best to find a solution that utilizes an existing part of the system. The existing system has two main sources of heat production, the hydrogen production and the fuel cell. The amount of heat the fuel cell produces is the amount of energy produced in the water formation reaction minus the power that is pulled from the cell. This quantity of heat is dependent solely on the load required to run the equipment and the efficiency of the work provided. If more hydrogen is supplied than is required for power, it will escape as a purge. It will not cause the reaction in the fuel cell to proceed any further. Due to this, the heat from the fuel cell must be treated as a function of power, rather than a variable that can be altered. The hydrogen production reaction is the other main form of heat production. The heat it gives off is the heat of reaction. This will be a function of power needed but may also be used as a variable. This will be further discussed in the modeling section of this project.

The hydrogen production reaction has several variables to be considered. The reactants have already been determined but their concentrations and physical form have to be considered

before the model or the physical setup can be determined. The metal hydride, SBH, comes in solid form. The original setup has this stored in the bottom of the reactor with the other reactants, both liquids, deposited from above as needed. There are concerns with this setup were it to be run for days at a time. Depending on the pH of the solution in the reactor, some of the products may be solids. If these solids form a crust, preventing the reactants from meeting, the reactor would fail to perform as designed. Additionally, even if the products remain liquid, the reactants being able to interact may be prevented or slowed depending on viscosity and temperature of the solution and reactants.

Due to these complications, it would likely be less cumbersome if the SBH could be stored in liquid form and deposited at the same time as the other reactants. This would allow the reaction to take place either in solution with, or on top of, the previously made products. This also allows better modeling since it allows concentrations to be utilized, rather than modeling the surface area of reaction. This will be the method utilized for creating the model for this project. The means of getting SBH in liquid form will also have to be determined. It is exceptionally soluble in water but reacts with it. It is moderately soluble in diglyme and doesn't react with it. These options will be further discussed in the following chapters.

Figure 1-4 shows the fuel cell setup that will be used when modeling the heat transfer. All physical equipment, aside from sensors, is colored grey in the figure. The two boxes at the top represent the containers that hold the reactants. These are held above the reactor to allow gravity to drive the flow of reactants. The flow of reactants is represented by the dark lines and arrow, indicating flow of mass. The container on the left will contain sodium borohydride and the liquid that is used to dissolve it. The one on the right will be the 50 weight % mixture of water and ethylene glycol. The flow of reactants will be controlled by two solenoid pinch valves that remain closed until they receive a signal from the controller. Hydrogen flows from the reactor to the fuel cell, represented with another dark arrow. There will be a pressure release valve on this line to prevent excess hydrogen buildup or injury to sensors. There are pressure and temperature sensors in the reactor and a temperature sensor in the fuel cell. The voltage for the battery as well as the voltage and current for the fuel cell are also monitored. This information will be sent to the controller (the lines for this were omitted in the diagram for clarity). For safety and simplicity, a breadboard will be used to electrically connect the battery, fuel cell, and controller. These connections are represented in the figure as zigzag lines. There is also a line going from the battery that indicates the load that will be drawn from by the equipment being powered by this setup. The reactor is represented as a cylinder because it will be assumed to be a large polyvinyl

chloride (PVC) pipe with appropriate lining to prevent as much hydrogen as possible from escaping.

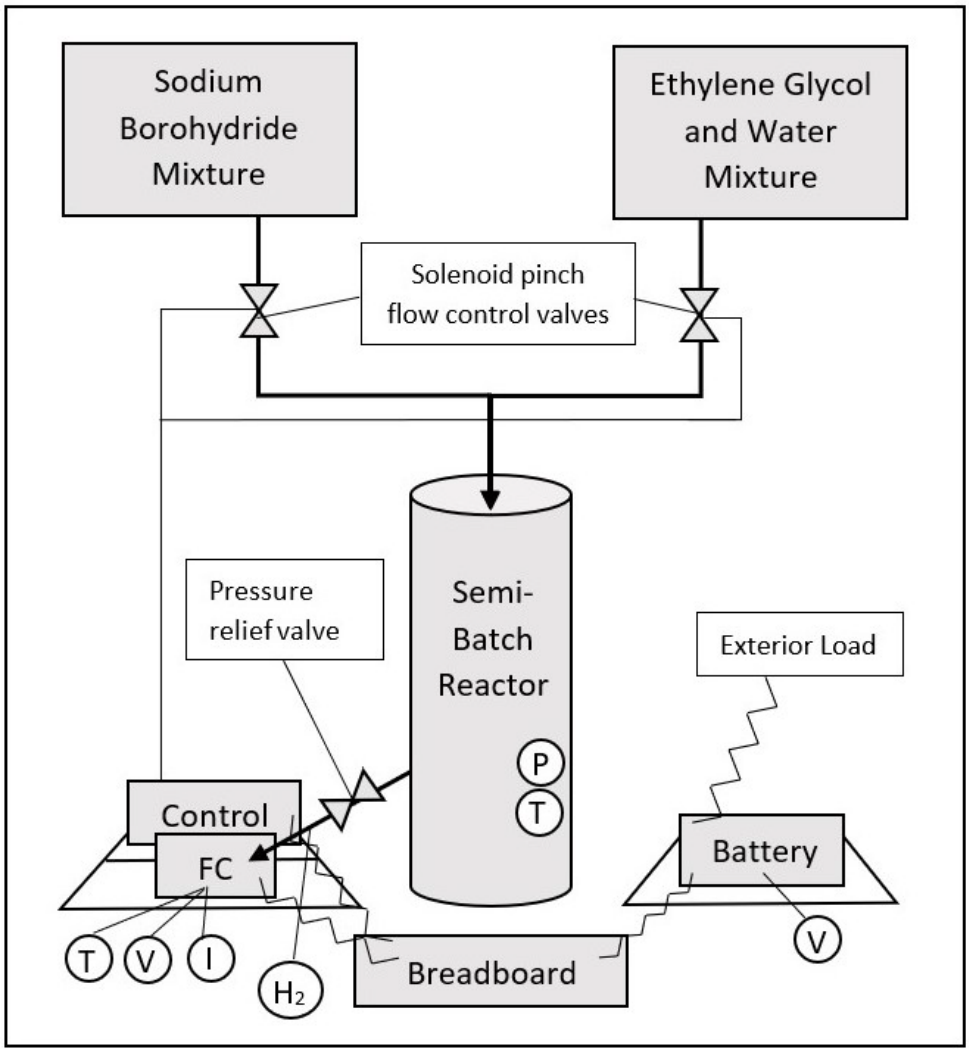

Figure 1-4 Model Fuel Cell Prototype

Chapter 2
Modeling the Fuel Cell

Modeling the heat given off by the fuel cell requires modeling the rate of reaction since that is the origin of heat production. The rate of reaction for the water formation in the fuel cell does not follow typical combustion kinetic models. Most reaction rates are directly related to the physical property of the reaction area. This can be concentration, such as in the case of a reaction occurring in a liquid solution, the surface area in the case of having one of the reactants in solid form, or the reaction may occur on a solid catalyst. The operation of the fuel cell differs in that it is instead driven by the load requirement. This will be verified in the modeling section of this report. This simplifies the heat model for the fuel cell significantly. As mentioned in the first chapter of this report, the heat given off by the fuel cell will be a function of power and efficiency. Power will be a known quantity when modeling. It is assumed that there will be an average power draw needed for the research equipment powered by the fuel cell. The efficiency will not be known so it will be modeled in order to estimate the heat given off by the fuel cell per amount of power required.

2.1 Fuel Cell Heat Production

The relation between power, efficiency, and heat given off is simple. The energy demand of the fuel cell is the power needed divided by the efficiency of the fuel cell, as shown in equation 2.1 where P is the power requirement, in joules per second (J/s), $\dot{E}$ is the actual energy production (J/s) required to produce that power, and η is the efficiency of the fuel cell (unitless). Any energy that is not used as electricity dissipates as heat following the conservation of energy. This is shown mathematically in equation 2.2, where h represents heat given off (J/s). Equation 2.3 combines the first two equations and is simplified to show the quantity of heat given off by the fuel cell. This heat can be measured directly by monitoring the change in temperature of the surrounding area or it can be determined indirectly. The heat is found indirectly using the enthalpy of reaction (J/mol) and the amount of reactants used (mol/s). For this reaction, the enthalpy of reaction simplifies to the heat of formation of water (J/mol). Equation 2.4 shows the heat of reaction equation using the reaction shown in equation 1.3 for the ratio of reactants to products, making the units substance specific (J/mol hydrogen or water). The f denotes formation, so each term is the enthalpy of formation of the substance in brackets. Since the heat of formation

of elements is by definition equal to zero, the enthalpy of reaction simplifies to being directly equal to the enthalpy of formation of water.

$$\dot{E} = \frac{P}{\eta} \tag{2.1}$$

$$h = \dot{E} - P \tag{2.2}$$

$$h = P * (\frac{1}{\eta} - 1) \tag{2.3}$$

$$\Delta H^{\circ}_{reaction} = \Delta H^{\circ}_{f}[H_2O] - \Delta H^{\circ}_{f}[H_2] - \frac{\Delta H^{\circ}_{f}[O_2]}{2} \tag{2.4}$$

While the efficiency of the fuel cell is easy to calculate, as shown above, modeling the heat given off requires being able to model the efficiency, rather than measure it as it occurs. The theoretical maximum efficiency is a good starting point for creating this model. Carnot efficiency is a well-known theoretical maximum efficiency model. It is the maximum efficiency for heat engines and is derived from thermodynamic laws that govern how the heat is transferred. The laws used to create the Carnot efficiency do not apply to fuel cells, however, since the power output is not driven by heat flow. There must be a similar efficiency, or physical limit to the efficiency that can be achieved for the fuel cell at certain operating parameters. Modeling this physical limit will be an important factor for validating the efficiency model. If the efficiency model produces an efficiency greater than the theoretical maximum, it will be clear that the model needs to be adjusted. As such, this limit will be important to have.

2.2 Fuel Cell Theoretical Maximum Efficiency

There are several sources that explore the maximum theoretical efficiency (unitless) of the fuel cell. The general form of this efficiency is the change in Gibbs free energy (J/mol) divided by the enthalpy (J/mol), shown in equation 2.5 [13]. Both Gibbs free energy and enthalpy are functions of temperature. Gibbs free energy is a measure of chemical energy potential. It is defined as the difference between enthalpy (H) and entropy (S, J/(mol*K)) multiplied by absolute temperature (T,(K)) shown in equation 2.6. The theoretical efficiency could be that of the reaction between pure oxygen and pure hydrogen or the reaction between pure (assumed) hydrogen and the oxygen content in air, as will be used in this design. Due to the difference in heat capacity (C_p, (J/mol*K)) and mass, the source of oxygen will alter the quantity of heat required to change

the temperature and thus will alter the theoretical efficiency. These relations are evident in equations 2.7 and 2.8, the equations of change with respect to temperature for entropy and enthalpy, respectively. T (K) is the temperature of the substances and T_{ref} (K) is the temperature where the entropy or enthalpy is considered to equal 0.

$$\eta = \frac{\Delta}{\Delta H} \tag{2.5}$$

$$= H - T * S \tag{2.6}$$

$$\Delta H = \int_{T_{ref}}^{T} C_p dT \tag{2.7}$$

$$\Delta S = \int_{T_{ref}}^{T} \frac{C_p}{T} dT \tag{2.8}$$

Equations 2.7 and 2.8 show the dependence of the enthalpy and entropy on the heat capacity of the products and reactants. Heat capacity is temperature dependent, so modeling the theoretical efficiency will require modeling the change in heat capacity of the substances with change in temperature. The source [1] originally used to model this change had an uncertainty of less than 1%. The models had an applicable range from 50 to 1500 kelvin. Operation of the fuel cell will be restricted to a much smaller range, so the model was simplified to cover the range of 273K < T < 330K. The applicable heat capacities are relatively linear with respect to temperature within that temperature range. Where there is significant variance, a piece wise linear function will be utilized. Table 2-1 lists the substances and the heat capacity models at the respective ranges. Oxygen is the only substance that was modeled using the same equation for the full temperature range. Appendix B has the applicable data and graphs for reference. The data used has an uncertainty of less than 1%.

Table 2-1 Heat Capacity Modeling Equations

Substance	Heat Capacity (J/(kmol*K) 273 K < T < 300 K	Heat Capacity (J/(kmol*K) 300 K < T < 315 K
Nitrogen	= 1.1412*T + 28773	= 0.7330*T + 28905
Hydrogen	= 9.8002*T + 25911	= 4.6650*T + 27448
Oxygen	= 4.5950*T + 27983	= 4.5950*T + 27983
Water$_{(v)}$	= 3.8505*T + 32430	= 6.2323*T + 31701

While the theoretical efficiency could be modeled on a per mole basis, it is better to find the theoretical efficiency of a fuel cell with flow rates or ratios included to ensure the effect of temperature is properly accounted for. The theoretical efficiency will be modeled in this project

by combining two separate sources [13], [14] and making some further adjustments. The combined model will have the same equation for efficiency as that shown in equation 2.5, but the difference in temperature is also accounted for, rather than just the change due to the reaction. For simplicity, the effect of temperature change will be modeled using the temperature of the products as the reference temperature. This means the enthalpy change of the products due to change in temperature becomes zero, and the only change due to temperature that needs to be modeled is that of the reactants.

To model the change in enthalpy and entropy due to temperature, terms will be combined by creating a molar basis to keep units consistent. All temperatures shown will be in units of Kelvin. Equation 2.9 is the enthalpy change of the reactants, ΔH_R, in J/mol reaction where T_R is the temperature of the reactants entering the fuel cell and T_P is the temperature of the products leaving. All heat capacities are in units of J/(mol [substance] *K). The integrals all have the same variable and limits of integration so they can be combined. Since addition requires identical units, combining these terms requires all heat capacities be converted to J/(mol H_2 *K). This unit conversion is achieved by using the input ratio of moles hydrogen to moles of respective substance. λ in equation 2.10 is defined as the ratio of moles of hydrogen to moles of oxygen. FE is the fractional excess of oxygen which will be a factor determined by the user. This equation was created by combining the mathematical definition of excess and the stoichiometric ratio of hydrogen to oxygen from the water formation reaction. Equation 2.11 is the enthalpy equation with all heat capacity terms converted. $\frac{y_{N_2,DA}}{y_{O_2,DA}}$ (mol N_2/mol O_2) is the ratio of nitrogen to oxygen in any dry air stream. This combined with λ (mol O_2/mol H_2) cancels all units of nitrogen and oxygen, leaving hydrogen units as desired. $\frac{y_{H_2O}}{y_{O_2}}$ (mol H_2O/mol O_2), similarly, is the ratio of water to oxygen. This can be found without knowing molar flow if the humidity is known. These concepts and material balances can be found in any elementary chemical engineering textbook so they will not be further explained here. Equation 2.12 shows the generic form of the heat capacity equations modeled in Table 2-1, where a_i (J/(mol*K)) is the slope and b_i (J/mol) is the intercept of substance i. With all heat capacities having consistent units, the a and b terms can be factored out and combined to a_R and b_R terms, shown in equation 2.13. Equation 2.14 is the culmination of the previous equations. It shows the enthalpy equation with everything combined and simplified, having units of J/mol H_2. Similarly, equation 2.16 shows the simplified equation for entropy in J/(mol H_2 *K). The entropy integral is just the enthalpy term divided by temperature, so the combination of terms and simplification is identical and thus omitted. Equations 2.15 and

2.17 are provided for completeness. They show the solutions for enthalpy and entropy, respectively, once integrated. Any further equation or discussion that references ΔH_R or ΔS_R will be referring to these simplified forms. Equation 2.18 is the entropy change of reaction (J/(mol H_2 *K)), identical to equation 2.4, but for entropy. This is necessary to define the Gibbs free energy ((J/mol H_2), shown in equation 2.19. This equation is derived from equation 2.6 defined for both the products and reactants, taking the difference thereof. It accounts for the change in energy due to both temperature and the reaction. Equation 2.20 is the enthalpy change (J/mol H_2) for an ideal reaction where oxygen is delivered pure and in stoichiometric proportions to hydrogen. This is the last piece necessary for creating the theoretical efficiency model, equation 2.21, defined as ε.

$$\Delta H_R = \int_{T_P}^{T_R} C_{p,O_2} dT + \int_{T_P}^{T_R} C_{p,H_2} dT + \int_{T_P}^{T_R} C_{p,N_2} dT + \int_{T_P}^{T_R} C_{p,H_2O}\, dT \tag{2.9}$$

$$\lambda = \frac{1 + FE}{2} \tag{2.10}$$

$$\Delta H_R = \int_{T_P}^{T_R} (C_{p,H_2} + \lambda * C_{p,O_2} + \frac{y_{N_2,DA}}{y_{O_2,DA}} * \lambda * C_{p,N_2} + \frac{y_{H_2O}}{y_{O_2}} * \lambda * C_{p,H_2O})\, dT \tag{2.11}$$

$$C_{p,i} = a_i * T + b_i \tag{2.12}$$

$$(a,b)_R = (a,b)_{H_2} + \lambda * (a,b)_{O_2} + \frac{y_{N_2,DA}}{y_{O_2,DA}} * \lambda * (a,b)_{N_2} + \frac{y_{H_2O}}{y_{O_2}} * \lambda * (a,b)_{H_2O} \tag{2.13}$$

$$\Delta H_R = \int_{T_P}^{T_R} (a_R * T + b_R)\, dT \tag{2.14}$$

$$\Delta H_R = \frac{1}{2} a_R * (T_R^2 - T_P^2) + b_R * (T_R - T_P) \tag{2.15}$$

$$\Delta S_R = \int_{T_P}^{T_R} \frac{(a_R * T + b_R)}{T}\, dT \tag{2.16}$$

$$\Delta S_R = a_R * (T_R - T_P) + b_R * \ln(\frac{T_R}{T_P}) \tag{2.17}$$

$$\Delta S_P = \Delta S_f^\circ[H_2O] - \Delta S_f^\circ[H_2] - \frac{\Delta S_f^\circ[O_2]}{2} \tag{2.18}$$

$$\Delta = \Delta H_R - \Delta H_P + T_P * \Delta S_P - T_R * \Delta S_R \tag{2.19}$$

$$\Delta H_{R,ideal} = (a_{H_2} + \frac{a_{O_2}}{2}) * (T_R^2 - T_P^2) + (b_{H_2} + \frac{b_{O_2}}{2})(T_R - T_P) - \Delta H_P \tag{2.20}$$

$$\varepsilon = \frac{\Delta}{\Delta H_{R,ideal}} \tag{2.21}$$

Figure 2-1 shows the effect of temperature change on the entropy, enthalpy, Gibbs free energy, and efficiency of the water formation reaction and substances. The numbers for these graphs were calculated using the model explained above. The percentages listed are the percent excess of oxygen supplied in an air stream with 2 weight % water in the air inlet. The temperature of all reactants for the excess calculations was 273K. The line labeled delta T = 0 is the only setup that has a changing reactant temperature. For this line, the reactant and product temperatures are instead set equal to show the effect of absolute temperature rather than just the temperature difference of the reactants and products. 273K was chosen as the reactant temperature for the other data because it is the lowest the reactants should be allowed to go in the application. If the temperature went lower than that, it would cause the membrane to freeze. This allows the full range of temperature change that may be experienced in this setup to be represented.

The source of the Carnot lack of efficiency is well known. Fuel cell loss of efficiency is not as well studied, however. The model shows the change in Gibbs free energy as the actual available energy. Given that the definition of Gibbs free energy includes the enthalpy of the reactants, shown in the denominator, the loss of efficiency must be due to the change in entropy and the enthalpy change of the excess reactants, by definition. One physical cause of efficiency loss in the entropy of the system/enthalpy of the excess reactants and inert gases is likely that the oxygen leaving must go against a diffusion gradient (the gas out of the fuel cell will have less oxygen than that going in since oxygen gets used to create water). Another loss is likely the expansion of the gases, evident in the increased loss of efficiency as temperature increases. These losses correlate with the irreversibility of the energy change, so they appear to be reasonable assumptions of loss.

Visual basic user defined functions were used to create the data for the graphs. These functions may be found in Appendix C.

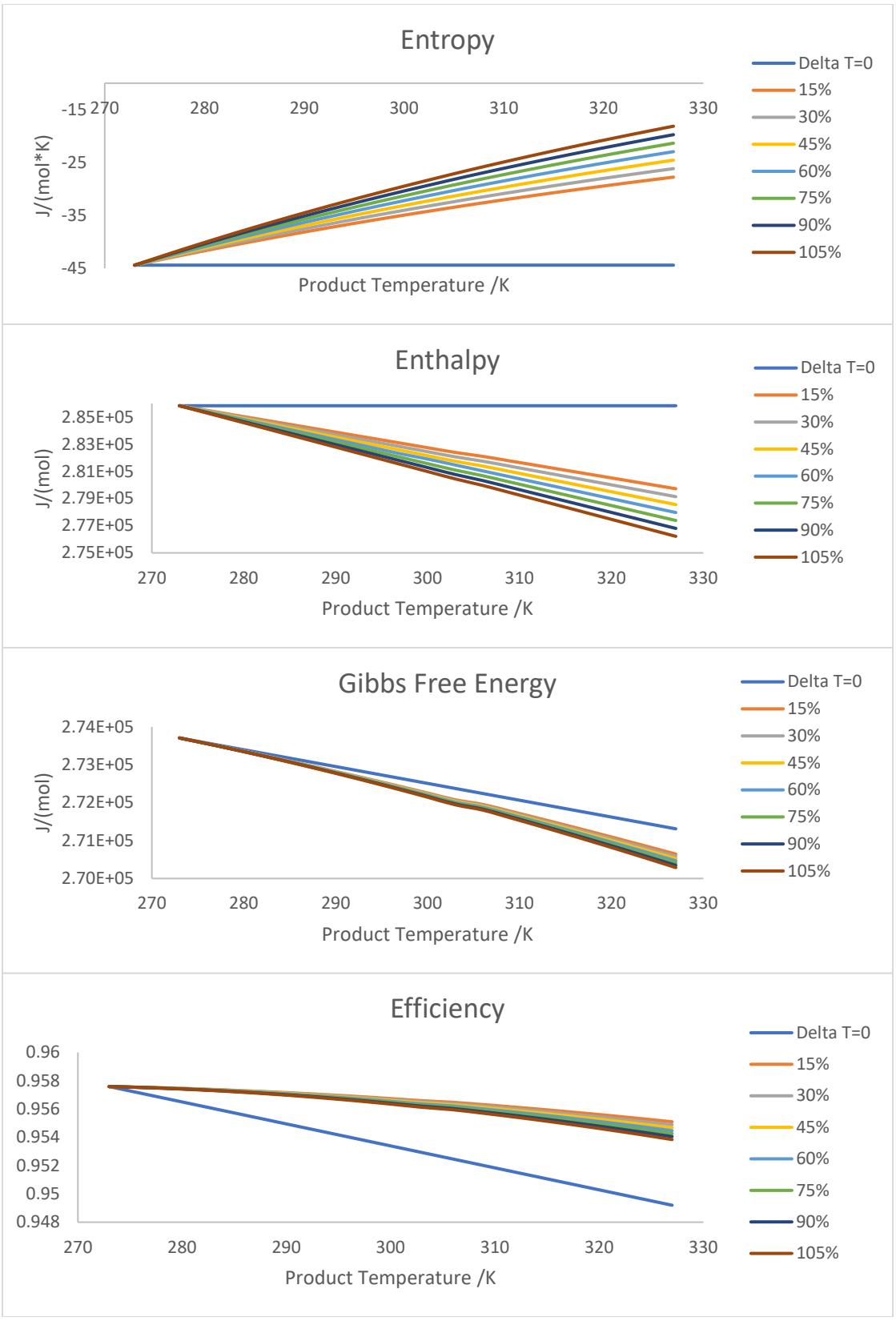

Figure 2-1 Energy and Efficiency Change by Temperature

2.3 Experimental Setup for Fuel Cell Efficiency Testing

Two fuel cells were used for efficiency testing and thus modeling. One was used as part of an apparatus that had flow, current, and voltage control built in. This will be referred to as the apparatus fuel cell (AFC) sold by TN. The other fuel cell used was the H-100 fuel cell stack, sold by Horizon [2]. The horizon fuel cell stack (HFC) has a cooling fan that is also the source of air input. This is helpful for keeping the cell from overheating but prevented the variance of reactant ratio when testing the efficiency of the fuel cell. Due to this, the AFC was used for most efficiency modeling experiments. Figure 2-2 shows the apparatus and fuel cell it controls. The tank in the picture stores the hydrogen used for the fuel cell and the air is supplied by a built-in line in the lab. The black and red valves are the hydrogen and air flow shut off valves, respectively. The setup is such that any hydrogen that is not used in the fuel cell does not get purged to the ambient air. Rather, the outlet for the hydrogen is connected to a pressure sensor. This allows the apparatus to determine if there is too much or too little hydrogen being supplied (based on if the pressure continues to climb) and alter the flow rate accordingly. The setup also has the reactants run through glass bottles that have water in them and a heating mechanism to allow temperature control and bring the reactants to 100% relative humidity before they go into the fuel cell.

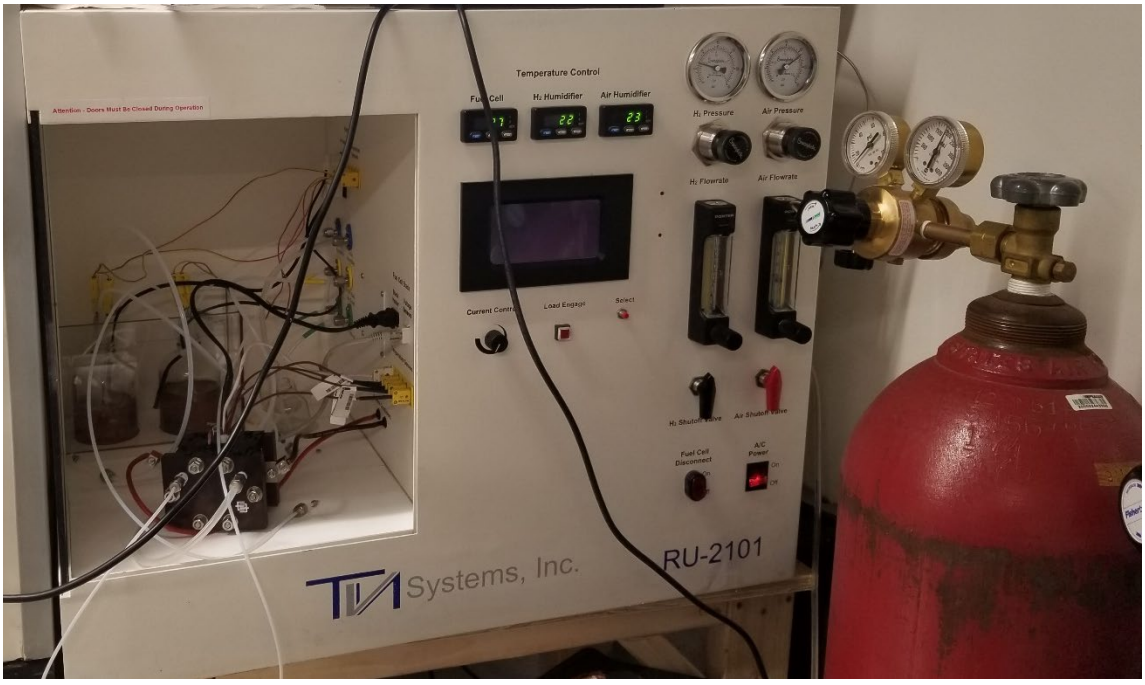

Figure 2-2 The Apparatus Fuel Cell

The AFC has software that allows the user to control the flow rates, current, and temperature of the reactant humidifiers. To increase the similarity in conditions of the AFC and the fuel cell that will be used in the field, the humidifiers were bypassed by attaching a separate piece of tubing that goes directly from the port out of the apparatus and into the fuel cell. The software stores all data in a file on the computer and displays it as it's being read in. The left side of Figure 2-3 shows this display. Being able to view this live data allows the user to see the adjusted flow rate and voltage for the individual cells, allowing for easier error management. For instance, if something prevented enough hydrogen getting to the fuel cell, the voltage in one or more of the cells would begin to drop. If the voltage in any of the cells drops below zero, the software is coded to decrease the load by 1 amp. It will continue to do so each time it reads a negative voltage until the load is completely removed if necessary. The right side of Figure 2-3 shows a closer picture of the flowmeters for reference. The flow meter on the left is the hydrogen flow meter, and the one on the right is the air flow meter.

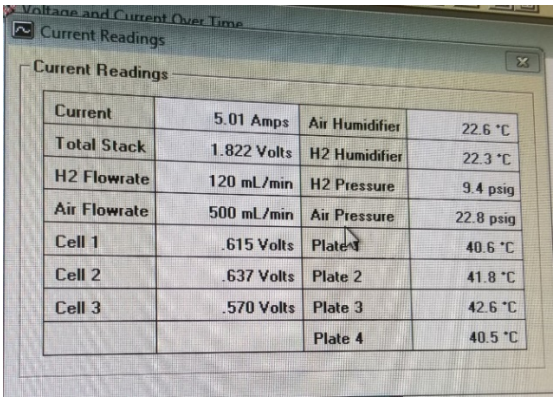

Figure 2-3 Real Time Reading User Display and Flow Meters

The meters were calibrated using the water displacement method [15]. The air flow meter was calibrated using a 4 L graduated cylinder inverted into a 5-gallon bucket, both filled with water. The outlet tube from the meter was threaded into the graduated cylinder. Since the hydrogen flow meter handles a smaller flow rate, it was calibrated using a 250 mL hydrogen burette, shown on the right of Figure 2-4. The tubing shown on the left side of the burette is the water outlet. The tubing shown on the right side is connected to the hydrogen source. This tubing had to be kept higher than the top of the burette to ensure the water flow didn't reverse when the hydrogen wasn't pressurized. The calibration curves and their corresponding equations are shown on the left of Figure 2-4. The graphs show a linear correlation between reading and flow rate, with the trend line going through all data points, so they appear to be a good fit. Reference Appendix B for the raw data used for these graphs.

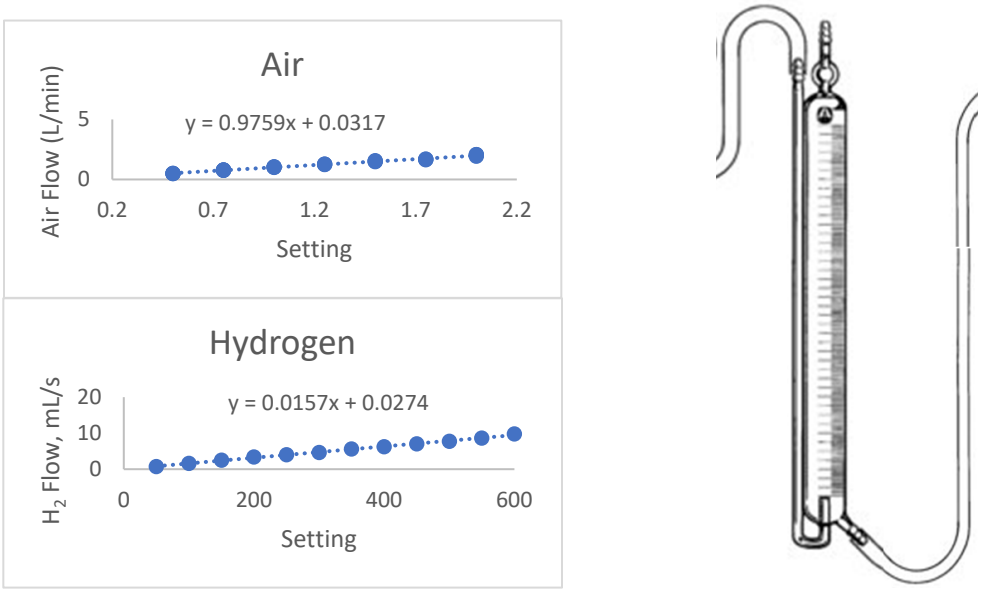

Figure 2-4 Flow Meter Calibration Curves and Hydrogen Burette

The calibration curves were used in combination with the ideal gas equation, equation 2.22, to determine the flow of reactants, where P is pressure (atm), V is volume (L), T is temperature (K), ṅ is the molar flow rate of air or hydrogen (mol/s), and R is the gas constant (0.08206 atm*L/(mol*K)). The necessary changes due to differences in ambient temperature and pressure between the day the curves were made and the day the experiments were run were also accounted for using ratios formed from rearranging equation 2.22. An example of this rearrangement is the classic $P_1*V_1=P_2*V_2$. Visual basic user defined functions were created to convert the flow meter readings to moles of applicable gas. The functions and applicable ratios are available for reference in Appendix C.

$$P * V = \dot{n} * R * T \qquad (2.22)$$

The Horizon fuel cell, seen at the top of Figure 2-5, is a more powerful fuel cell than the AFC. It has 20 cells and produces an average voltage of 12 V rather than the 3 cells and average 2 V observed with the AFC. The HFC does not have its own measurement hardware and software as the AFC does. Instead, it has a controller, shown on the bottom left of Figure 2-5. Table 2-2 has the description of the parts of the fuel cell and controller, as given by the manufacturer [2]. The controller and fuel cell have three points of connection. The first two are the positive and negative power output for the fuel cell, labeled B and C, respectively, in the fuel cell diagram, and G and H, respectively, in the controller diagram. The third point of connection, labeled E in the fuel cell diagram and D in the controller diagram, is where the information and control are

transferred. These connections and the full setup are shown visually in a connection diagram, shown at the bottom right of Figure 2-5. The transfer to the controller from the fuel cell consists of temperature readings, control of the purge and hydrogen flow valves, and control of the blower. This allows the controller, coded by the manufacturer, to prevent damage to the fuel cell and run a short circuit that allows better performance of the fuel cell. The controller prevents damage to the fuel cell by shutting the fuel cell load and hydrogen flow off if the operating conditions are such that they could injure the fuel cell. This can occur both during start up and run of the fuel cell. The conditions that will prevent the fuel cell being run include an internal or external temperature that is too high, not enough hydrogen fed to the fuel cell, and low fuel cell voltage. The specific voltage and current limits as well as power and efficiency specifications can be found in Appendix A.

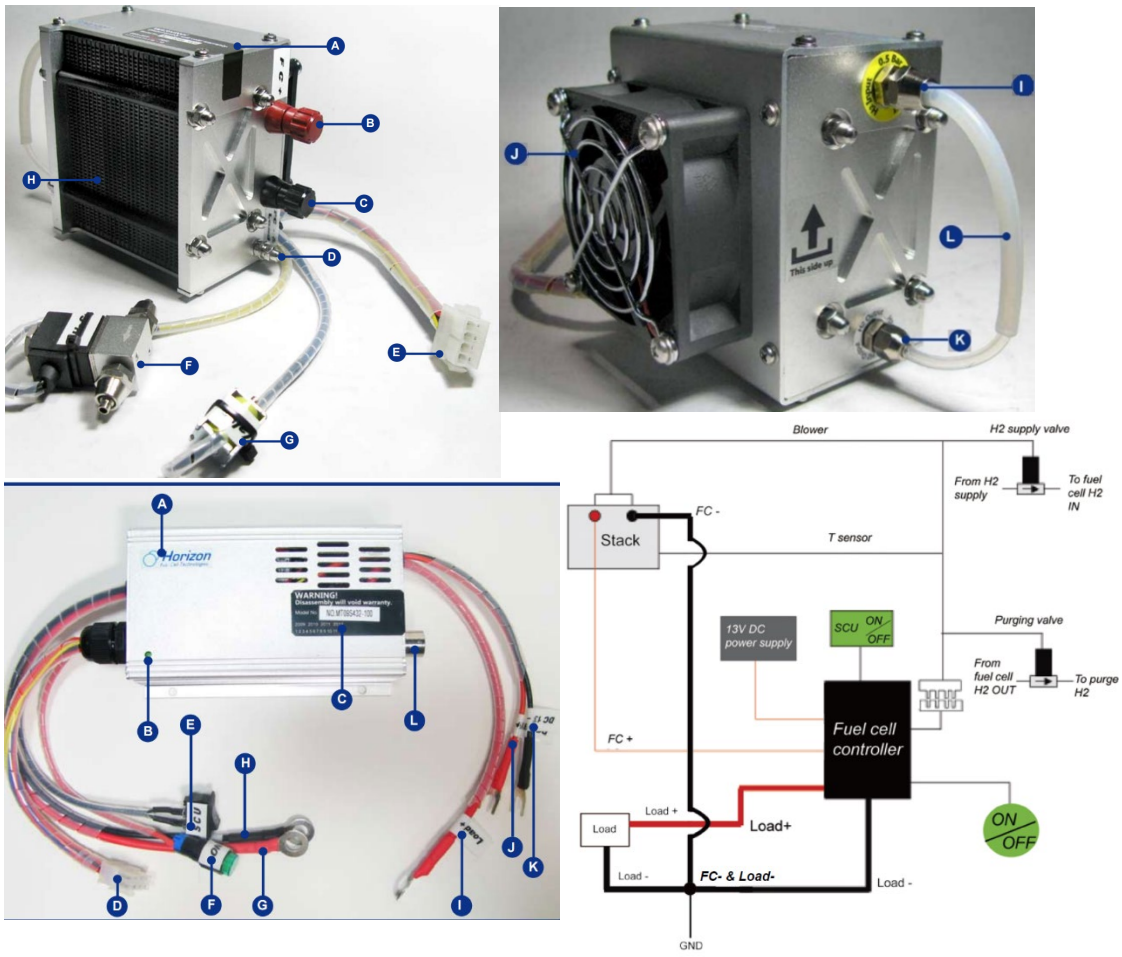

Figure 2- 5 Horizon Fuel Cell, Controller and Connection Diagram [2]

Table 2- 2 Horizon Fuel Cell and Controller Descriptions

	Fuel Cell	**Controller**
A	Warning labels	Horizon Logo
B	FC (+) Connector	LED
C	FC(-) & load(-) connector	Product No. Label
D	Grounding cable connector	Connect Plug
E	Controller multi-connector	SCU (short circuit units) switch
F	H2 supply valve	ON/OFF button
G	H2 purge valve	Connect to FC (+)
H	Fuel cell air inlet side	Connect to FC (-)
I	H2 inlet connector	Connect to Load (+)
J	Blower	Controller power supply DC 13V(+)
K	H2 outlet connector	Controller power supply DC 13V(-)
L	Silicon tube	LCD connector

The hardware used to measure data for the HFC consisted of two parts, the sensors and the data acquisition devices. The sensors used were a pressure sensor and a type J thermocouple [16], [17]. The data acquisition devices were the compact data acquisition, (CDAQ), and my data acquisition, (MYDAQ) systems, made by National Instruments [18]. The MYDAQ was used for the pressure sensor and current data acquisition. The CDAQ chassis had multiple modules in it. The ones used for the fuel cell were the NI9221, for thermocouple data acquisition, and NI9211, for fuel cell voltage acquisition. The MYDAQ current acquisition hardware required a current of 1 A or less, else it would be damaged. This limit, combined with the 100W rating of the fuel cell, required a resistance of at least 10 Ω, calculated using equation 2.23, the definition of power rearranged and substituted to solve for resistance.

$$R = \sqrt{\frac{P}{I}} \tag{2.23}$$

The last piece of hardware required to run and measure output from the HFC was the 12V battery, shown in the prototype in chapter 1. The battery is necessary to power the pressure transducer and the fuel cell controller. The one used was rated for 12 V at 7 amp hours [19]. A circuit was created to measure the efficiency of the HFC. The circuit consisted of resistors, the MYDAQ current acquisition, and the fuel cell controller placed in series, with the CDAQ acquisition card setup in parallel to the controller. (The controller is where the load is attached, not the fuel cell. See Figure 2-5 for reference.) Two sizes of resistors were used, 2.75 and 5 Ω. One setup had two 5 Ω resistors and the 2.75 Ω resistor set up in series in the circuit, giving a combined resistance of 12.75 Ω. Figure 2-6 shows the wiring diagram for this setup. Pictures of the hardware and experimental setup may be referenced in Appendix A.

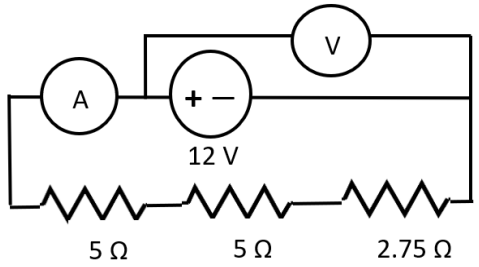

Figure 2-6 HFC Circuit Wiring Diagram

The hardware used for data acquisition had its own software. This software is a program called Labview [20], also designed by National Instruments. It is a programming software that uses a graphical interface to design the code. The version of the software used for this project is the 2013 release. Figure 2-7 shows the graphical code, or block diagram as it is called in the program, used for the efficiency experiments. The grey line represents a while loop. It is set up to collect data and time passed every second, display it to the user, and amend it to the end of a file until the user clicks the stop command. The wire shown going to the outside of the loop is a command that only occurs once the while loop is complete. This command adds the date to the end of the file at the end of each run. The numbers seen connected to the pressure readings are used to convert the mV input from the pressure transducer to units of psi. These numbers were found via calibration using two different, already calibrated, pressure sensors. The data and graph for this calibration can be found in Appendix B.

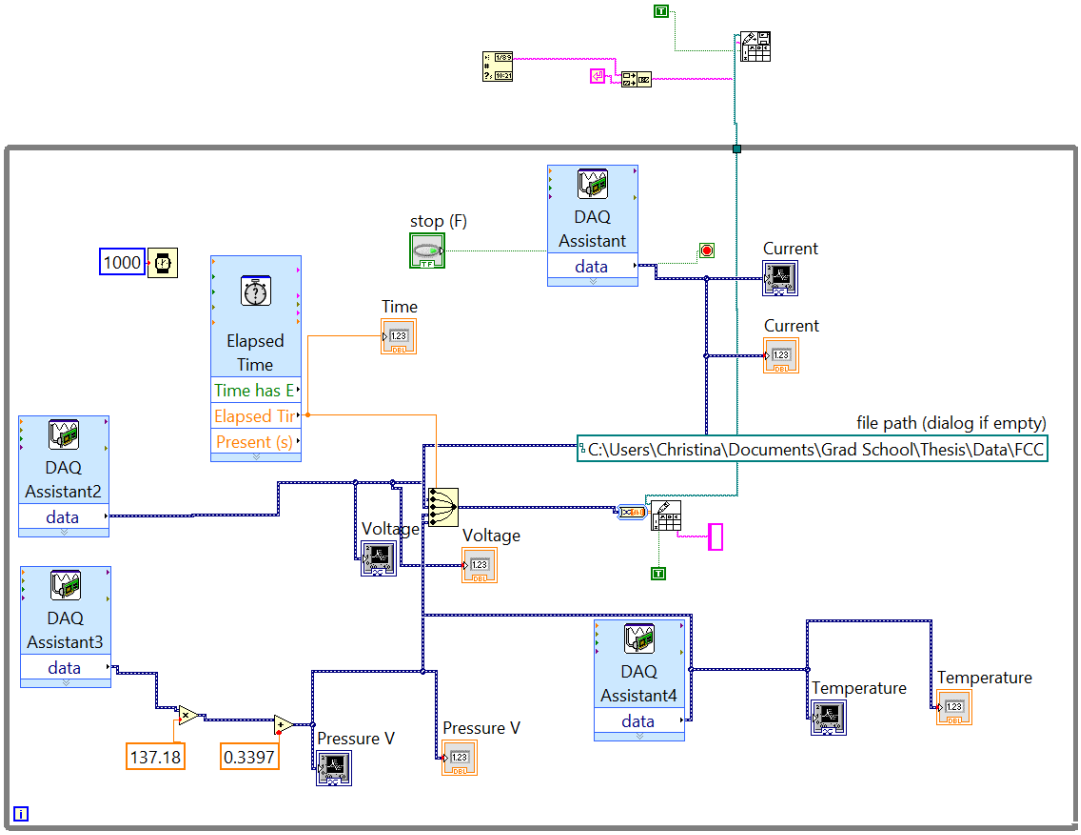

Figure 2-7 Labview Block Diagram for Efficiency Experiments

The purge stream mentioned prior introduced error into the expected heat produced since it means some hydrogen is not converted into water and heat. Due to this, the hydrogen lost in the purge stream was measured. To do so, the purge outlet was connected to the hydrogen burette used when calibrating the flow meters. This was measured, but it was noted that the pressure would get low enough between purges that the level wasn't consistent, meaning hydrogen was leaking or diffusing faster than it was being produced. No leaks were able to be found. It was still measurable, but the accuracy seemed questionable. Further, if the flow of hydrogen was varied too significantly, it would trigger the controller to shut the fuel cell off. The inaccuracy in measuring the hydrogen lost, in addition to the restriction on the range of hydrogen flow and load, meant the HFC was not a good source for efficiency testing. A couple runs were performed for completeness, but these were not used to create the fuel cell efficiency model.

2.4 Fuel Cell Efficiency Results

While the graphs shown in Figure 2-1 indicate that temperature affects the maximum theoretical efficiency, temperature does not appear to be the main component that will affect the

experimental efficiency. Preliminary tests showed little correlation between the efficiency and temperature. Instead, they appeared to indicate that current would be the largest determining factor of both efficiency and voltage. This was the main variable tested in the experiments.

All efficiency discussed in experimental data was determined via use of equation 2.1, rearranged and solved for the efficiency rather than the total energy. The moles of hydrogen, the limiting reagent, consumed per second ($\dot{n}_{H_2}$), were used to determine the moles of water produced via stoichiometric ratios. The expected energy flow, $\dot{E}$, in J/s, was determined using these moles of water multiplied by the heat of formation of water, assuming complete conversion of the limiting reagent. This correlation is shown in equation 2.24.

$$\dot{E} = \dot{n}_{H_2} * \frac{1 \text{ mol } H_2O}{1 \text{ mol } H_2} * \Delta H_f^{\circ}[H_2O] \tag{2.24}$$

To ensure there were no unknown factors affecting the efficiency, the AFC was run for just short of an hour with loads of 1 and 2 amps. The fuel cell was malfunctioning when the smaller load was run, as is evident in Figure 2-8. It was apparent from the voltage differences that the hydrogen was not getting distributed to the 3rd cell properly. The part of the graph where the efficiency rebounds to the initial starting conditions shows where the hydrogen flow was disconnected and reattached to flush hydrogen back through the cells. This was included as part of the graph because, despite erroring, it provides evidence of consistency in efficiency despite the start and stop. It also shows that even without being continuously run, there is no apparent change due to time. Both of these factors are applicable and important to the model since the hydrogen will be supplied as needed, not continuously. The 2-amp load displays no significant change due to time. The initial decreasing slope correlates to the expected loss in efficiency due to the temperature increase. This data, and all other used in figures and models in this chapter, are provided in Appendix B.

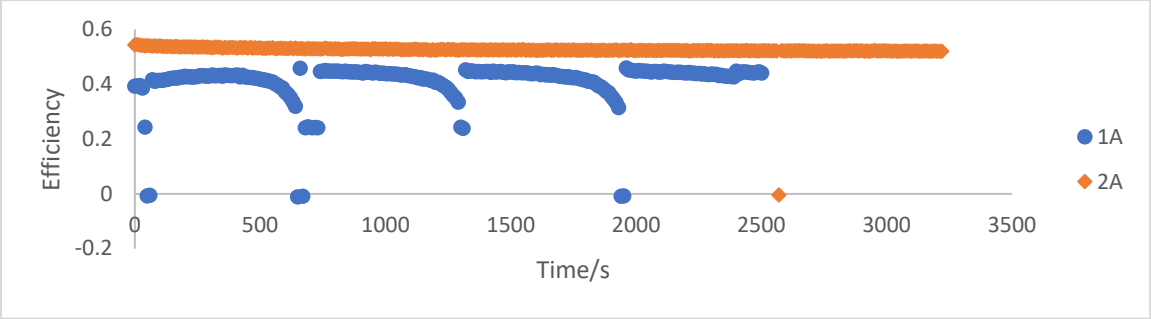

Figure 2-8 Graph of Efficiency vs. Time for 1- and 2-Amp Loads

Several experiments were run to test the fuel cell efficiency. Some had the current held constant and left to run for a period of time while others had the current varied during the same run. Those that had the current varied were labeled by date while those with the current held constant were labeled with the current quantity. This will be further explained in the results. The temperature continuously rose during all the trials due to the heat given off. Due to the error described previously, any experiments with currents higher than 5 amps (A) were not able to be run in identical starting conditions as the lower currents, as the fuel cell required time running in steady state before these higher currents could be achieved. Due to this, the higher currents were not able to be modeled at the lower temperatures and it was not possible to observe non-steady state operation at the higher current rates. This will be further discussed when describing the results.

In an attempt to keep the temperature lower as it will be when run outside, the fuel cell was put into an ice-water bath with very little water, for two runs. The weight of the ice placed in the container at the beginning of the experiments was measured, as was the ice remaining at the end. The difference was taken to determine heat produced from the fuel cell. A control run was also performed where the fuel cell was placed in the bath, covered, and left for several hours to determine heat gained from the environment rather than that produced by the fuel cell. It was not fully submerged in any of these trials to avoid risk of harming it. The fuel cell and the ice bath were placed in a thermally insulated container with Styrofoam packing placed on top to try to mitigate heat escape. The bath did not keep the inside of the cell cold. The thermocouples are in the fuel cell, so they give accurate internal readings and there was no significant decrease in temperature as compared to other runs. The ice melted in the control run correlated to a loss of 13.9 kJ/hr to the environment. This, combined with the expected heat production from the efficiency and energy correlation, gave an expected 77 grams of ice melted for the first run and 64.5 for the second. The ice that melted was 210 and 204.5 grams, respectively. While this difference is significant, there were significant differences between the control run and the experiment that would have increased heat transferred from the environment to the ice. One difference was that the fuel cell was not covered the full length of the experiments. This was due to having to make regular adjustments to the fuel cell and external thermocouple placement as the ice melted. The second difference was the user, and therefore body heat, presence. The control run did not require a user, but the apparatus required consistent monitoring. The final difference is the heat produced by the apparatus and computer being run that was not present in the control run. Due to the inconsistencies being within reason and the ice not affecting the operating

temperature of the fuel cell, no further runs with ice were performed. The ice run results were included as part of the main data and included in efficiency calculations performed.

Once calculated, efficiency was graphed compared to temperature for all experiments run, as shown in Figure 2-9. One of the cells in the AFC would error if the load was increased too quickly. The voltage of the cell would either decrease to negative over the course of approximately 30 seconds, or it would immediately decrease to a negative voltage directly after load increase. This erroring was omitted from the remaining graphs since the source of it was known and the same erroring has not been experienced in the other fuel cell. Further, this level of failure would require user intervention and thus would not represent how the fuel cell would operate when in the field. For integrity and completeness, this data is available for reference in Appendix B. "i1" and "i2" shown in the graph are the two sets of data taken while the fuel cell was placed in an ice bath. "st1" and st2" were the first trials run. They are the staircase setup that can be auto run by the program, where it increases the current from 0 to 2.5 A in steps of 0.5 A every 2 minutes. The graph appears as if the efficiency is strongly temperature dependent between 295 and 300K, but this is the temperature range where steady state is achieved. This is evident since 295K is the ambient temperature and the efficiency and heat transfer is such that the time required to reach steady state correlates to a 5 degree increase. This assumption was initially realized when it was observed that the data sets that follow this trend perfectly correlate to those that experienced significant erroring before steady state could be achieved. The rest of the graph makes it evident that there is no correlation between temperature and efficiency. The straight lines correlate to the data that was kept at constant current with time, which explains the lack of variance in efficiency for that data and supports the notion that the efficiency is solely dependent on current.

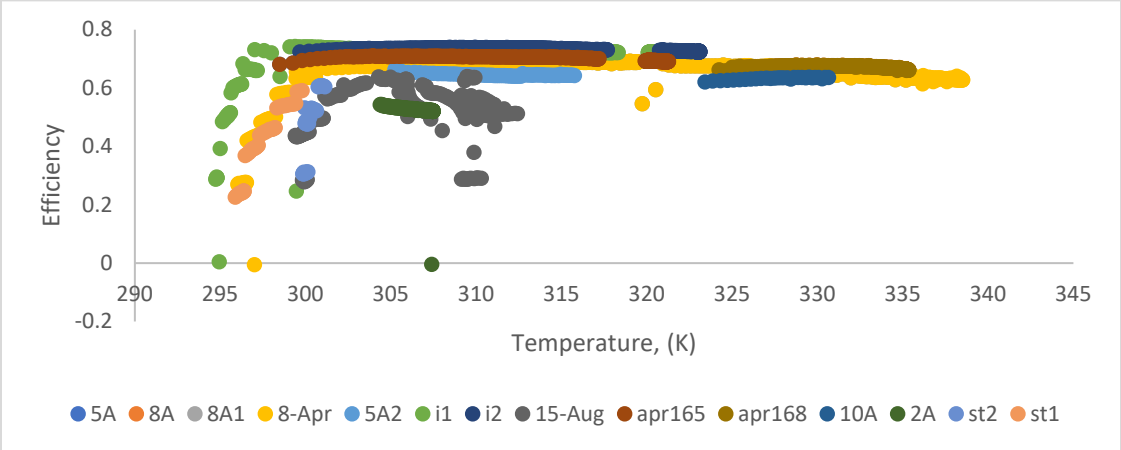

Figure 2-9 Graph of Efficiency and Temperature Correlation at Steady State

As stated previously, the current appears to be the variable that the efficiency is dependent on. Figure 2-10 displays this correlation in a graph of efficiency vs current. There appears to be a distinct pattern where efficiency increases with current until roughly 5 amps, where it slowly begins to decrease.

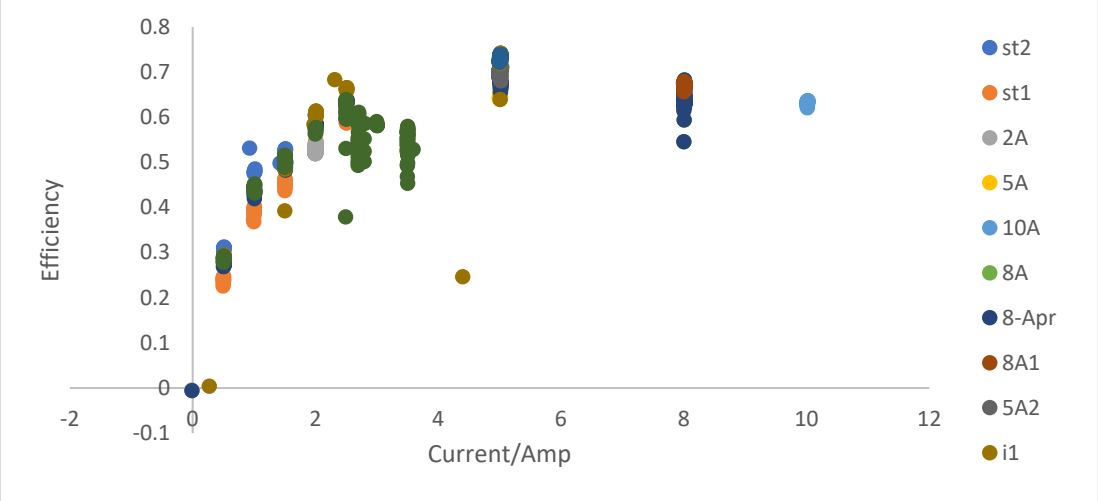

Figure 2-10 Graph of Efficiency and Current Correlation at Steady State

The variance in the current seems within reason given the lack of precision in the flow rate meters of the apparatus, shown in Figure 2-3. The picture shows the markings at 0, 50, and 100 mL, with a decreasing length between them. This uncertainty will be quantitatively evaluated in the modeling section of this chapter.

2.5 Fuel Cell Efficiency Model

To create the model, the current was set as the independent variable and the efficiency the dependent variable. To mitigate the weight of samples that were run for longer times when testing, the data was broken up into pieces. Any data set with 5 or more points that differed from the previous set by 0.01 A or more was considered a unique set. The average current and efficiency were then calculated for each unique set and used as a point. This also allowed the measurement with the greatest uncertainty, the flow rate, to be the weighted factor since this was only changed/recorded when the current was altered, thus, another set was created. Once the averages were determined, the model was able to be created. Equation 2.25 was the equation used to create the model, where y is efficiency, x is current (A), and a and b (A) are the variables that can be changed to fit the data. Newton's method (via Excel's Solver), was used to minimize the sum of squares, shown in equation 2.26, to find the values for a and b that allow the best fit for

the model. Table 2-3 shows some of the data used for the model. To conserve space, the data shown was limited to the current that directly correlates to the settings used. The sum of squares and variable values shown were found using all the averaged data. The raw data and the averages used can be found in Appendix B.

$$y = \frac{x}{a * x + b} \tag{2.25}$$

$$SS = (y_{real} - y_{model})^2 \tag{2.26}$$

Table 2-3 Efficiency Model Data

Current (A)	Avg Eff	Mod Eff	Difference Squared
0	0	0	0
0.501	0.264	0.300	0.001
0.999	0.424	0.424	0.000
1.50	0.492	0.492	0.000
2.00	0.529	0.536	0.000
2.49	0.623	0.565	0.003
3.00	0.584	0.587	0.000
3.50	0.548	0.604	0.003
5.00	0.710	0.636	0.006
8.00	0.663	0.667	0.000
10.0	0.630	0.678	0.002

a	1.376
b	0.982
SS	0.0403

The model and its standard error limits were graphed with the averaged data, shown at the top of Figure 2-11. For clarity, the model's error is omitted for the graph with the raw data, shown on the bottom of Figure 2-11. The error bars shown in the average data in the graph at the top of Figure 2-11 were determined using 95% confidence based on the physical measurements of the data. This error was computed using the jitter macro in Visual Basic [21]. The error shown for the model is the standard error, shown informally in equation 2.27 where SS is the sum of squares defined in equation 2.26 and the degrees of freedom (DOF) is number of points used minus one. The model appears to be a good fit with error that is similar magnitude to that found in the data.

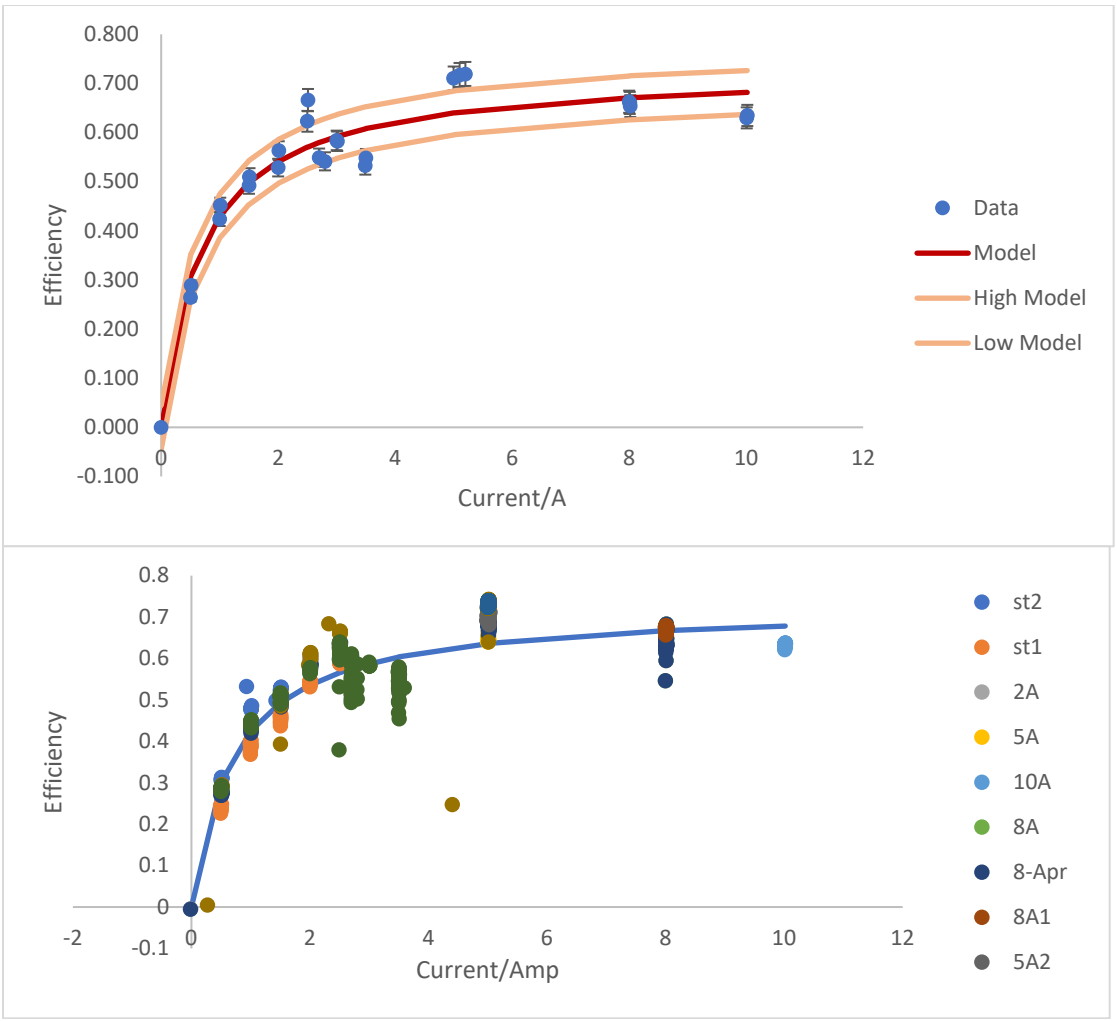

Figure 2-11 Model and Raw Data Comparison

$$\text{Error} = \sqrt{\frac{\text{SS}}{\text{DOF}}} \tag{2.27}$$

Chapter 3
Modeling the Rate of Hydrogen and Heat Production

The complexity in modeling the heat given off by the hydrogen production reaction lies in the rate of reaction. This rate is what must be modeled since the rate of reaction occurring is directly related to the rate of heat production. Unlike the rate of reaction for the fuel cell, the hydrogen production reaction rate is directly related to the physical properties of the reaction area, in this case, concentration. Concentration will change as the reaction proceeds, based on the ratio of products to reactants and the physical state of the products formed. Equations 3.1 and 3.2 show the reactions for SBH with water and SBH with ethylene glycol, respectively. For ease of discussion, the reaction with water will be referred to as hydrolysis and with ethylene glycol as alcoholysis.

$$NaBH_{4(s)} + 2H_2O_{(l)} \rightarrow NaBO_{2(l)} + 4H_{2(g)} + \text{heat} \quad (3.1)$$

$$NaBH_{4(s)} + 2CH_2OHCH_2OH_{(l)} \rightarrow NaB(OCH_2)_{4(aq)} + 4H_{2(g)} + \text{heat} \quad (3.2)$$

The "heat" term shown in these equations is the difference in heat of formation between the products and the reactants. This heat of formation, shown on the right side of the equation, will be considered positive as heat output to the environment. Similar to equation 2.4, equations 3.3 and 3.4 are the equations for the enthalpy of reaction for the reactions. The hydrolysis heat of reaction was determined using equation 3.3. However, the aqueous product of the alcoholysis reaction is not a known molecule with heat of formation listed in any sources found. The heat of reaction found experimentally in a separate publication was used in place of using the formation equation. The enthalpy values used for calculations were -212.1kJ/mol and -227kJ/mol for the hydrolysis and alcoholysis reactions, respectively [22].

$$\Delta H^{\circ}_{\text{hydrolysis}} = \Delta H^{\circ}_f[NaBO_2] + 4 * \Delta H^{\circ}_f[H_2] - 2 * \Delta H^{\circ}_f[H_2O] - \Delta H^{\circ}_f[NaBH_4] \quad (3.3)$$

$$\Delta H^{\circ}_{\text{alcoholysis}} = \Delta H^{\circ}_f[NaB(OCH_2)_4] + 4 * \Delta H^{\circ}_f[H_2] - 2 * \Delta H^{\circ}_f[E\ ] - \Delta H^{\circ}_f[NaBH_4] \quad (3.4)$$

While both the alcoholysis and hydrolysis will occur together, they will first be modeled individually. This will allow a better understanding of what is happening in the reactor.

3.1 Modeling Reaction Rate

Modeling rate of reaction is highly dependent on the reactor type being used. As labeled in the prototype in chapter 1, this reactor is a semi-batch reactor. Semi-batch typically means one or more reactant is placed in the reactor at time 0 and is not added during the progression of the reaction while one or more of the other reactants are added several times, if not continuously, after time 0. This reactor will stray from that slightly in that both reactants are added after time 0. It is still considered batch, however, since there is no outlet stream for the products or reactants. The general form of reaction rate is created via use of the general material balance equation that can be represented as in – out + generation = accumulation. Equation 3.5 is the material balance equation represented for reactant A, where F_{A0} is the flow of A in to the reactor (mol A/s), F_A is the flow of A out (mol A/s), r_A is the reaction rate (mol A/L*s), V is the volume of the reactor (L), and N_A is the moles of reactant A (mol A). The reactor for this application has no flow out, as stated previously, and complete mixing is assumed so the rate of reaction is not dependent on position in the reactor. This simplifies the material balance to the form shown in equation 3.6. Reactant A is chosen to be the limiting reactant, and the other reactants and products, as applicable, are modeled after the change in the limiting reactant.

$$F_{A0} - F_A + \int_0^V r_A \, dV = \frac{dN_A}{dt} \tag{3.5}$$

$$F_{A0} + r_A * V = \frac{dN_A}{dt} \tag{3.6}$$

The flow of reactants in is as needed, not on a continuous basis, so models with respect to time will treat this as a batch reaction, thus setting F_{A0} equal to 0. The reactants and products already present can be considered as part of the initial concentration of the limiting reagent. The rate of reaction for both the alcoholysis and hydrolysis reactions have been found to be linearly, and solely, dependent on the concentration of SBH. The rate of reaction model equation takes the form shown in equation 3.7, where k is the rate constant (s^{-1}) and C_A is the concentration of species A (mol A/L solution). k can be modeled via use of the Arrhenius equation, shown in equation 3.8, where A is the frequency factor (s^{-1} in this context), E_a is the activation energy of the reaction (J/mol), R is the universal gas constant (= 8.314 J/(mol*K) in this context), and T is the temperature of the reaction (K). This equation can be rearranged to solve for the rate constant at a different temperature, as seen in equation 3.9.

$$-r_A = k * C_A \tag{3.7}$$

$$k = A * e^{\frac{-E_a}{R*T}} \tag{3.8}$$

$$k = k_0 e^{\frac{E_a}{R}(\frac{1}{T_0}-\frac{1}{T})} \tag{3.9}$$

Since the reaction rate is dependent on concentration, which varies with time, the rate was modeled via use of a differential equation modeling software called Polymath. The differential equation used was a derivation of equation 3.6, with the negative of the reaction rate used and both sides of the equation divided by N_{A0} (mol A) to build the model as a function of fractional conversion, x (mol A consumed by time t/mol A at time 0). 3.10 is the resulting equation. This equation should be valid for any batch reactor. Polymath finds a solution via the initial value problem (IVP) solving strategy. Due to this, it requires all variables that change with the independent variable (time in this case) to be defined at the starting conditions, indicated with the subscript "0". The initial and final time were also specified. Initial mass of SBH (reactant A) and volume of either EG or H_2O (reactant B) were set directly equal to the measurements so the equation is unnecessary here. The other variables were defined based on these measurements and known quantities such as molecular weight. The initial concentration of SBH, C_{A0} (mol/L), is shown in equation 3.11, where V_0 (L) is the volume of reactant B added (the volume of SBH is assumed to be negligible and irrelevant since it is solid phase and the reaction occurs on its surface, not throughout the solid volume)). The calculation of N_{A0} (mol A) is shown in equation 3.12 where m_A is the initial mass (g) of SBH added and MW_A is the molecular weight (g/mol) of SBH. The volume changes as the reaction proceeds. This change is modeled, shown in equation 3.13, as the original volume minus moles of B consumed, divided by the molecular density, $\rho_{M,B}$ (mol B/L B). The concentration of A at some time, C_A (mol A/L) is modeled similarly, shown in equation 3.14. It is set equal to the moles remaining divided by the volume remaining.

$$\frac{dx}{dt} = \frac{-r_A * V}{N_{A0}} \tag{3.10}$$

$$C_{A0} = \frac{N_{A0}}{V_0} \tag{3.11}$$

$$N_{A0} = \frac{m_A}{MW_A} \tag{3.12}$$

$$V = V_0 - \frac{2 * N_{A0} * x}{\rho_{M,B}} \tag{3.13}$$

$$C_A = \frac{N_{A0} * (1 - x)}{V} \tag{3.14}$$

Modeling the reaction rate requires knowing the rate constant. This is an issue in that the activation energy and frequency factor are unknown variables that require measuring the reaction rate to find them. There are sources that provided the activation energy for the alcoholysis reaction but did not provide the raw data or calculated rate constant. This was inferred from the graph and a model was created, but it did not appear to match their results. The left side of Figure 3-1 shows the code (modified from code written by Dr. Steven Sternberg) to create the ethylene glycol model in Polymath and the right side has the graph that the reaction constant of 0.001136 (1/s) at a temperature of 323K was estimated from. This model didn't show full conversion until around 22 hours, where the source gave the conversion at those conditions as 3 minutes. Similar results were found for the hydrolysis model. Due to these discrepancies, further modeling was not pursued until the reaction rate constant, the activation energy, and the frequency factor, could be experimentally determined.

```
d(x) / d(t) = -rA*V/Na0 #Alcoholysis batch
x(0) = 0
rA=-k*Ca
m=10 #g
Na0=m/37.83#mass/MW = moles A


V0=.01 # liters
V=V0-Na0*x*2/17.887 #liters
Ca0=Na0/V0 #mol/L

Nb0=V0*17.887 #moles = volume EG added*molar de
#Nc0=0
#a=1
#b=2
#c=1
#zieB=Nb0/Na0
#zieC=Nc0/Na0

Ca=Na0*(1-x)/V
#Since reactant B is the solvent, concentration is not
#Cc=Na0*(zieC+c/b*x)/V
T0=323
T=303
#T=T0+227*x/(0.15*Na0*(zieB-b/a*x)) #Based on heat
#by heat capacity of B since the other heat capacities
k=0.001136*exp(25800/8.314*(1/T0-1/T)) #min^-1
# Initial and Final Conditions
t(0) = 0
t(f) = 800
```

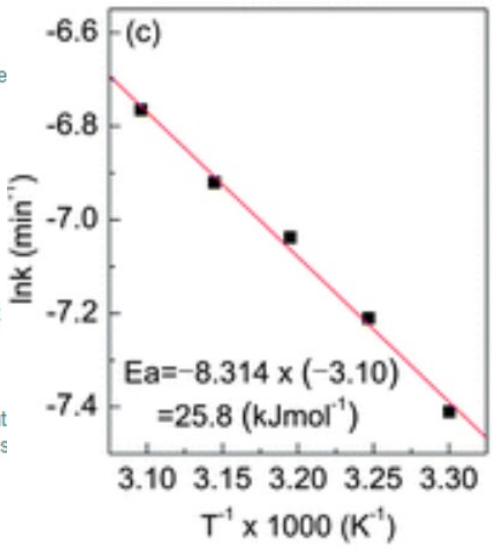

Figure 3-1 Model Code and Graph of Data

3.2 Reaction Rate Experimental Setup

Both the alcoholysis and hydrolysis reactions involve gas evolution. Since gas leaves the solution at approximately the same rate it is formed, this was the easiest measurement for the rate and extent of reaction. The hydrogen burette was used to measure the gas, hydrogen, as it was produced. The burette was connected to one neck of a 250-mL 3-neck round-bottom flask. The other two necks of the flask were used for sensors. The middle, and largest, neck was used for the pressure sensor while the right neck was used for the temperature sensor. The left side of Figure 3-2 shows the full experimental setup before the pressure sensor was attached. The right side of the figure shows a closeup of the 3-neck flask and attachments with residual products in the bottom. To connect the pressure sensor to the flask, a glass tube was pushed through the stopper. This was done by pushing the tube through without removing any rubber, thus increasing the pressure around the tube to reduce amount of hydrogen lost through the stopper. A silicon tube was pushed over the glass tube, creating a pressure seal. The end of the silicon tube was then connected to the pressure sensor via use of a "T" junction. A pressure relief valve and the pressure sensor were attached to the other ends of the junction. The pressure relief valve was put in to protect the pressure sensor in case enough hydrogen was supplied to cause the pressure to rise above 15 psi, the rated maximum pressure for the sensor. The connection with the relief valve was identical to that with the stopper since the valve was made primarily of glass tubing. The connection to the pressure sensor was done via use of compression fittings that screwed onto the pressure sensor. The thermocouple was a larger concern since the sensor must be directly in the reactor, not attached at the end of tubing. To do so, a glass tube was pushed through the stopper just as with the pressure sensor. Silicon tubing was then attached to the glass tube and the thermocouple was threaded through both. The other end of the thermocouple had to be attached to the CDAQ, so there was no way to directly cut off potential flow of hydrogen to these areas. A clamp was attached to the silicon tubing and tightened by hand. The end of the tube was filled with liquid silicone to give as much flow resistance as possible. The end of the thermocouple in the reactor was kept above the volume of the flask used for reaction to make sure the metal of the thermocouple couldn't act as a catalyst for the reaction. These connections are present in the picture shown on the left of Figure 3-2 but missing in the picture on the right because the thermocouple had not yet been added. Snoop [23] was used periodically to check for leaks in each point of connection. Finally, the flask was placed in a water bath to keep the temperature more consistent to allow better evaluation of the rate constant.

Figure 3-2 Experimental Setup of Reaction

The thermocouples and pressure sensors were monitored via use of the Labview software for this experiment as well. The setup is shown in Figure 3-3. The setup is identical in concept to that shown in chapter 2, section 2.3, so further explanation will be omitted here.

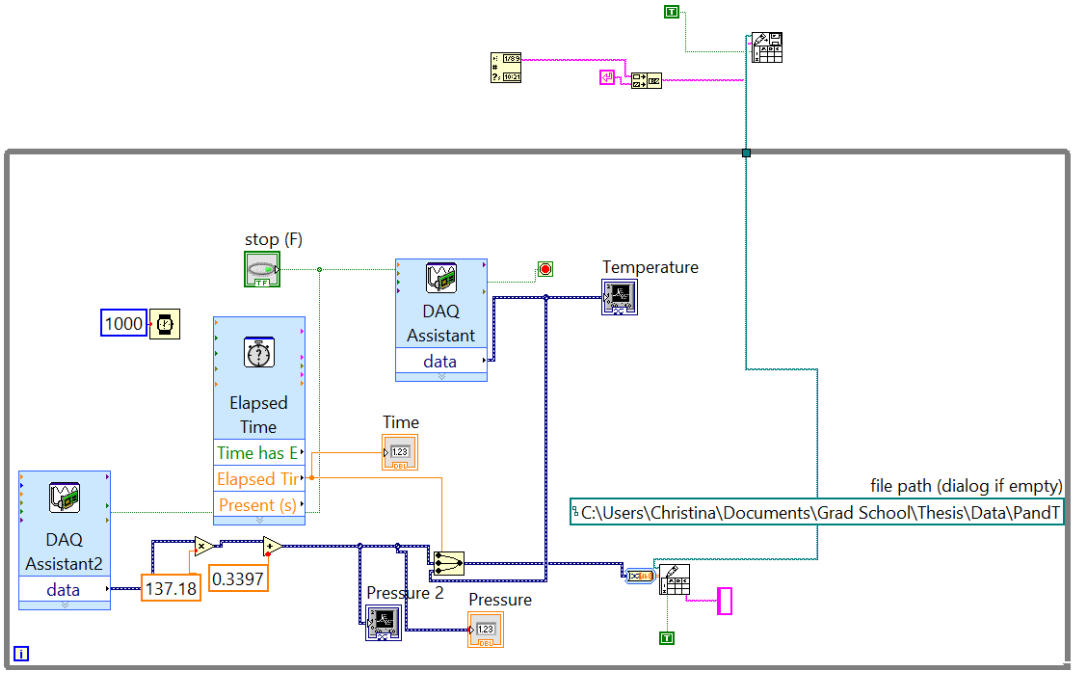

Figure 3-3 Labview Virtual Instrument Setup for Rate of Reaction Experiments

The reactants were added to the flask via use of micropipettes when the SBH was already in the reactor. The neck of the flask that the thermocouple was inserted into was the one used for reagent addition. As soon as the reactants were added the stopper/thermocouple combination was

placed back in the neck and the measurement software was started. Vaseline was used on all 3 stoppers to create a better hydrogen seal. A second thermocouple was used for the burette to get the temperature of gas for determining the moles of hydrogen present.

3.3 Reaction Rate Results

The rate experiments were performed for ethylene glycol and water separately and in the mixture that will be used in the prototype. The concentration was determined by measuring weight of SBH added, converting to moles, and dividing by the volume of reagent added, either EG or water, as shown in equations 3.11 and 3.12. The natural log of the concentration was taken and graphed with time to verify that the reaction was first order with respect to the SBH, as assumed. Figure 3-4 shows these graphs for the room temperature and 15 degrees Celsius mixed reactant experiments. The graphs cover the length of the reaction that had temperature variance of less than 1 degree Celsius. Thus, they don't start at time 0. Their linear pattern strongly supports the assumption that the reactions are first order with respect to the SBH concentration [24].

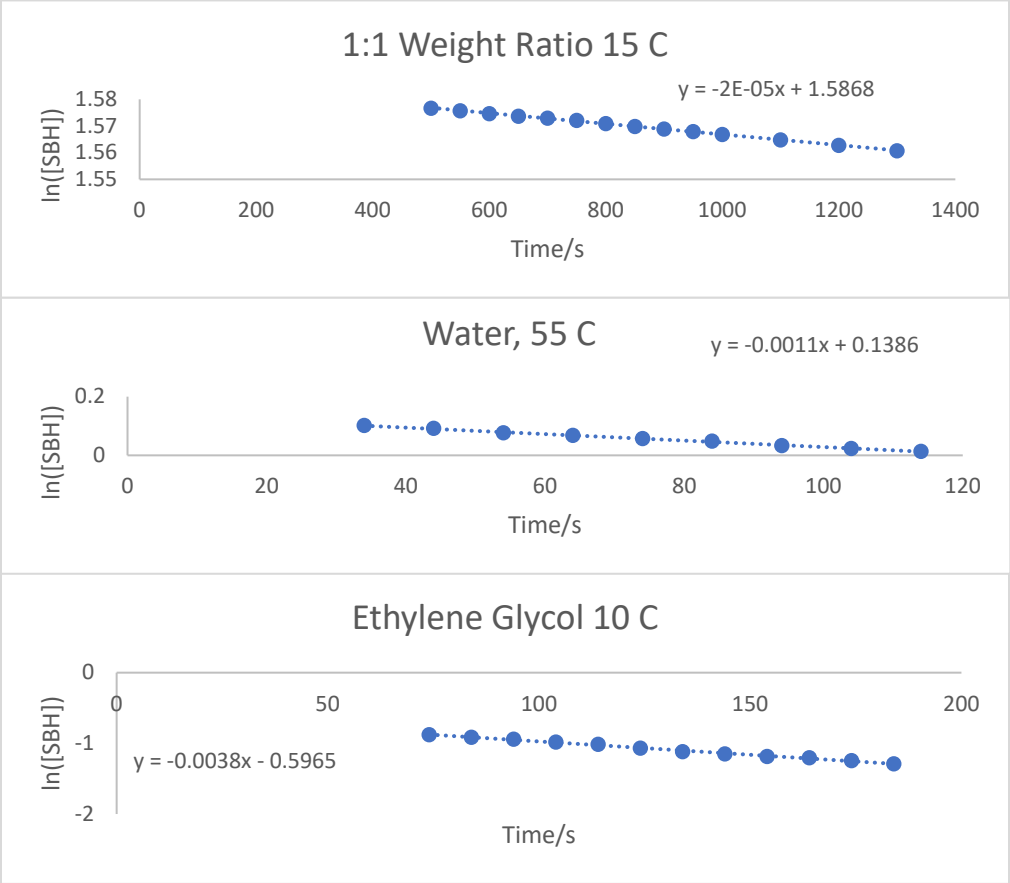

Figure 3-4 Graphs of Natural Log Concentration per Time used to verify order of reaction

Since the rate constant, k, varies with temperature, data from all experiments was grouped by change in temperature within the experiment, where any data within 1 degree Celsius of one another was a group. Each group of data then had the average temperature, concentration, change in concentration, and rate constant determined. These points were used to create an Arrhenius plot for each reactant individually as well as the mixture. While the mixture won't have a true activation energy, this allowed an effective activation energy to be estimated to create the model. This was done for the frequency factor as well. Figure 3-4 has these plots as well as linear trendlines with the equations shown. The intercept (=ln(A)) was used to calculate the frequency factor and the slope of the line was used to find the activation energy (slope = -Ea/R). These values were used to calculate the rate constant, k, in further modeling.

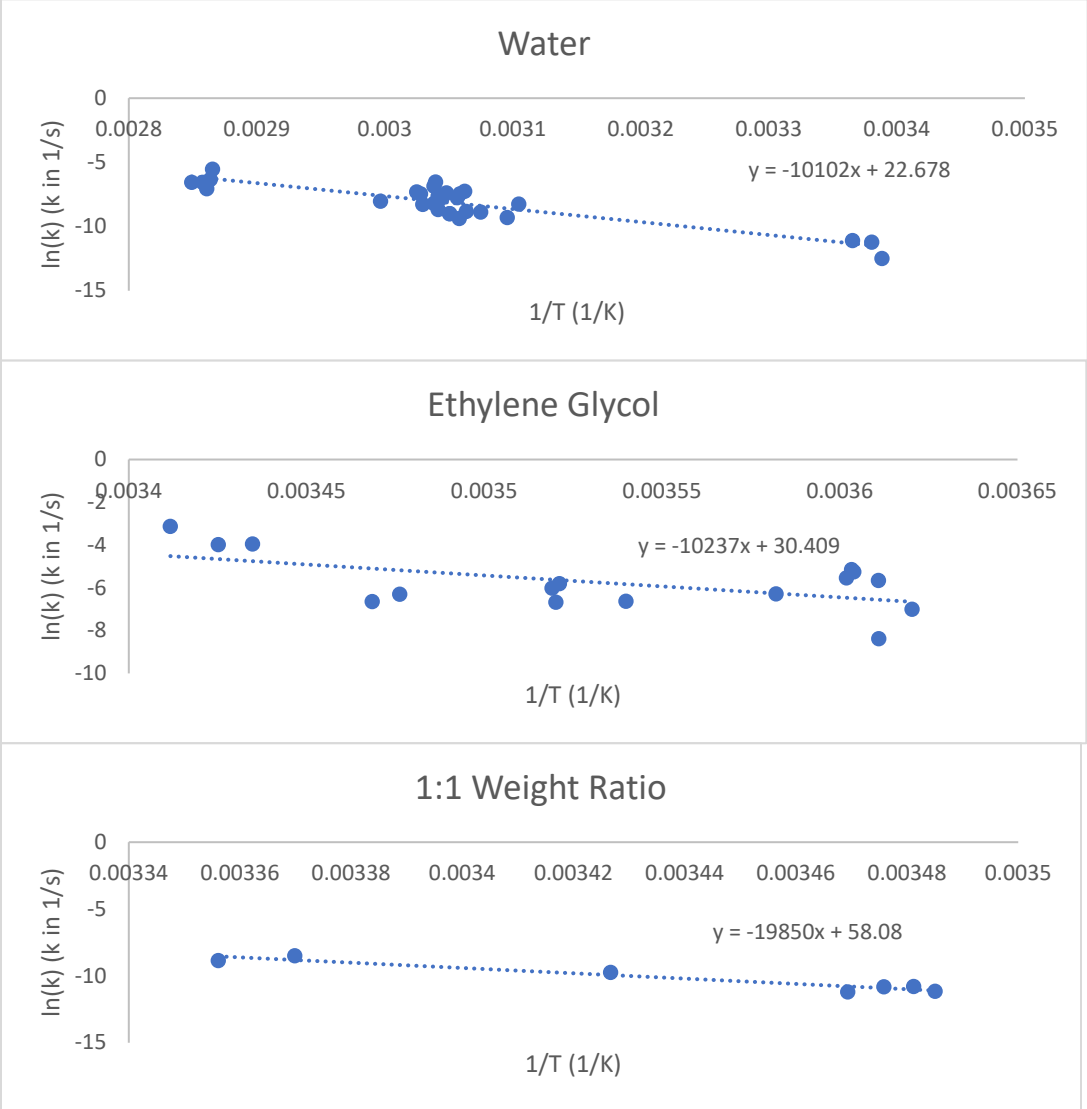

Figure 3-5 Arrhenius Plots used to determine the activation energy and frequency factor constants for the rate law

Table 3-1 shows the resulting activation energies and frequency factors found via use of the linear trendline equations displayed in Figure 3-5.

Table 3-1 Respective Activation Energy and Frequency Factor

	Ea (kJ/mol)	A (1/s)
Alcoholysis	85.1	1.61E+13
Hydrolysis	84.0	7.06E+09
Mixture	165	1.67E+25

A few errors were encountered with most experiments. The water experiments couldn't be run at temperature below room temperature because the reaction proceeded slowly enough the hydrogen would diffuse or escape before it could be effectively measured. The EG experiments had the opposite issue where the temperature had to be reduced to slow the rate enough to get good measurements of the gas evolved. Another issue was encountered with the ethylene glycol experiment anytime the reactants were added at a temperature below 5 degrees Celsius. They would go through a period of time where no reaction would be observed until suddenly the reaction proceeded very quickly. This was likely due to the sodium borohydride not dissolving readily, but once dissolved, creating enough heat from the reaction to increase the rate significantly. Unfortunately, these results correlated with having a chunk of the SBH still remaining at the end when the reaction wasn't proceeding fast enough to get results. This prevented any usable data from being gathered. This was not further pursued since ethylene glycol wasn't going to be used on its own, but it gave strong support of not using pure ethylene glycol as the only reactant in temperatures near freezing.

There were also intermittent issues with hydrogen leaks where no leak would be observed via the physical test (i.e. no bubbles were observed when snoop was used), yet the pressure would suddenly drop while the reaction would be observed to still be continuing. This was assumed to be the point where the leak became greater than the amount of hydrogen produced in the reaction. The experiments had to be stopped at this point because the volume of hydrogen produced could no longer be measured. This error will tend toward a more conservative model in that it will underestimate the amount of hydrogen, and therefore heat, produced. This will be discussed quantitatively in the model.

The above issues were resolved prior to the mixture experiments being conducted, so fewer experiments had to be run. The temperature was also varied less because the setup was planned to be such that the temperature didn't go below 10 degrees Celsius to prevent risk of the fuel cell getting injured by cold reactants being run to it.

3.4 Reaction Rate Model

The rate of reaction was modeled using Polymath as mentioned in section 3.1. The activation energy and frequency factor found experimentally were used for this model. The new code is shown in Figure 3-6. The program experienced overflow when the frequency factor, A, was kept outside the exponential function as it is written in the Arrhenius equation, equation 3.8. The natural log of A was used to avoid this issue. This change is shown numerically in the code and algebraically in equation 3.15. As mentioned in section 3.1, each run of the model is based on one addition of reactants (could be any time during the week that this setup is to be run), where the reactants still present in the reactor are accounted for using m, the sum of the mass of SBH still in the reactor and the mass added at the beginning of the model. V0 accounts for the amount of the other reactants, where it is the sum of the volume of the other reactants left and the volume of mixture added at the beginning of the model.

```
d(x) / d(t) = -rA*V/Na0 #Alcoholysis batch
x(0) = 0

rA=-k*Ca
m=.01 #g
Na0=m/37.83#mass/MW = moles A

V0=.01 # liters
V=V0-Na0*x*2/17.887 #liters
Ca0=Na0/V0 #mol/L

Ca=Na0*(1-x)/V

T=303

k=exp(30.409-85110.42/(8.314*T)) #s^-1
# Initial and Final Conditions
t(0) = 0
t(f) = 200
```

```
d(x) / d(t) = -rA*V/Na0 #Hydrolysis batch
x(0) = 0
rA=-k*Ca
m=10 #g
Na0=m/37.83#mass/MW = moles A

V0=.01 # liters
V=V0-Na0*x*2/54.4 #liters

Ca0=Na0/V0

Ca=Na0*(1-x)/V
T=295

k=exp(22.678-84000/(8.314*T)) #s^-1

# Initial and Final Conditions
t(0) = 0
t(f) = 100000
```

```
d(x) / d(t) = -rA*V/Na0 #50/50 batch
x(0) = 0
rA=-k*Ca
m=.2082 #g
Na0=m/37.83#mass/MW = moles A

V0=.012 # liters
V=V0-Na0*x*0.775*2/55.4-Na0*x*0.225*2/17.887
Ca0=Na0/V0 #mol/L

Ca=Na0*(1-x)/V

T=296.2

k=exp(55.078-175525/(8.314*T)) #s^-1
# Initial and Final Conditions
t(0) = 0
t(f) = 1500
```

Figure 3-6 Polymath Code for Alcoholysis, Hydrolysis, and Mixture Batch Reactions

$$k = e^{\ln(A)-\frac{E_a}{R*T}} \tag{3.15}$$

Fractional conversion, x, was used to give the best error estimation and comparison of data versus model. Model runs were created for each hydrolysis (model H), alcoholysis (model A), and mixture (model M), experiment that was run in lab (those that had significant leaks or other hardware issues were excluded). The models required one temperature be used to estimate the rate constant for the experiment they modeled. This was the greatest source of error in the models, especially those correlated to experiments that had significant change in temperature. To reduce the error, the models were run with the average measured temperature in the experiments they replicated. The initial mass (m in the code) and volume (V0 in the code) used in each experiment were input to the model, directly modeling the moles and concentration at time 0 for the experiments. Models H and A were created to validate model M since model M used effective

values for the rate constant and activation energy. Further discussion of models H and A will not be included in this report since model M is the reaction model for the 50 % mixture that will be used to react with the SBH to create the hydrogen for the fuel cell.

Replicating the experiment parameters in the model allowed direct comparison of model and experiment for error analysis. Figure 3-7 shows this comparison. The experiments labeled "cool experiments" refer to the experiments run in a beaker that was held in a water bath at approximately 15 degrees Celsius and an initial concentration of approximately 5 mol SBH/L. Those labeled "RT Experiment" refer to the experiments run with the beaker kept in a room temperature water bath and an initial concentration of roughly 3 mol SBH/L. The 1st cool experiment and both room temperature experiments appear to fit the model well. The 2nd cool experiment, however, has significantly better conversion than the model predicts. This could be due to the hydrogen being better contained or the heat from the reaction being produced faster than the water bath could remove it, thus giving a higher operating temperature than the model is based on. The temperature difference is the most likely cause of the discrepancy because the temperature of the bath was used to model the temperature of reaction, so a significantly higher temperature in the reaction area than in the bath would not have been observed with the experimental setup.

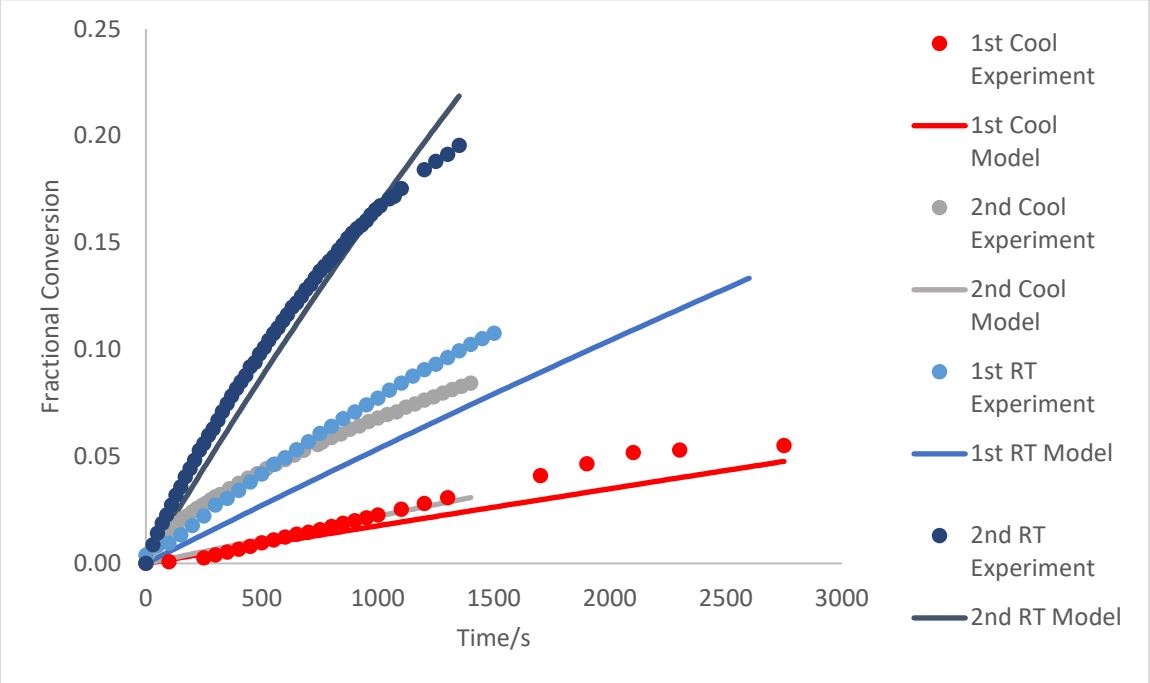

Figure 3-7 Model and Experimental Conversions for Mixture

The data for the models and experiments is available in Appendix B. Uncertainty was evaluated and an average uncertainty of 2% was found, (calculated using fixed and combined uncertainties) but the error bars were not long enough to be observed on the graph. The real error of the data is likely higher than calculated, but there was no standard deviation to calculate and give a better estimate since there were no averages taken in the calculations. The only uncertainty that could be directly determined was that due to readability of the physical measurements.

Chapter 4
Creation of the Heat Transfer Model

Modeling the heat transfer requires modeling the sources of heat, heat sinks, and how the heat is transferred within the environment. The simplest heat production is the heat loss from the fuel cell, based on the efficiency, as modeled in chapter 2, section 5. The specifications given in the original project [8] had a power requirement of 20 W at 12 V for one week. Using equation 4.1, rearranged to solve for current, I, this requirement was found to have a 1.667 A current. Using the efficiency model, this correlated to a fuel cell efficiency of 51.3%. An efficiency of 50% will be used to model the heat transfer to ensure a conservative model. Equation 2.2 was used to find the heat output from this power requirement and efficiency. The heat output was 20 J/s. This will be used as a constant in the heat transfer model.

$$P = I * V \tag{4. 1}$$

4.1 Transient Heat Conduction Approximation

It is assumed that there is negligible mass transfer between the system and surroundings (the surroundings being anything outside of the large box that represents the boundary of the container in Figure 1-4). It is further assumed, based on the lack of mass transfer, that heat transfer due to convection is negligible. Equation 4.2 is the equation for heat conduction, where q is heat transfer per unit time, h_c is the heat convection coefficient, A is the cross sectional area of heat transfer, and dT is the change in temperature. The heat convection of air with negligible velocity is 10.75 W/(m^2*K) [25]. The applicable transfer area for the fuel cell is 0.015 m^2. If the difference in temperature between the air in the environment and the fuel cell is 10 K, the heat transfer would be 1.66 J/s, less than 10% of the heat generated by the fuel cell.

$$q = h_c * A * dT \tag{4. 2}$$

(Equations 4.3 through 4.10 are basic heat transfer equations. The particular nomenclature and explanation of their derivation is based on notes from the Mechanical Engineering Department of Auburn University [26].) The assumptions of negligible mass transfer

and negligible heat transfer via convection reduces the heat transfer model to that for conduction. Equation 4.3 is the equation for energy change with time in a system with fixed volume and constant mass where E is the energy of the system and $\dot{Q}$ is the rate of heat into (or out of) the system. If the system is not in equilibrium, then E cannot be related to a single temperature of the system and the equation must be expanded to model the heat transfer. To do so, the heat transfer is modeled by taking the sum of the energies of infinitesimally small volumes assumed to be in thermodynamic equilibrium at any instant, t. This can be taken as a limit as the size goes to zero, thus allowing integration by volume to find the energy transfer. Equations 4.4 and 4.5 show both sides of the equation expanded with integration to show change in energy per unit volume per time. ρ is density (g/m^3), c is the specific heat ($J/(g*K)$), e is the specific energy (J/g), T is temperature (K), t is time (s), A is area (m^2), q'' is the heat flux vector (W/m^2), q''' is the volumetric heat source function (W/m^3), n is the normal vector out from the surface dA, and V is volume (m^3).

$$\frac{dE}{dt} = \dot{Q} \tag{4. 3}$$

$$\frac{dE}{dt} = \int_V \rho \frac{\partial e}{\partial t} dV = \int_V \rho c \frac{\partial T}{\partial t} dV \tag{4. 4}$$

$$\dot{Q} = -\int_A q'' \cdot n \, dA + \int_V q''' dV \tag{4. 5}$$

Equation 4.6 is a translation of the flux term in equation 4.5 (the integrated term with area, A, as its bound). This change was done via use of the divergence theorem to express the flux in terms of volume, allowing both integrals from equation 4.5 to be combined. The combination of integrals allows equations 4.4 and 4.5 to be substituted back into equation 4.3 and the combination simplified. Equation 4.7 is the resulting combination. Physical understanding of the problem allows equation 4.7 to be simplified to the form shown in equation 4.8. Equation 4.8 is not very useful for modeling because it is expressed using two different variables, flux and temperature. To resolve this, equation 4.9, Fourier's law for heat conduction, where k is thermal conductivity ($W/(m*K)$), is substituted into equation 4.8. The resulting equation, equation 4.10, is the energy change, first shown in equation 4.3, expressed in terms of one variable, temperature. This version of the equation is applicable to any coordinate system since the Laplacian is expressed generically. The coordinate system and origin have to be determined to be able to create a heat exchange model function.

$$\int_A q'' \cdot n \, dA = \int_V \nabla \cdot q'' dV \tag{4. 6}$$

$$\int_V (\rho c \frac{\partial T}{\partial t} + \nabla \cdot q'' - q''')dV = 0 \tag{4. 7}$$

$$\rho c \frac{\partial T}{\partial t} + \nabla \cdot q'' - q''' = 0 \tag{4. 8}$$

$$q'' = -k\nabla T \tag{4. 9}$$

$$\rho c \frac{\partial T}{\partial t} = \nabla \cdot k\nabla T + q''' \tag{4. 10}$$

Cylindrical coordinates were chosen to represent the environment around the fuel cell. Specifically, it was treated as a hollow cylinder with a solid inner cylinder, in this case, the reactor. The origin was chosen to be the exterior of the reactor. Equation 4.11 is the heat exchange model that was expressed in equation 4.10, now expanded for cylindrical coordinates. Equation 4.11 was altered further for clarity. k from equation 4.10 was replaced with λ and I was substituted in for q'''. The variable r in the equation is the radius of the hollow cylinder, phi is the angle, and z is the height of the cylinder, all expressed in meters. This equation is generally referred to as the transient heat conduction equation.

$$\frac{1}{r}\frac{\partial}{\partial r}\left(\lambda_r * r \frac{\partial T}{\partial r}\right) + \frac{1}{r^2}\frac{\partial}{\partial \phi}\left(\lambda_\phi \frac{\partial T}{\partial \phi}\right) + \frac{\partial}{\partial z}\left(\lambda_z \frac{\partial T}{\partial z}\right) + I(r, \phi, z, t) = \rho c \frac{\partial T}{\partial t} \tag{4. 11}$$

4.2 Heat Conduction Model

Several assumptions were made when modeling the heat transfer in the environment around the fuel cell. To accommodate assumptions and simplify the model, the environment around the fuel cell was treated as a hollow cylinder, as mentioned in section 4.1. To do so, an effective radius, R, was used. This radius is taken to be the average length between the exterior of the reactor and the exterior environment. The physical setup referenced in the prototype in chapter 1 has a height of 42 inches, a depth of 18 inches, and a width of 36 inches. The diameter of the reactor is 4 inches. This means that the shortest length between the exterior of the environment and the reactor (radially, excluding height) is 7 inches, while the longest, from

reactor to corner, is 17.5 inches. The average of these two lengths is 12.25 inches or 0.3 meters, roughly. This will be the effective radius used for calculations. The only change in position from the prototype is that of the fuel cell. This will be placed next to the reactor rather than equidistant between reactor and the exterior wall as shown in the prototype.

The main assumption used in the model was that the temperature is constant with respect to time. This assumption is justified if the system is designed to have a reaction rate that is sufficient, if not greater than, that required to produce the hydrogen necessary to continually produce the required 20 W of power in the fuel cell. The constant reaction rate assumption assumes that the power requirement is also continuous, an assumption implied at the beginning of this chapter when it was stated that the heat production from the fuel cell would be treated as constant. The second and third assumption used when designing the heat model pertain to the direction of heat transfer. The reactor is treated as a solid cylinder that is significantly taller than the fuel cell. It is assumed, then, that temperature is invariant with z in respect to the fuel cell. Similarly, it is assumed that there is no angular change in temperature. This assumption is justified with the use of the effective radius. Finally, the heat generation, I, was assumed constant along the radial length. This assumption seems the least reasonable in this derivation, but it tends toward a more conservative model when an effective heat generation constant is used. The effective heat generation constant is created by taking the average heat generation and dividing it by the length of the container.

Assuming steady state conditions with negligible variance with respect to height and angle simplifies equation 4.11 to that shown in equation 4.12. The thermal conductivity, λ, of air, is shown to be linearly dependent on temperature in the applicable range. The applicable range, however, correlates to a change in thermal conductivity of less than 10%. To simplify the model, the thermal conductivity was treated as a constant. To optimize the accuracy of the thermal conductivity used, the constant was allowed to change with temperature by treating it as a piece wise function where the constant used for the conductivity was determined by the range of the temperature. (i.e. for T between x1 and x2, constant A is used, else for T between x2 and x3, constant B) This reduced the maximum error in the thermal conductivity to less than 1.5%. Additionally, the conductivity was left within the equation despite being assumed constant to allow easy substitution of a linear correlation when a more robust model is sought. Table 4-1 has the data used for the thermal conductivity piece wise function.

$$\frac{1}{r}\frac{\partial}{\partial r}\left(\lambda * r\frac{\partial T}{\partial r}\right) + I = 0 \qquad (4.\ 12)$$

Table 4- 1 Temperature Dependence of Thermal Conductivity of Air

Temperature, K	Thermal Conductivity of Air in W/(m K)
253.35	0.0227
263	0.0234
272.65	0.0241
282.3	0.0248
291.95	0.0255
301.6	0.0262
311.25	0.0269
320.9	0.0276

Equation 4.12 must be integrated twice to model temperature as a function of radius. Wolfram Alpha was used to integrate the equation. The details of the computation can be found in Appendix C. The initial solution was simplified by using the ratio of position r to the effective radius, R as the independent variable. Equations 4.13 and 4.14 show the function and first derivative expressed with general constants of integration. Equations 4.15 and 4.16 are the boundary conditions and resulting expressions for the constants of integration (bolded for clarity). Equation 4.17 is the complete version of the equation used to model the temperature as a function of radius.

$$T(r) = -\frac{1}{2}\frac{I}{\lambda} * \frac{r^2}{R} + \frac{I * r}{\lambda} + c_1 e^{-\frac{r}{R}} + c_2 \tag{4. 13}$$

$$T'(r) = -\frac{r}{R} + \frac{I}{\lambda} - \frac{c_1 e^{-\frac{r}{R}}}{R} \tag{4. 14}$$

$$\text{At } r = 0,\ \frac{dT}{dr} = 0 \ \rightarrow\ 0 = \frac{I}{\lambda} - \frac{c_1}{R} \ \rightarrow\ \mathbf{c_1 = \frac{I*R}{\lambda}} \tag{4. 15}$$

$$\text{At } r = R,\ T = T_{out} \ \rightarrow\ T_{out} = \frac{I*R}{2\lambda} + \frac{I*R}{e*\lambda} + c_2 \ \rightarrow\ \mathbf{c_2 = T_{out} - \frac{I*R}{\lambda}\left(\frac{1}{2} + \frac{1}{e}\right)} \tag{4. 16}$$

$$T(r) = -\frac{I * r^2}{2 * \lambda * R} + \frac{I * r}{\lambda} + \frac{I * R}{\lambda} e^{-\frac{r}{R}} + T_{out} - \frac{I * R}{\lambda}\left(\frac{1}{2} + \frac{1}{e}\right) \tag{4. 17}$$

The final step to create the model was finding the appropriate value for the heat generation constant, I. This value was determined by dividing the amount of heat generated per time by the length of the system. The heat generated per time is the sum of the heat from the fuel

cell and the heat from the reactor. The heat from the fuel cell was determined to be 20 J/s as mentioned at the beginning of this chapter. The heat generated from the reactor was determined based on the constant reaction rate assumption. The amount of hydrogen required to constantly produce 20 watts of power at a fractional efficiency of 0.5 is 100 moles H_2 per week. This was found by dividing the actual energy needed, found via equation 2.1, by the heat of formation of water, as shown in section 2.2. Stoichiometry requires 25 moles of SBH and 50 moles of the EG-water mixture to produce 100 moles of H_2. The water mixture contains 0.775 molar fraction water and 0.225 molar fraction EG. Assuming 1:1 selectivity of the two reactions and using the associated heats of reaction, the reactions will produce 4,400 kJ/week from the hydrolysis and 1,300 kJ/week from the alcoholysis. Converting back to units of seconds, the sum of the heat produced by the reactions is 9 J/s, giving a total of 29 J/s heat produced from the fuel cell and reactor. The heat generation constant was determined to be 33 J/s.

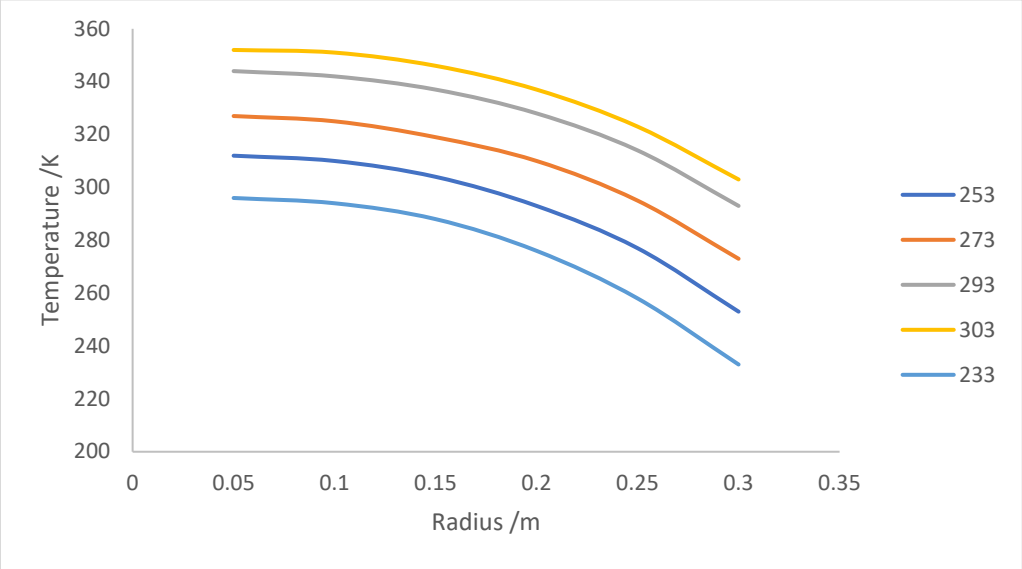

Figure 4- 1 Effect of Outside Temperature on System Temperature with Respect to Distance From Reactor

The lowest temperature reached at the reactor, assuming the environment reaches 233 K, was roughly 290 K as derived by the model. This temperature is more than adequate to maintain the necessary reaction rate, even at the end of the cycle when the volume of reaction exceeds 4 liters. Specifically, the model used in chapter 3, with 4 L volume and 6 grams SBH (the amount required to run for an hour at a time and assumes no residual SBH), gives over 10 percent conversion within an hour at this temperature.

4.3 Adding Sodium Borohydride

One of the main components of the heat transfer model, as discussed in 4.2, is the assumption that the rate of reaction would be sufficient to produce the necessary hydrogen for the required load for the fuel cell. Further, the rate of reaction model was created as a function of concentration, assuming the sodium borohydride would be in solution with the other reagents. Given how unpredictably the SBH reacted when in solid form (referring to the discussion at the end of section 3.3 of the experiments where the SBH didn't dissolve due to temperature), the sufficient and constant reaction rate assumption would likely be invalid if the SBH reactions occur on the surface of the solid. To ensure these assumptions and models were reasonable and applicable, means of storing SBH in solution needed to be addressed. During review of literature that addressed fuel cell efficiency, it was found that sodium hydroxide (NaOH) could be added to the water to stunt the reaction between the water and sodium borohydride [27]. If true, this would allow the SBH to be stored in water until it was added to the fuel cell reactor. To test this hypothesis, approximately 5 grams of SBH was added to 100 mL of 1, 0.1, and 0.01 concentrations of NaOH with water. The 0.01 molarity had significant observable reaction. 0.1 molarity had very little reaction. The reaction proceeded slowly enough that the hydrogen production was insufficient to be able to be measured with the hydrogen burette. The 1 molar solution had very little, if any, gas evolved in the space of an hour. Pictures were taken at the end of an hour for both the 1 molar and 0.1 molar solutions. The left side of Figure 4-2 shows the 0.1 molar solution and the right side is the 1 molar solution.

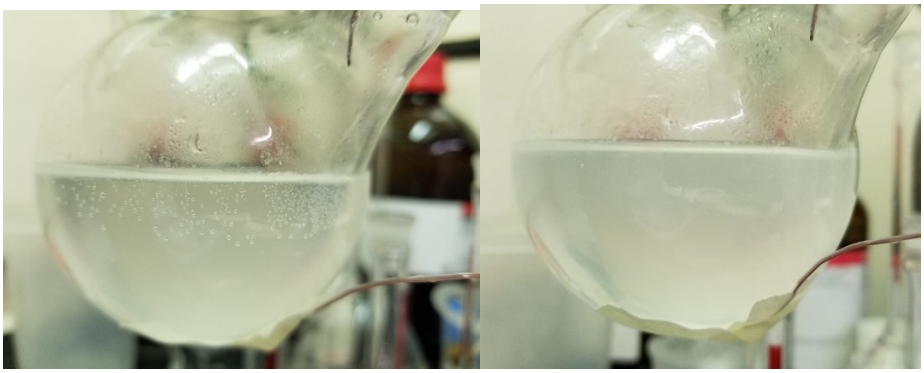

Figure 4- 2 Sodium Hydroxide Storage Beaker Experiments

The results show that the NaOH water solution at 0.1 molarity could work for SBH storage. It was found that running the fuel cell for a week with a load of 20 W and an efficiency rounded down to 0.5 required 950 g SBH and 1500 mL of the 50% weight solution. With a solubility of 550 g SBH/ 1 L water [28], depositing the SBH in the reactor as a basic, aqueous

solution, requires roughly double the amount of water required to react with the SBH. Accommodating this solubility would require a reactor volume at least 4 L, preferably 5L. The large reactor and the excess water will greatly reduce the reactant concentrations by the end of the week. Given that the reactor must be kept above 280 K to prevent the hydrogen sent to the fuel cell causing damage, these lower concentrations should not be a problem since significant conversion was still achieved at these temperatures. Further, the reaction rate model run with a volume of 4L and temperature of 280 K still showed significant conversion. An initial concern was that a 5L reactor may be too big for the available space, so the necessary height to achieve a volume of 5 L while still keeping a 4 inch diameter was calculated. The height required was 24 inches, well within the capacity of the container system that has a height of 42 inches, so it was determined that size would not be an issue. Further discussion of this storage option and the necessary safety considerations will be included in chapter 5. It will be assumed to be the storage used in the model, however, since it appears the best option at this point.

Chapter 5
Results and Future Steps

The temperature around the reactor, according to the model, stayed slightly below room temperature with the temperature outside the setup being 40 degrees Celsius below the freezing point of water. A test of the model using engineering error was run. A decrease of 20% heat generation was still able to keep the area around the fuel cell above the freezing point of water. (20% error resulted in a temperature of 279 K at the fuel cell). To further test the limits of the model, the heat produced by the reaction to form water was assumed to be absorbed by the reactants and thus did not diffuse to the area around the fuel cell. (This parameter was tested because the reactants added may be at a lower temperature than that of the reactor and thus may absorb some of the heat.) The temperature in the area around the fuel cell was found to still remain above the freezing point of water with an outside temperature of -40 degrees Celsius. As such, the hypothesis was considered to be supported.

5.1 Further NaOH Storage Considerations

As stated at the end of chapter 4, the 0.1 NaOH solution looks like a promising means of storage and delivery of the SBH. A few issues must be addressed before this means of storage may be utilized. One issue is that the 0.1 molar solution did show some reaction. This may actually be a significant benefit, however, because it will help balance the pressure on both sides of the valve and help prevent hydrogen rushing from the reactor area to the storage areas when the valves are opened to deposit reactants. Another potential issue with NaOH and water as a means of storage is the basicity of the solution. Since a basic solution hinders the reaction rate, acid would need to be added to the reactor to neutralize the base. This could easily be achieved by adding the appropriate amount of acid to the EG such that every dose of EG added to the reactor has enough acid to neutralize the amount of NaOH added with the water. This means of storage would require the EG be stored separately from the water and added in equal volume to keep the effective 50% weight solution, so adding acid to the EG would be quite simple. There is a safety concern for this, however, in that acid is a known accelerant for the hydrolysis and alcoholysis of SBH. There could be an unsafe acceleration of reaction when the ethylene glycol and acid mixture is first introduced to the reactor. This will need to be further explored to ensure the setup is safe.

5.2 Future Model Considerations

Despite the model showing the heat provided by the simple running of the setup is sufficient to keep the environment warm, it will still be necessary to create the setup with process control that allows the ethylene glycol and acid mixture to be added any time the fuel cell or reactor get below 280 K to prevent freezing of the fuel cell membrane. This may require an additional amount of reactants be added at the beginning of the week, or it may necessitate a signal being sent to the operators to replenish the reactants sooner than initially planned. It is noteworthy, however, that no solid precipitate was observed during rate of reaction tests. If this precipitate is pH dependent, adding the extra ethylene glycol and acid may cause a crust to form and prevent mixing of the reactants. pH dependency on rate and solubility will need to be further examined before this process control can be created.

Another process consideration that needs to be addressed before this can be created is the amount of reactant addition necessary to maintain the desired rate of reaction. This amount would vary dependent on temperature and amount of reactant and product already present in the reactor, so this would need to be modeled and experiments run for it. Similarly, the time required to dispense the reactants will need to be determined before the valve opening can be coded into a program to run autonomously. The time that the valve must be open to dispense the appropriate reactants would likely be dependent on amount of reactants remaining due to pressure differences caused by changes in fluid height, so this would likely require a significant set of experiments to test before this model and code could be created.

5.3 Safety Considerations

There is significant concern that the heat of reaction could cause the temperature to rise high enough that there would be risk of a runaway reaction. Pressure and temperature settings and limits would need to be created and evaluated before this setup could be used. The storage consideration appears to present a potential built in safety mechanism, however. Were the water and NaOH mixture added without adding the EG and acid, the excess base could potentially stunt the reaction significantly, in addition to cooling it down. This safety issue will be especially pertinent in warmer weather. It could be that warmer weather necessitates keeping the solution in the reactor slightly basic to keep the reaction rate lower overall, assuming the pH variance didn't create physical barriers to the reaction proceeding properly, as mentioned in section 5.2.

5.4 The Final Step

Once everything is coded and setup, the ability of the fuel cell to be run autonomously would need to be tested. Essentially, the physical device needs to be setup once it has been validated that the setup designed in the initial prototype can be run in Duluth's beautiful and brisk winters. This would be one more step toward using energy produced without emissions, especially that produced without the production of carbon dioxide.

Bibliography

[1] Brigham Young University, “Public Database - DIPPR801,” 2019. [Online]. Available: https://dippr.aiche.org/FullDb. [Accessed: 18-Jun-2019].

[2] “H-100 Fuel Cell Stack User Manual.”

[3] J. T. Henry, *The early and later history of petroleum :with authentic facts in regard to its development in western Pennsylvania ... the Parkers’ and Butler County oil fields; also, life sketches of pioneer and prominent operators, with the refining capacity of the Un*. Philadelphia: New York :, 1873.

[4] William Robert Grove, “On the Gas Voltaic Battery. Voltaic Action of Phosphorus, Sulphur, and Hydrocarbons,” pp. 557–558.

[5] L. J. Nuttal and L. R. Stevens, “Test of Gemini Fuel Battery Section,” 1965.

[6] J. M. Andújar and F. Segura, “Fuel cells: History and updating. A walk along two centuries,” *Renew. Sustain. Energy Rev.*, vol. 13, no. 9, pp. 2309–2322, 2009.

[7] Smithsonian Institution, “Collecting the History of Proton Exchange Membrane Fuel Cells,” 2004. [Online]. Available: https://americanhistory.si.edu/fuelcells/pem/pemmain.htm. [Accessed: 18-Jun-2019].

[8] S. Sternberg, A. R. Hasan, and V. Mereddy, “A Prototype System for Chemical Hydrogen Generation and Storage for Operating ITS Devices,” Duluth, 2013.

[9] D. Langmuir, P. Chrostowski, B. Vigneault, and R. Chaney, “Issue Paper on the Environmental Chemistry of Metals (corrected reference on 1/25/05),” 2046.

[10] “Lab Equipment and Lab Supplies | Fisher Scientific.” [Online]. Available: https://www.fishersci.com/us/en/home.html?gclid=CjwKCAjw-ITqBRB7EiwAZ1c5Ux1VvqUR20gEvA6BLlKYpkAcjzHroiQj8g0dSSkFSkNTVvpNtWAJ6BoC8UgQAvD_BwE&cid=SEM_GAW_20190715_1N8MYH&ppc_id=FisherSciBrand_goog_979894225_47449837574_fischer scientific_e_232169621685_18. [Accessed: 31-Jul-2019].

[11] H. Ould-Amara, D. Alligier, E. Petit, P. G. Yot, and U. B. Demirci, “Sodium borohydride and propylene glycol, an effective combination for the generation of 2.3 wt% of hydrogen,” *Int. J. Hydrogen Energy*, vol. 43, no. 15, pp. 7237–7244, 2018.

[12] B. G. W. Kemp, “The Second Kemp Process for the Use and Reuse of Sodium Borohydride as a Solid State Hydrogen Storage Medium,” no. 4, pp. 11–12, 2018.

[13] F. Barbir, “Fuel Cell Basic Chemistry and Thermodynamics,” *PEM Fuel Cells*, pp. 17–32, 2007.

[14] Y. Haseli, “Maximum conversion efficiency of hydrogen fuel cells,” *Int. J. Hydrogen Energy*, vol. 43, no. 18, pp. 9015–9021, 2018.

[15] “Multimedia: The Water Displacement Method | Chapter 3, Lesson 2 | Middle School Chemistry.” [Online]. Available:

https://www.middleschoolchemistry.com/multimedia/chapter3/lesson2. [Accessed: 13-Aug-2019].

[16] “Ready-Made Insulated Thermocouples | Omega Engineering.” [Online]. Available: https://www.omega.com/en-us/sensors-and-sensing-equipment/temperature/sensors/thermocouple-probes/5tc/p/5TC-TT-J-40-72. [Accessed: 18-Aug-2019].

[17] “Pressure Transducer 0-15PSIG MV/V, +/-0.20%, 1/4-18 NPT Male, Cable (2m, 6ft), CE MARK (no charge).” [Online]. Available: https://www.omega.com/en-us/sensors-and-sensing-equipment/pressure-and-strain/pressure-transducers/p/MMG015V1P4C0T4A5CE. [Accessed: 18-Aug-2019].

[18] “CompactDAQ Chassis - National Instruments.” [Online]. Available: http://www.ni.com/en-us/shop/select/compactdaq-chassis. [Accessed: 18-Aug-2019].

[19] “Lithium-Ion Battery 12V - 7.5Ah - 96Wh - PowerBrick+ / LiFePO4 battery.” [Online]. Available: https://www.powertechsystems.eu/home/products/12v-lithium-battery-pack-powerbrick/7-5ah-12v-lithium-ion-battery-pack-powerbrick/. [Accessed: 18-Aug-2019].

[20] National Instruments, “What is LabVIEW?” [Online]. Available: https://www.ni.com/en-us/shop/labview.html. [Accessed: 18-Aug-2019].

[21] R. A. Davis, *Practical Numerical Methods for Chemical Engineers*. 2013.

[22] J. Zhang, T. S. Fisher, J. P. Gore, D. Hazra, and P. V. Ramachandran, “Heat of reaction measurements of sodium borohydride alcoholysis and hydrolysis,” *Int. J. Hydrogen Energy*, vol. 31, no. 15, pp. 2292–2298, 2006.

[23] “Snoop Liquid Leak Detector | Swagelok | Swagelok.” [Online]. Available: https://www.swagelok.com/en/product/Leak-Detectors-Lubricants-Sealants/Snoop-Liquid-Leak-Detector. [Accessed: 21-Aug-2019].

[24] H. S. Fogler, *Elements of Chemical Reaction Engineering*, Fifth. Pearson, 2016.

[25] Engineering Toolbox, “Convective Heat Transfer.” [Online]. Available: https://www.engineeringtoolbox.com/convective-heat-transfer-d_430.html. [Accessed: 27-Aug-2019].

[26] D. W. Mackowski, “Conduction Heat Transfer Notes for MECH 7210.”

[27] J. Goldade, T. Haagenson, H. Salehfar, and M. Mann, “Design of a laboratory experiment to measure FC stack efficiency and load response,” *ASEE Annu. Conf. Expo. Conf. Proc.*, 2010.

[28] Y. Shang and R. Chen, “Thermodynamic study on the solubility of NaBH4 and NaBO 2 in NaOH solutions,” *SAE Tech. Pap.*, 2011.

Appendix A: Supplementary Materials

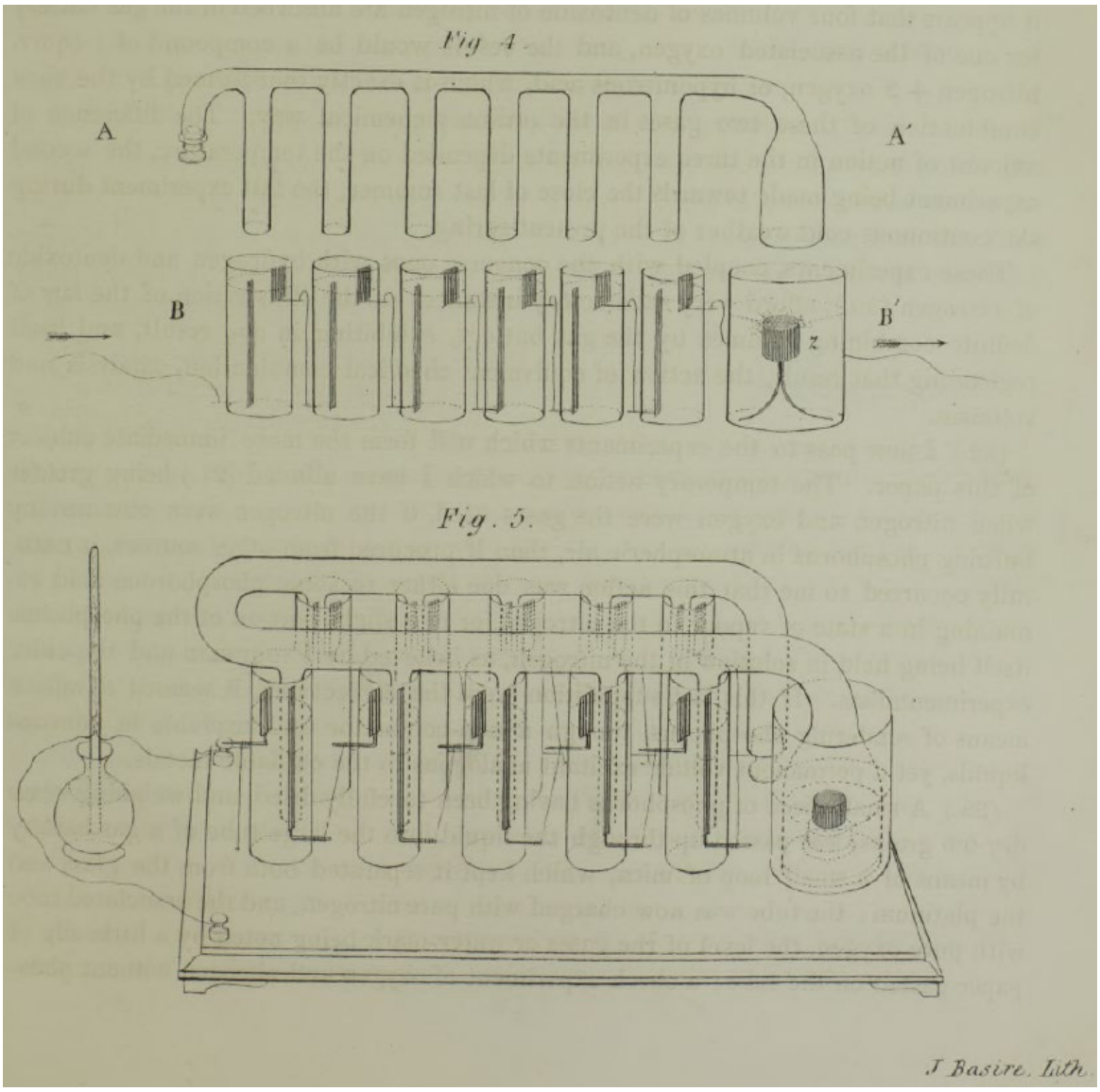

Figure A-1 Grove's Hypothetical Fuel Cell Setup

(53.) The results embodied in my present and my former paper, I think sufficiently indicate the field of research opened by the gas battery, a field which may of course be indefinitely extended. I have never thought of the gas battery as a practical means of generating voltaic power, though in consequence of my earlier researches, which terminated in the nitric acid battery, having had this object in view, I have been deemed by some to have proposed the gas battery for the same purpose; there is, however, a form of gas battery which I may here describe, which, where continuous intensity or electromotive force is required, but the quantity of electricity is altogether unimportant, appears to me to offer some advantages over any form of battery hitherto constructed, and which, independently of any practical result, is, from circumstances peculiar to the gas battery, not without interest. It is shown at figs. 4 and 5. A A′ is a long glass tube, with a series of legs or glass tubes attached to and opening into it; the lower extremities of these are open, and the main tube or channel A A′ terminates at the extremity A in a glass stopper, and at A′ opens out into a funnel, as shown in the figure. Into a series of glasses B B′ are cemented platinum wires having attached to them strips of platinized platinum foil, two to each glass, the one being four inches long and half an inch wide, the other $1\frac{1}{2}$ inch long by one inch wide; the former set are placed lower than the latter, so that when the glasses are filled with liquid the former set shall be just covered, and the latter bisected by the water-mark; the last glass B has no platinum. These platinum strips are connected metallically by external wires, the narrow platinum of one cell with the wide one of the next, and so on in series. The glasses having been filled to the top of the narrow platinum with acidulated

Figure A-1 Grove's Explanation of his Hypothetical Zinc Fuel Cell Setup

water, let a piece of zinc be placed on a pedestal in the vessel B, and the stopper being out of the extremity A, the apparatus A A′ lowered into the glasses, the tubular legs covering each one of the narrow platinum plates. The tubes will of course be full of water, and the main channel full of atmospheric air; this will gradually be displaced by the hydrogen ascending from the zinc, which hydrogen, in consequence of the curve at A, will retain its position. When it is judged that the greater portion of air has been expelled, the stopper at A, covered with a little grease, is to be inserted; the hydrogen now will rapidly descend in all the tubes until the zinc is laid bare, and then remain stationary.

We have now a gas battery, the terminal wires of which will give the usual voltaic effects, the atmospheric air supplying an inexhaustible source of oxygen, and the hydrogen being renewed as required by the liquid rising to touch the zinc; by supplying a fresh piece of zinc when necessary, it thus becomes a self-charging battery, which will give a continuous current; no new plates are ever needed, the electrolyte is never saturated, and requires no renewal except the trifling loss from evaporation, which indeed is lessened, if the battery be in action, by the newly composed water. There is an aperture in the pedestal with a moveable slide, through which the vessel B′ can be removed, when necessary, to replace the zinc, and the remaining part of the apparatus is never disturbed. This battery would form an elegant substitute for the water battery; it would much exceed in intensity a similar number of series of that apparatus; it would be applicable to experiments of slow crystallization and possibly to the telegraph. Its construction is difficult and makes its prime cost expensive, but after that it is the most durable, the most easily charged, and the most free from local action of any known form. I have had one of ten cells constructed, shown at fig. 5, which succeeds perfectly, giving sparks, decomposing water, &c., and is ever ready for use. Any number of such sets might be united by adapter-tubes; or indeed it would be much more economical, and reduce to a minimum the damage from breakage, to have the main channels A A′ made of varnished wood or porcelain, with apertures into which separate glass tubes might be cemented.

Figure A-2 Continued

4. Technical Specification

Type of fuel cell	PEM
Number of cells	20
Rated Power	100W
Performance	12V @8.3A
H2 Supply valve voltage	12V
Purging valve voltage	12V
Blower voltage	12V
Reactants	Hydrogen and Air
External temperature	5 to 30°C
Max. stack temperature	65°C
H2 Pressure	0.45-0.55bar
Hydrogen purity	≧99.995% dry H2
Humidification	self-humidified
Cooling	Air (integrated cooling fan)
Stack weight (with fan & casing)	1290 grams(±50grams)
Controller weight	400 grams(±30grams)
Dimension	11.8cm x 10.4cm x 9.4cm
Flow rate at max output*	1.3 L/min
Start up time	≦30S at ambient temperature
Efficiency of stack	40% @ 12V
Low voltage shut down	10V
Over current shut down	12A
Over temperature shut down	65℃
External power supply**	13V (±1V), 5A

** The flow rate may change with the power output.*
*** System electronics need external power supply.*
**** The Specification is subject to change without notice.*

Figure A-2 Horizon Fuel Cell Specifications

Figure A-3 Experimental Setup for HFC Efficiency Model

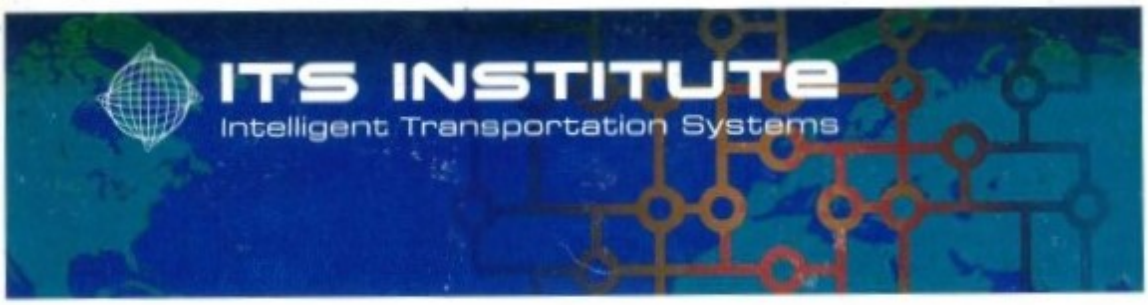

A Prototype System for Chemical Hydrogen Generation and Storage for Operating ITS Devices

Final Report

Prepared by:

Steven P. Sternberg
A. Rashid Hasan

Department of Chemical Engineering

Venkatram R. Mereddy

Department of Chemistry and Biochemistry

Northland Advanced Transportation Systems Research Laboratories
University of Minnesota Duluth

CTS 13-11

CENTER FOR TRANSPORTATION STUDIES UNIVERSITY OF MINNESOTA

Technical Report Documentation Page

1. Report No.	2.	3. Recipients Accession No.
CTS 13-11		

4. Title and Subtitle	5. Report Date
A Prototype System for Chemical Hydrogen Generation and Storage for Operating ITS Devices	April 2013
	6.

7. Author(s)	8. Performing Organization Report No.
Steven P. Sternberg, A. Rashid Hasan, and Venkatram R. Mereddy	

9. Performing Organization Name and Address		10. Project/Task/Work Unit No.
Department of Chemical Engineering University of Minnesota Duluth 1303 Ordean Court Duluth, MN 55812	Department of Chemistry and Biochemistry University of Minnesota Duluth 1110 Kirby Drive Duluth, MN 55812	CTS Project #2012018
		11. Contract (C) or Grant (G) No.

12. Sponsoring Organization Name and Address	13. Type of Report and Period Covered
Intelligent Transportation Systems Institute Center for Transportation Studies University of Minnesota 200 Transportation and Safety Building 511 Washington Ave. SE Minneapolis, Minnesota 55455	Final Report
	14. Sponsoring Agency Code

15. Supplementary Notes

http://www.its.umn.edu/Publications/ResearchReports/

16. Abstract (Limit: 250 words)

This research project sought to develop a prototype hydrogen-based fuel cell system for ITS devices. The project investigated hydrogen storage capacities of the various candidate chemical hydride analogs; selected the most efficient of the candidates for energy storage based on volume, mass, and cost; developed a prototype system; and estimated the capital and operating cost for such a system.

A hydrogen fuel cell combines hydrogen and oxygen to produce electricity, providing a clean, high-efficiency energy source that circumvents the problems associated with conventional batteries. A major drawback that limits its utility, however, is the use of heavy and bulky compressed metal cylinders as the source of hydrogen. The chemical-based hydrogen generation used in this project can provide a compact, atmospheric-pressure storage option for the controlled release of hydrogen. Many ITS-based applications can be envisaged with hydrogen-based fuel cells, such as alternating-traffic signs, directional signals, speed-limit signs, blinkers in series, warning blinkers, and backup power sources at traffic signals during power outages. This system is particularly attractive because many remote traffic signals on northern Minnesota roads lack access to a power grid, requiring the use of batteries that must be changed often, thus incurring maintenance costs.

17. Document Analysis/Descriptors	18. Availability Statement
Off-grid power, Fuel cells, Hydrogen power, Hydrides, Hydride chemistry	No restrictions. Document available from: National Technical Information Services, Alexandria, Virginia 22312

19. Security Class (this report)	20. Security Class (this page)	21. No. of Pages	22. Price
Unclassified	Unclassified	50	

A Prototype System for Chemical Hydrogen Generation and Storage for Operating ITS Devices

Final Report

Prepared by:

Steven P. Sternberg
A. Rashid Hasan

Department of Chemical Engineering

Venkatram R. Mereddy

Department of Chemistry and Biochemistry

Northland Advanced Transportation Systems Research Laboratories
University of Minnesota Duluth

April 2013

Published by:

Intelligent Transportation Systems Institute
Center for Transportation Studies
University of Minnesota
200 Transportation and Safety Building
511 Washington Ave. S.E.
Minneapolis, Minnesota 55455

The contents of this report reflect the views of the authors, who are responsible for the facts and the accuracy of the information presented herein. This document is disseminated under the sponsorship of the Department of Transportation University Transportation Centers Program, in the interest of information exchange. The U.S. Government assumes no liability for the contents or use thereof. This report does not necessarily reflect the official views or policies of the University of Minnesota.

The authors, the University of Minnesota, and the U.S. Government do not endorse products or manufacturers. Any trade or manufacturers' names that may appear herein do so solely because they are considered essential to this report.

Acknowledgments

The authors wish to acknowledge those who made this research possible. The study was funded by the Intelligent Transportation Systems (ITS) Institute, a program of the University of Minnesota's Center for Transportation Studies (CTS). Financial support was provided by the United States Department of Transportation's Research and Innovative Technologies Administration (RITA).

The project was also supported by the Northland Advanced Transportation Systems Research Laboratories (NATSRL), a cooperative research program of the Minnesota Department of Transportation, the ITS Institute, and the University of Minnesota Duluth College of Science and Engineering, departments of Chemistry and Chemical Engineering.

Table of Contents

List of Tables

List of Figures

Executive Summary

This project explores the development of a power source that is independent of the power-grid, does not need frequent recharging, can work in cold weather, and is dependable. In particular, the project explores the use of a hydrogen powered fuel cell for constant, local charging of a battery pack. The battery pack would be much smaller than a battery-only system since the power storage medium is hydrogen and the waste heat from the fuel cell can be used to keep the system warm. This project proposed research to develop a reliable H_2-based portable power system that can be used to operate various traffic systems including DSRC-based wireless applications, variable message signs, traffic sensors, and intersection traffic signals. The primary goals of this project are to: (1) investigate the hydrogen storage capacities and operational safety of the various candidate chemical hydrides, (2) further develop a short listing of an appropriate candidate chemical hydride, (3) develop a prototype system, and (4) estimate the capital and operating cost for such a system.

Results for this project include:

1) Several hydrogen generating materials were investigated. The most promising consisted of the alkali-hydrides and -borohydrides. An ammonia borohydride was also explored.

2) The selection of a hydrogen generating reaction system was based on the ability to control the reaction such that it produced hydrogen at approximately the rate at which it would be consumed by the fuel cell, that the reaction would work between temperatures of -40 °C to 30 °C, that the reactants would be inherently safe to humans and the environment, and be inexpensive. The system chosen uses sodium borohydride combined with a 50/50 mixture of ethylene glycol and water. A small amount of acetic acid can be added to accelerate the reaction at colder temperatures. In a late addition to the project, tartaric acid was explored as an alternative to acetic acid. This acid provided better control of the reaction at higher temperatures (above 0°C).

Results of our work show that we were able to successfully produce hydrogen at temperatures as low as -50°C. However, the production rate was significantly slowed at temperatures lower than -40°C. The yield of hydrogen was observed to be >90% for temperatures between 25°C to -20°C, and at -40°C, the yield was observed to be ~80%.

3) A prototype reactor was designed and constructed. This system provides a 20 watt, 12 volt load with electricity for one week using 2.5 pounds of sodium borohydride and one gallon of the liquid mixture. Potential problems not addressed in this report include water / ice buildup within the equipment enclosure, hydrogen release during refueling, and unintended buildup of hydrogen within the equipment enclosure due to unknown leakages.

4) The cost of the prototype system was approximately $7,500. Costs of fuel materials for operation will be approximately $35 /week or about $2,000 / year.

Chapter 1. Introduction

Intelligent Transportation System (ITS) technologies advance transportation safety and mobility and enhance American productivity by integrating advanced communications technologies into transportation infrastructure and into vehicles. ITS devices encompass a broad range of wireless and traditional communications-based information and electronic technologies. They are used to measure, collect, analyze, and inform users of transportation services. For roadway transportation this may mean monitoring traffic and speed, warning drivers of changes in traffic conditions, and collecting information needed to enhance use of or re-design of existing infrastructure. The monitors, sensors, and communication equipment needed to do this require electricity. In urban areas this rarely presents a problem as grid power sources are generally widely available or easy to bring to a site. In rural areas it may be miles between power grid locations, limiting the use and deployment of ITS devices. These off-grid locations could be used if there was a reliable, inexpensive, all-weather alternative power source. Typical off-grid power sources include battery packs or diesel generators. However, these sources require constant maintenance to recharge/ replace batteries or to refuel generators. The frequency of such trips can be daily. If a site is far from a maintenance area, the trip may require multiple hours for the maintenance crew. An additional issue in Northern Minnesota is the winter weather (snow, ice) and cold temperatures (-30 to -40 °F at night) both of which can greatly reduce the efficiency and up-time of these power sources.

This project explores the development of a power source that is independent of the power-grid, does not need frequent recharging, can work in cold weather, and is dependable. In particular, the project explores the use of a hydrogen powered fuel cell for constant, local charging of a battery pack. The battery pack would be much smaller than a battery-only system since the power storage medium is hydrogen and the waste heat from the fuel cell can be used to keep the system warm. This project proposed research to develop a reliable hydrogen (H_2)-based portable power system that can be used to operate various traffic systems including (DSRC)-based wireless applications, variable message signs, traffic sensors, and intersection traffic signals. The primary goals of this project are to: (1) investigate the hydrogen storage capacities and operational safety of the various candidate chemical hydrides, (2) further short listing of an appropriate candidate chemical hydride, (3) develop a prototype system, and (4) estimate the capital and operating cost for such a system.

Results for this project include the selection of a reactor system for generating hydrogen at temperatures between -40 °C to 30 °C: sodium borohydride combined with a 50/50 mixture of ethylene glycol/ water with a small amount of acetic acid to accelerate the reaction at colder temperatures. Also, a prototype reactor was designed and constructed. This system will provide a 20 watt, 12 volt load with electricity for one week using 5 pounds of sodium borohydride and one gallon of the liquid mixture. Potential problems not addressed in this report include water / ice buildup within the equipment enclosure, hydrogen release during refueling, and unintended buildup of hydrogen within the equipment enclosure due to unknown leakages. The cost of the prototype system is approximately $7,500. Costs of materials for operation are approximately $35 /week or about $2,000 / year.

Chapter 2. Background

There are several electric power choices for off-grid applications. The main considerations for this project are portability, cold weather suitability, and safety. This project requires the power source to be easily transported for deployments of a few days to several months and that it not endanger maintenance workers or the public. The main commercially available choices for this equipment are battery packs and diesel engines. Alternative equipment includes solar power, wind turbines, and fuel cells. These alternatives are just beginning to be commercialized and offer several potential advantages over battery packs or combustion engines. In this chapter we will briefly discuss each of these technologies and look at their utility for off-grid power supplies for Intelligent Transportation Systems (ITS) devices.

Battery Pack

A battery pack is a set of any number of (preferably) identical batteries or individual battery cells. They may be configured in a series, parallel or a mixture of both to deliver the desired voltage, capacity, and power density. The components of a battery pack include the individual batteries or cells and the interconnects which provide electrical conductivity between them. Rechargeable battery packs usually contain a temperature sensor, which the battery charger uses to detect the end of charging. Interconnects are used to connect each cell in either a series or parallel connection. Battery regulators are used to keep the peak voltage of each individual battery or cell below its maximum value so as to allow weaker batteries to be fully charged, bringing the whole pack back into balance. A well-balanced pack lasts longer and delivers better performance, (Engineering.com, 2013).

The main advantages of battery packs are that they are portable, so they can be swapped into and out of any device. This allows the pack to be charged at a central location, while a replacement pack is used to power the device. Battery packs can be added together to obtain higher power or to last longer. A small device (sensor, communication) may be able to be run for a week from a battery pack, whereas a larger, more energy intensive device (lighting) may need to have the batteries replaced daily. A user would need approximately twice as many battery packs as devices so that one set is charging while the other pack is being used.

The main disadvantages of battery packs are their cycle life and their reduced efficiency in cold weather. Batteries have a cycle life, which could also be described as the number of times it may be recharged. The typical range is 200 – 1000 cycles, depending on usage environment and maintenance level of the battery equipment. Batteries have a working temperature range of -20 °F to 60 °F. The temperature will also control the charging and discharge rate. Batteries need more frequent recharging in colder weather (or need to be that much larger). Batteries cannot be charged if they are cold (<20 °F), but will recover if they are heated. Indeed, some battery pack systems include a battery warming circuit which uses electricity from the battery in a heating resistor.

The performance of all battery chemistries drops drastically at low temperatures. At –20°C (–4°F) most nickel-, lead- and lithium-based batteries stop functioning. Specially built Li- ion brings the operating temperature down to –40°C, but only on discharge and at a reduced

discharge. Lead acid batteries have the danger of the electrolyte freezing, which can crack the battery casing. Cold temperature also increases the internal resistance and diminishes the capacity. Batteries that would provide 100 percent capacity at 27°C (80°F) will typically deliver only 50 percent at –18°C (0°F). The capacity decrease is linear with temperature. Batteries achieve optimum service life if used at temperatures of 20°C (68°F) or slightly below.

Table 1: Rechargeable battery characteristics.

Battery Type	Whr/kg	Joules/g	Whr/liter	$/Whr
Lead-acid	41	146	100	0.17
Alkaline long-life	110	400	320	0.19
Carbon-Zinc	36	130	92	0.31
NiMH	95	340	300	0.99
Ni-Cd	39	140	140	1.50
Lithium-ion	128	460	230	0.47

Diesel and Biofuel Generators

Diesel engines are a well-developed technology. A quality unit starts at around $10,000 and is capable of running full time. The limitations are need for constant refueling, fuel efficiency, and equipment maintenance. Fuel tanks start at 20 gallons and can be considerably larger. The engine and generator can produce electricity at levels starting at 10,000 watts. Equipment is about 3' x 3' x 2' and larger if given a weather resistant enclosure. Fuel usage is typically 0.5 to 1.0 gallons per hour, so they require daily refueling (including holidays and weekends). Basic maintenance requires oil and filter changes every 500 hours (every three weeks). Typically these maintenance activities are done in a central shop, so the unit must be transported to and from the shop to work site. This is a great choice for short term applications that require 1000+ Watts, such as lighting. Winter weather tends to decrease efficiency and increase maintenance requirements. Weight starts at 500 – 1000 lbs, which requires the engine be mounted on a trailer. Typical cost of fuel is 0.0004$/Wh. This does not include cost of routine maintenance and replacement of oil and air filters, which can double or triple the cost depending on distance it must be transported for the maintenance. For small electric loads this choice is not economical due to the large size and initial cost of the equipment, (Wikipedia, Diesel Engine, 2013).

Solar Panels

A solar panel is a packaged assembly of solar cells, electricity inverter, a battery, perhaps solar tracking hardware, and a mounting system. The solar cells directly convert sunlight into electricity. The inverter is used to correct the voltage to a single value. It is needed because the voltage output (and power) will vary with solar intensity and time of day. Time of day effects can be partially offset by solar tracking hardware. Solar tracking allows the panel to always be perpendicular to the sun's rays. The mounting system holds the panels in place and is used to locate the panels above surrounding buildings and vegetation, (Wikipedia, Solar Panel, 2013).

Solar panels work when light, in the form of photons, hits the solar cell. If the photon has sufficient energy it can energize a single electron. This creates an electron-hole pair within the cell. The electron is prevented from rejoining the hole due to the inherent electric field in the

solar cell. These electrons can be collected on one side of the solar cell and then routed through a load and back to the solar cell's other side where the electron holes have collected. The electron flow provides current, and the cell's electric field causes a voltage. With both current and voltage, power is created, which is the product of the two. The actual voltage output of the panel changes as lighting, temperature and load conditions change, so there is never one specific voltage at which the panel operates. The panel is sized by its nominal voltage. Nominal voltage refers to the voltage of the battery that the package is best suited to charge, and it is a semi-empirical quantity.

Obviously solar panels only work during the daytime. These systems require a charged battery to work at night. The panel must be sized large enough to provide for the power requirements of the device plus enough to charge the battery to provide power until the next day. This size would need to be 3 - 4 times the daytime size to account for the reduced daylight available in winter. Batteries may return 70% of the incoming energy as electricity; the rest is unavoidably expended as heat due to thermodynamic constraints. Most batteries cannot be fully recharged if the temperature is below 20°F. Cold weather applications must provide for heating of the battery, which in turn uses more of the stored energy which requires larger solar panels and a larger battery pack to store the charge.

While this system is similar to the battery packs described above, the battery pack is smaller or can be swapped out less frequently. The system can even send out a signal to warn that its batteries are getting too low in reserve power and may need to be serviced. This would happen during periods with overcast skies, when the solar panels are dirty or get covered in snow or ice. Also in the winter there is less light, and the cold temperatures will cause the batteries to have slower recharge and quicker drain. Any of these conditions will require maintenance personal to visit the site more frequently.

The cost of solar panels is decreasing because they are becoming more efficient and less expensive to manufacture. The battery is typically the main capital expense, and these systems may soon become less expensive than the battery-only system, if only because of fewer maintenance visits to recharge the batteries. The solar panel system works well in summer time in Minnesota, but performs poorly in winter.

Wind Turbines

Another potential method for generating off-grid power is the wind turbine. These systems consist of a turbine, a battery pack for low wind time periods, inverter to correct voltage to a single value, and a tower upon which the turbine is mounted. The turbine converts wind motion into mechanical motion (rotating fan blades) which is then converted into electricity This system, like the solar panels, will require a battery pack. The system needs energy storage for when wind speeds are too low to generate electricity (< 8 mph), although the required battery would be smaller in size than the battery-only option. A typical installation would require a 50 to 100 foot tower with a rotor diameter of about 5 to 20 feet. The size of the equipment, especially the tower, and the previous mentioned battery recharge in cold temperature issues make this system unadvisable for cold weather, portable, ITS applications (Wikipedia, Wind Turbine, 2013).

Fuel Cells

A fuel cell is a device that converts chemical energy into electricity. The fuel cell uses a chemical reaction that typically involves a hydrocarbon fuel and oxygen. Hydrogen gas is the most common fuel, although natural gas or methanol can also be used. Fuel cells work almost the same as a battery, except the fuel cell requires the addition of external reactants (fuel and oxygen) rather than storing them completely within the battery. Indeed, fuel cells have been called gas batteries. They may also produce electricity for much longer time periods – as long as the reactants are provided in sufficient quantity (Wikipedia, 2012), (Barbir, 2005).

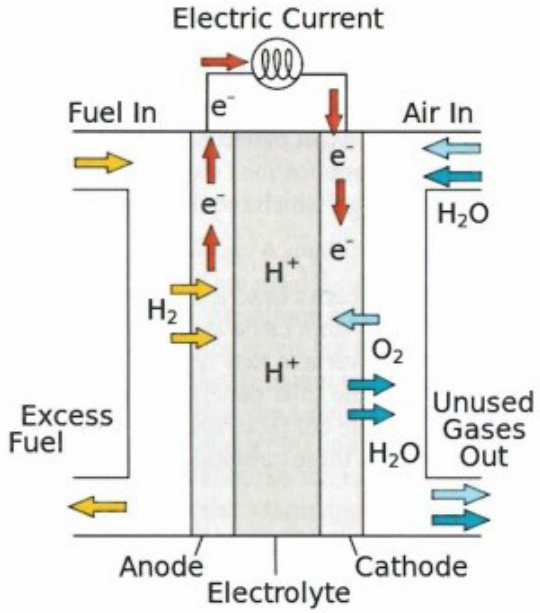

Figure 1: Schematic of a Fuel Cell [(Wikicommons, 2007)].

There are several types of fuel cells. All types consist of an anode, a cathode, and an electrolyte which allows charges to move between the electrodes (Larminie, et al., 2003). Electrons are drawn from the anode to the cathode through the external circuit as direct current (DC) electricity. The main difference between types of fuel cells is the electrolyte. Fuel cells are capable of converting approximately half of the chemical energy into electricity, with the remaining energy converted to heat. Fuel cells also produce standard combustion products for the fuel that is used – typically water and carbon dioxide.

A hydrogen fuel cell uses a catalyst (platinum) at the anode to convert the hydrogen atom into a hydrogen ion (bare proton) and an electron. The electrolyte which connects the anode to the cathode allows the positively charged proton to pass and it prevents the electron from moving through it. If an external circuit is provided, the electron may pass through it to travel to the cathode. A second catalyst (nickel) is used at the cathode to combine the electron, proton and oxygen to create water and heat, which drives the mass transfer potential by converting and removing the protons. The most widely used fuel cell for portable applications uses hydrogen at

ambient conditions in a proton exchange membrane (PEM). The membrane is a polymer material that does not conduct electricity but allows protons to diffuse through it.

Major concerns with PEM fuel cells are water/ air management and temperature management. The fuel cell requires that the electrolytic membrane be sufficiently hydrated. Too little water will reduce the proton mobility, increasing resistance and reducing efficiency. Too much water will flood the cell and prevent the mass transfer of oxygen to the cathode which also reduces / stops the cell from functioning. Temperature management must be used to maintain the same temperature throughout the cell in order to prevent destruction of the cell through thermal loading. This is particularly challenging as the hydrogen combustion reaction is highly exothermic, so a large quantity of heat is generated within the fuel cell. Both concerns are addressed by having a controlled fan on the cathode side to draw off water and heat. The fan uses the fuel cell as its power source and uses a calibrated power curve and temperature measurement to determine when the fan should be run.

Fuel cells are not as efficient as batteries, but do have the potential to augment batteries by reducing the need to exchange/ replace batteries. They also supply heat which can keep the battery operating at a high efficiency even in cold weather. Professor Jeremy P. Meyers, (Meyers, 2008) wrote, "While fuel cells are efficient relative to combustion engines, they are not as efficient as batteries, due primarily to the inefficiency of the oxygen reduction reaction (and ... the oxygen evolution reaction, should the hydrogen be formed by electrolysis of water). ... [T]hey make the most sense for operation disconnected from the grid, or when fuel can be provided continuously. For applications that require frequent and relatively rapid start-ups ... where zero emissions are a requirement, as in enclosed spaces such as warehouses, and where hydrogen is considered an acceptable reactant, a [PEM fuel cell] is becoming an increasingly attractive choice [if exchanging batteries is inconvenient]".

Fuel cell advantages include their efficiency, size, and safe operation. A PEM fuel cell can convert approximately 30-50% of the fuel chemical energy into electricity, with the remainder forming heat. The electricity can be used to charge a battery, which is used to power any electrical load requiring DC power (or AC power if a power inverter is used). The heat generation can be used to keep the battery and auxiliary equipment warm. The incoming air will also need to be heated to prevent temperature changes from damaging the fuel cell. The size of a fuel cell is quite small, a 100 W system is the size of a brick, and a 1 kW system is about the size of a small laptop computer. The system size will depend on what other equipment is needed: battery pack, power inverter, measurement and control hardware, air pre-conditioning (a heat exchanger for controlling air temperature and an adsorption column to remove contaminants), and a hydrogen source. The battery pack is used to smooth the power supply and to cover peak loads. Fuel cells are quick to adapt to power changes, but are not instantaneous devices - requiring several seconds to respond to power changes. The power inverter is used to supply the proper type of electricity to the load (voltage, AC or DC). Measurement and control hardware are used to keep the system operating at high efficiencies. These include temperature and moisture levels in the fuel cell which are used to control the fuel cell fan, pressure device to monitor and control fuel input to the fuel cell, and hydrogen sensor to monitor for safety within the system. Air pre-conditioning is used to maintain a steady air inlet temperature to prevent thermal stresses within the fuel cell. This is especially important for winter conditions. Also, certain contaminants in the air could damage the fuel cell: particulate matter, carbon monoxide,

nitrogen oxides, and sulfur oxides could all cause problems. Each of these is associated with road traffic so some sort of filter may be needed to remove /reduce these contaminants from the inlet air stream. The hydrogen source is the main variable consideration for this project, see next chapter on hydrogen fuel.

Fuel cell disadvantages mainly center on the fact that it is a new technology: slow start-up times, low power output, sluggish response on power demand, poor loading capabilities, narrow power bandwidth, short service life and high cost. Similar to batteries, the performance of all fuel cells degrades with age, and the stack gradually loses efficiency. The relatively high internal resistance of full cells also poses a challenge. Each cell of a stack produces about one volt when in open-circuit condition, and a heavy load causes a notable voltage drop. Fuel cells operate best at a 30 percent load factor; higher loads reduce efficiency. A load factor approaching 100 percent, as is common with a battery, is not practical with the fuel cell. In addition, the fuel cell has poor response characteristics and takes a few seconds to react to power demands. This requires that the fuel cell provides a support function to a master battery, whereby the fuel cell provides the charge duty. This relationship enables both parts to deliver continuous service.

Chapter 3. Hydrogen Storage

Hydrogen is very abundant on earth, however very little hydrogen exits as the gas H_2. Instead hydrogen is chemically bound in other molecules. Hydrogen exists in water (H_2O), natural gas (CH_4) or other hydrocarbons (oil and coal), and many minerals. In order to use the hydrogen as fuel it must be chemically converted to generate the gas form (H_2). Once the hydrogen has been generated it may be used, stored for later use, or transported to the fuel using device.

There are many ways in which hydrogen can be stored for use in a fuel cell: ambient gas, compressed gas, liquefied gas, or a hydrogen compound, [(Puru, 2011), (Mandal, 2009), (Klebanoff, 2010), (V. Pe´rez-Herranz, 2010)]. This last form requires the compound to be transformed into hydrogen before use within the fuel cell device.

Ambient Gas

This is the easiest to use form, but it is also the least dense, containing only 1 mol in 22.5 liter, or 0.09 g/liter. This is equivalent to 1.5 Whr/liter. This form is not practical for long term storage, but is acceptable for generation at the source, where the low density is not an issue.

Compressed Gas

Hydrogen can be compressed to 150 - 350 bar (2000 - 5,000 psi) or with specialty storage materials up to 700 bar. This increased pressure changes the gas density to about 14 mols/liter. The energy storage density increases to an equivalent heating value of 450 Whr/liter. However, compressed hydrogen requires a storage vessel that can contain these pressures and creates a safety risk if a leak occurs due to corrosion or accident. Such containers are by necessity quite heavy even for small amount of hydrogen. A standard compressed gas cylinder (26 x 140 cm outside dimensions) can store about 50 L at 2500 psi (7 mol/liter) or 350 mol of hydrogen but it weighs nearly 70 kg (165 lbs). This amount will provide nearly 3 weeks of hydrogen for the prototype case described later in this report, compared to the 1 week time for the chemical storage as a metal hydride. However the metal hydride and reactor will weigh considerable less, and have greater safety.

Liquid Hydrogen

Hydrogen liquid has a high storage capacity (35 mol/liter or 71 g/liter), but requires a tremendous amount of energy to convert to the liquid form, and also requires continuous energy inputs to remain liquid. This is because hydrogen liquid boils at −252.882 °C or −423.188 °F. This is not an appropriate technology for small scale off grid electricity generation.

Metal Hydrides

Hydrogen can also be chemically stored as a metal hydride. The hydrogen can be generated from the hydride on an as needed basis (Soloveichik, 2002), (Gervasio, et al., 2005), (Breault, et al., 1999). This storage medium has the benefit of good energy density by volume, and low reactivity in the atmosphere. The low reactivity means they are safe to handle during maintenance or during and after an accident. Some of the more well-known mineral forms

include lithium hydride (LiH), lithium borohydride ($LiBH_4$), sodium borohydride ($NaBH_4$), lithium aluminum hydride ($LiAlH_4$), and sodium aluminum hydride ($NaAlH_4$), (McClaine, et al., 2000). The overall reactions for each mineral with water are as follows. Note that intermediary reactions are not included, even though each reaction proceeds through several steps. Also, the exact form of the products may differ depending on other characteristics such as pH. These reactions are all normalized to the same product form for the comparison presented in table 2.

Eqn 1: $2\ LiH + H_2O \rightarrow Li_2O + 2H_2$

Eqn 2: $LiBH_4 + 2\ H_2O \rightarrow LiBO_2 + 4\ H_2$

Eqn 3: $NaBH_4 + 2\ H_2O \rightarrow NaBO_2 + 4\ H_2$

Eqn 4: $LiAlH_4 + 2\ H_2O \rightarrow LiAlO_2 + 4\ H_2$

Eqn 5: $NaAlH_4 + 2\ H_2O \rightarrow NaAlO_2 + 4\ H_2$

Table 2 lists the hydrogen weight fraction for each of these compounds and the overall weight ratio of hydrogen generated as a fraction of all the reactants.

Table 2: Amount of hydrogen in several metal hydrides.

Compound	wt% H	wt% H reactants
LiBH4	18.4	13.8
LiH	14.4	11.6
NaBH4	10.6	10.8
LiAlH4	10.5	10.8
NaAlH4	7.4	8.9

Some alternative hydride complexes can be made from ammonia, aluminum, and borohydrides (Staubitz, et al., 2010). These materials have a hydrogen yield of 9% by weight or even less. Several of these compounds have been studied including some that contain only B, N, and H (both positive and negative ions), such as; amine boranes, boron hydride ammoniates, hydrazine-borane complexes, and ammonium octahydrotriborates or tetrahydroborates. Of these, the amine boranes have been investigated as hydrogen carriers the longest (during the 1970s and 1980s by the U.S. Army and Navy). Their chief benefit was that they contained no metal ions, otherwise they performed similarly to the metal hydrides.

This project explores the use of the metal hydride compounds for storing hydrogen. This choice is due to the lower overall weight, the high energy density, and the safety considerations for on-site storage.

Chapter 4. Hydrogen Fuel

Generation

The technologies involving hydrogen storage have only recently been under investigation and they are not well understood. They are also economically non-viable for routine and commercial applications. The most widely understood hydrides for hydrogen storage are sodium borohydride ($NaBH_4$ or SBH) and ammonia-borane (NH_3BH_3 or AB) (Demirci, et al., 2009). These compounds are safe, compact, and readily provide large quantities of hydrogen on demand. Sodium borohydride especially is nontoxic, nonflammable and is available in large supplies; in fact, the United States has the world's largest reserves of borax, an ore from which sodium borohydride is readily prepared.

The reaction of sodium borohydride with water leads to the slow release of hydrogen gas along with sodium borate as shown below. Sodium borohydride has been previously studied as a hydrogen storage material. The other reactants most studied are water and methanol.

Eqn 6: $NaBH_{4\,(s)} + 4\,H_2O_{(l)} \rightarrow NaB(OH)_{4\,(s)} + 4\,H_{2\,(g)}$ [High pH conditions]

Eqn 7: $NaBH_{4\,(s)} + 2H_2O_{(l)} \longrightarrow NaBO_{2\,(aq)} + 4H_{2\,(g)}$ [Low pH conditions]

Eqn 8: $NaBH_{4\,(s)} + 4CH_3OH_{(l)} \longrightarrow NaB(OCH_3)_{4(aq)} + 4H_{2(g)}$

These reactions represent the reaction mechanism for sodium borohydride with water and methanol respectively. The reaction is exothermic with the heat of reaction of (-210) kJ/mol. Both these reactants provide excellent reaction kinetics, but both are limited by temperature, and the reaction almost seizes at temperature below 0 °C. To enhance the rate of reaction at cold temperatures various metal catalysts have been used such as copper, aluminum, zinc, silica gel, ruthenium, nickel, or platinum (Amendola, et al., 2000). The application of catalyst enhances the rate of reaction but at the same time increase the cost of operations. One of the project goals was to develop a chemical reaction system that could operate at cold temperatures, and be economical.

One project parameter was set by the cold climate in Minnesota where, during the winter, an evening low may approach -40°C (-40°F). At this low temperature, both water and methanol will freeze solid. We explored several substances that could depress the freezing point of water. We eventually found a simple mixture of ethylene glycol (found in anti-freeze in car cooling systems) mixed with water kept the solution from freezing (Wikipedia, 2012). When a suitable accelerant is also added, the reaction can use the glycol as well as the water for hydrogen generation. We were able to successfully produce hydrogen at temperatures as low as -50°C without freezing. However the production rate was significantly slowed at temperatures lower than -40°C. The low temperature experiments required the use of an accelerant (protic or Lewis acids). The yield of hydrogen was observed to be >90% for the temperature range between 25°C to -20°C and at -40°C the yield was observed to be ~80%.

The data was gathered for the reaction between 2 mmol $NaBH_4$ and 5 ml of solvent using the laboratory setup as shown below in figure 2. Lower temperatures were attained using dry ice

around the round bottom reaction flask. The gas dryer was used to remove any moisture from the product gases. The moisture could occur during evaporation of the water reactant due to the heat generated from the reaction. The clear bulb was for observation of the gas (hydrogen is colorless). The gas burette was used to measure the quantity of gas generated by the reaction. The water reservoir was used to refill the burette between experiments. Each experiment reacted approximately 0.08 g of SBH with an excess of the glycol / water mixture. This amount was chosen to develop approximately 200 ml of hydrogen, which could be easily measured in the 250 ml gas burette. Actual amounts varied for each run, see table 3 for more detail.

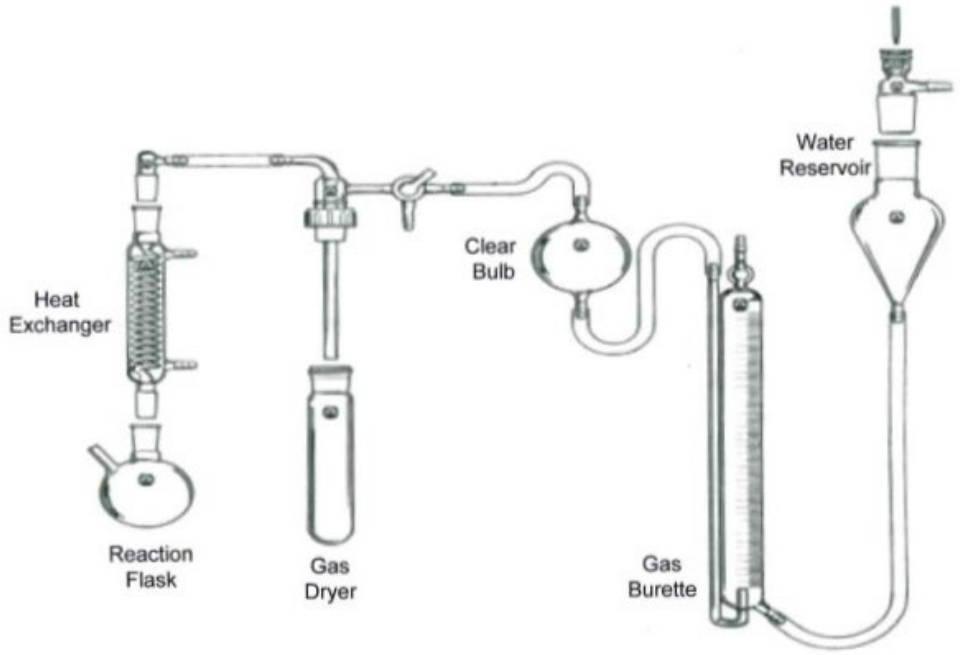

Figure 2: Experimental equipment schematic for determining hydrogen generation rates.

Table 3: Yield of hydrogen at different temperature conditions.

Experiment	Temperature °C	Mass of $NaBH_4$/g	Theoretical H_2 volume/ml	Experimental H_2 volume/ml	Yield %
1	22	0.0763	180.72	164	90.75
2	0	0.0733	173.61	160	92.16
3	-10	0.088	208.43	207	99.31
4	-20	0.0965	228.56	223	97.57
5	-40	0.0837	198.24	160	80.8

This table shows an increase in efficiency of hydrogen generation as temperature decreases until -20°C. The reaction is exothermic, so this trend is expected.

The detailed temperature dependent hydrogen evolution studies using sodium borohydride (SBH) and ethylene glycol without (table 4) and with (table 5) the presence of acetic acid (vinegar) as the protic acid are reported in the following tables. Acetic acid was added to the solvent to create a slightly acidic mixture (pH=5.5)

Table 4: Reaction of SBH with various solvents under non-accelerated conditions.

Solvent	Temperature [°C]	Reaction Time	Reaction Completion [% of maximum hydrogen evolved]
Water	25	24 hours	~50%
Methanol	25	15 minutes	>95%
Ethanol	25	30 minutes	>95%
2-Methyl-2-propanol	25	24 hours	Trace
Ethylene glycol	25	15 minutes	>95%
Propylene glycol	25	15 minutes	>95%

Table 5: Reaction of SBH with ethylene glycol/water mixture using acetic acid accelerant.

Temperature	Time	Actual Hydrogen Produced	Theoretical Hydrogen	Yield
°C	minute	ml	ml	%
25	3	164	180	91
0	5	183	200	92
-10	6	207	210	99
-20	7	215	220	98
-40	9	160	200	80

These results show that a 50/50 mixture of water and antifreeze, with a small addition of acetic acid, is suitable for generating hydrogen from the SBH at temperatures as low as (-40) °C. As the reaction in equation 7 shows, one mole SBH requires 2 moles of the ethylene glycol / water mixture and releases 4 moles of H_2. The yield of hydrogen is found to be greater than 90% at temperatures as low as (-20) °C and 80% at (-40) °C. The time to reaction completion was approximately 5 - 10 minutes.

Figure 3 presents the kinetic results for the yield of hydrogen from SBH in the ethylene glycol/ water mixture with acetic acid accelerant for different temperatures .The graph provides the volume of hydrogen collected in the equipment (see figure 2). It must be noted that only the reactor itself was kept at the reaction temperature conditions, and the remainder of the equipment was at room conditions. The results are corrected to standard conditions for presentation in this figure.

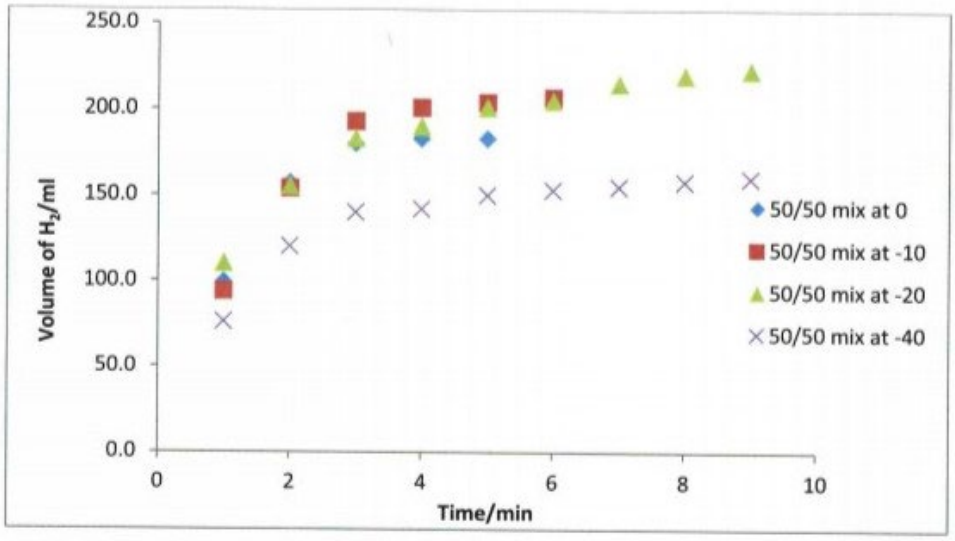

Figure 3: Rate of hydrogen production from SBH and mixture of ethylene-glycol and water at different temperatures.

Fuel Cell Operation

During the second phase of the project, a 20Watt fuel cell was used to generate electricity using the hydrogen generated as discussed above. Voltage and current were measured from the fuel cell using a multi-meter and stopwatch. The power was calculated using the following equation:

Eqn 9: $$P = VI$$

Where:

V is for voltage potential (Volt), and
I is the current (Amp).

The efficiency of the fuel cell was calculated using the following equation:

Eqn 10: $$\eta = \frac{IVt}{H_{H_2} V_{H_2}}$$

Where:

t is time (sec),
η denotes the energy efficiency,
H_{H2} is the heating value of hydrogen, which is a constant 10.8 (J cm^{-3}), and
V_{H2} is the volume of hydrogen (cm^3) supplied to the fuel cell.

The efficiency of the fuel cell was measured as a function of temperature and loads (the resistance). The data are shown in table 6. These results show that both efficiency and maximum

power output of the fuel cell are higher at higher temperatures. This observation is in agreement to other reports on fuel cells. It suggests that the best operation will occur if the fuel cell is kept warm (above freezing as the minimum operating temperature). The data presented in Table 6 used approximately 2 mmols (0.08 g) of $NaBH_4$, which was able to run the fuel cell for approximately 2.5 minutes

Table 6: Efficiency of fuel cell at different temperatures and resistance.

Trial	Reactor Temperature [°C]	Temperature of the fuel cell [°C]	Resistance [Ω]	Max Voltage [V]	Max Current[A]	Max power [W]	η [%]
1	21	18	6	9.26	1.543	14.291	76
2	21	18	20	10.23	0.5115	5.233	29
3	21	17	13	9.26	0.723	6.797	78
4	21	19	120	9.3	0.0775	0.7208	4.6
5	21	18	10000	9.25	0.00092	0.0086	-
6	0.1	18	6	9.96	1.66	16.534	94
7	0.1	18	13	9.77	0.7515	7.343	42
8	0.1	17	20	9.32	0.466	4.341	25
9	-9	-5	6	8.01	1.335	10.693	50
10	-17	-15	13	7.23	0.5562	4.021	-
11	-10	-6	20	9.63	0.4815	4.64	18

Figures 4, 5, and 6 show how the fuel cell operated once an experiment was begun. These plots show the effects of load (resistance) and temperature. Each of the results shows a quick increase to a steady value. This suggests that there is short start-up time. This is probably due to the reactor being initially filled with air which is displaced by the hydrogen from the reaction. The 40 ml volume suggested by these figures is approximately 2 times the gas space in the reactor. This observation is noted and any operating procedures must include a warning to operators that they must account for this start-up each time the hydrogen generation reaction is started.

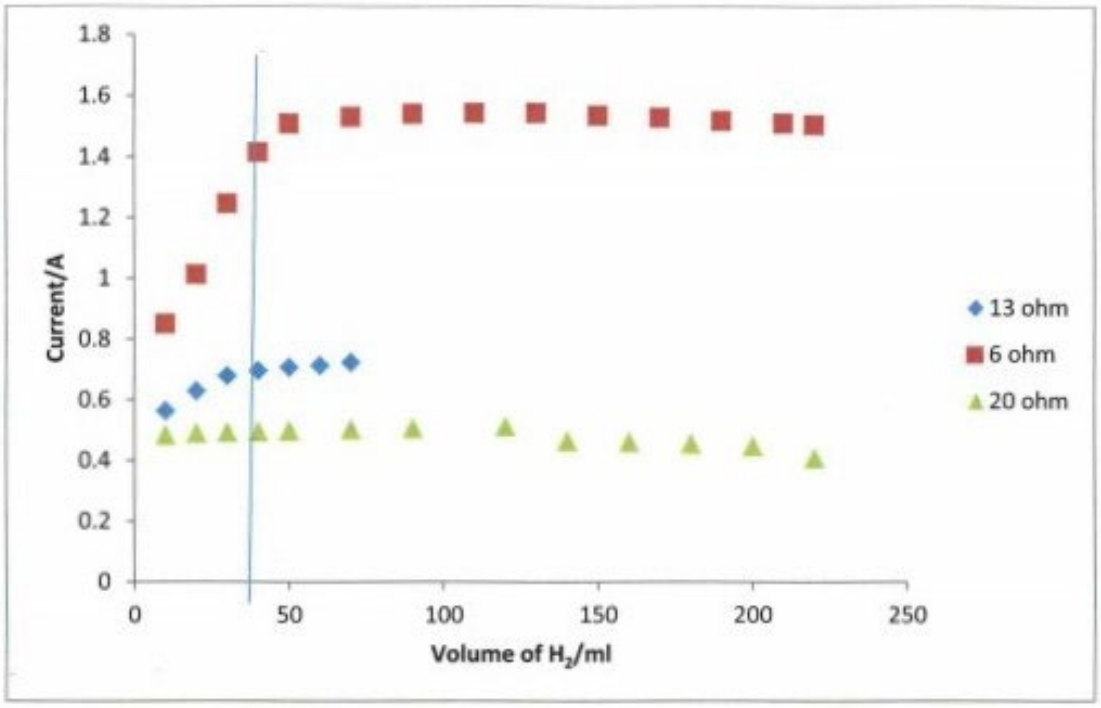

Figure 4: Fuel cell operation at room temperature.

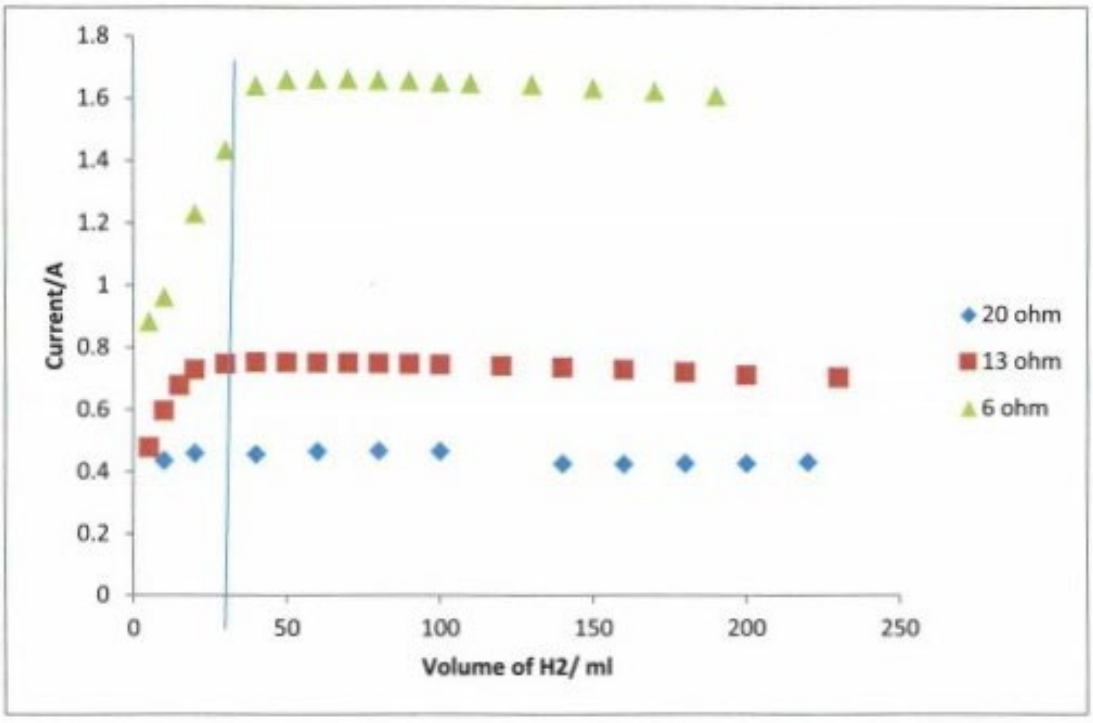

Figure 5: Fuel cell operation at 0.1 °C.

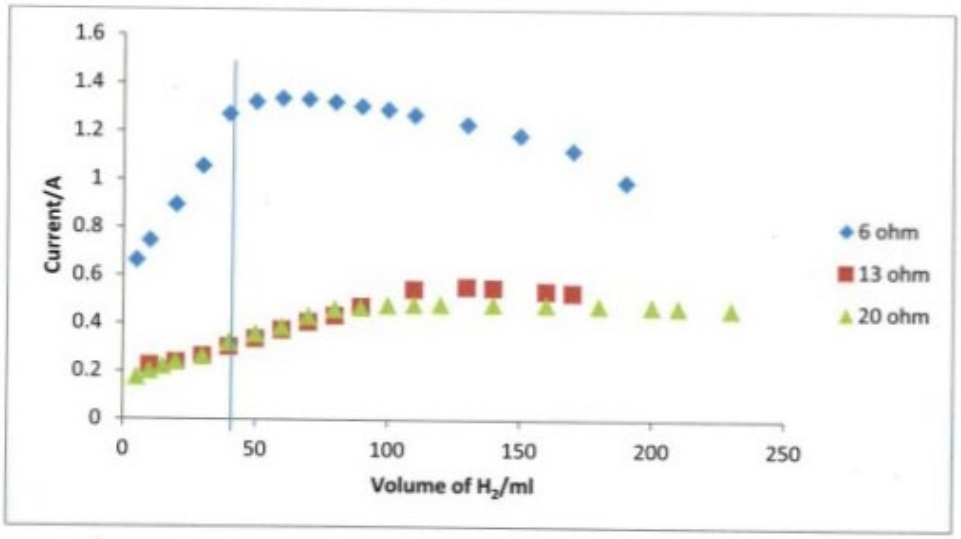

Figure 6: Fuel cell operation at (-9 <T<-20)°C.

To observe the performance of the fuel cell over an extended period of time, approximately 0.75 g of $NaBH_4$ was reacted at room conditions to supply H_2 to the fuel cell. The results are provided below in Table 7.

Table 7: Results of 0.75 grams of $NaBH_4$.

Time [min]	Voltage [Volt]	Reactor Temperature °C [°C]	Injection volume mL	Current [Amp]	Power [Watt]
1	8.9	18.6	2	0.68	6.09
2	9.0	18.7	3	0.69	6.16
3	9.0	18.9	4	0.69	6.16
4	9.0	19.3	5	0.69	6.22
5	9.0	19.6	6	0.70	6.29
6	9.1	20.0	6	0.70	6.33
7	9.1	20.3	6	0.70	6.37
8	7.3	20.6	6	0.56	4.10
9	9.2	20.7	8	0.71	6.47
10	9.2	20.7	8	0.71	6.48
11	9.2	20.7	8	0.71	6.50
12	9.2	20.6	10	0.71	6.54
13	9.2	20.6	10	0.71	6.57
14	9.1	20.6	10	0.70	6.40
15	9.3	20.7	11	0.71	6.64
16	7.3	20.8	11	0.56	4.11
17	9.0	20.8	12	0.70	6.29
18	9.3	20.8	14	0.71	6.61
19	7.1	20.8	15	0.54	3.86
20	4.4	20.8	15	0.34	1.47
21	3.0	20.8	15	0.23	0.71
22	3.0	20.8	17	0.23	0.70
23	3.0	20.7	17	0.23	0.67
24	2.7	20.7	18	0.21	0.55
25	1.2	20.6	20	0.09	0.11

This experiment was run with a 13 ohm resistor at room temperature. The temperature of the gas space of the reactor was recorded at each time interval. The glycol/water mixture was added slowly by injecting some solution every minute. The fourth column reports the cumulative amount of the liquid mixture added. The final two columns report the measured current in the resistive load, and the calculated power form the fuel cell.

The maximum power attained during this experiment was 6.638 watts, and the temperature inside the reactor increased 2.2 degrees after 16 minutes. At 19 minutes into reaction, the reaction rate decreased, and further injection of the solvent did not prolong or increase the rate of reaction. Figures 7 and 8 graphically present the fuel cell performance. Figure 7 shows the power output during the experiment, showing a small increase during the first 18 minutes, then a quick

decrease as the hydrogen supply was exhausted. Figure 8 shows the temperature profile of the reaction, again demonstrating the exothermic nature of the reaction.

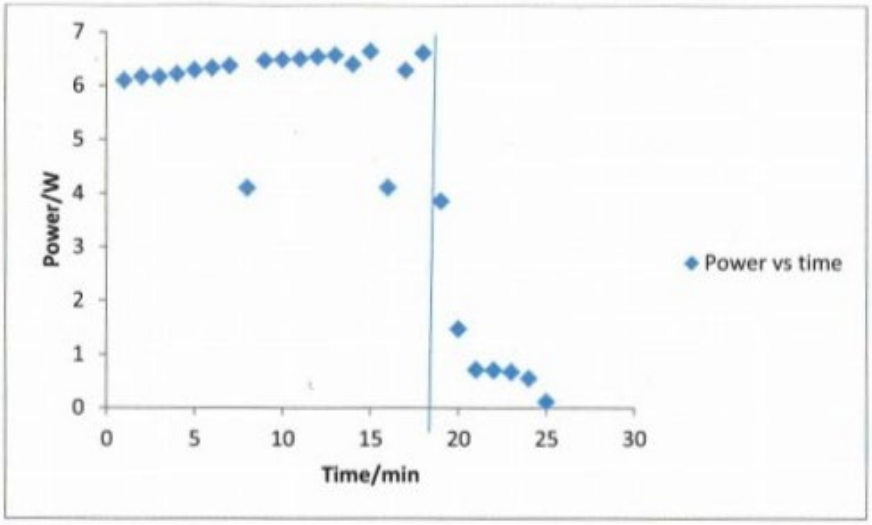

Figure 7: Power generation during experiment described in table 7.

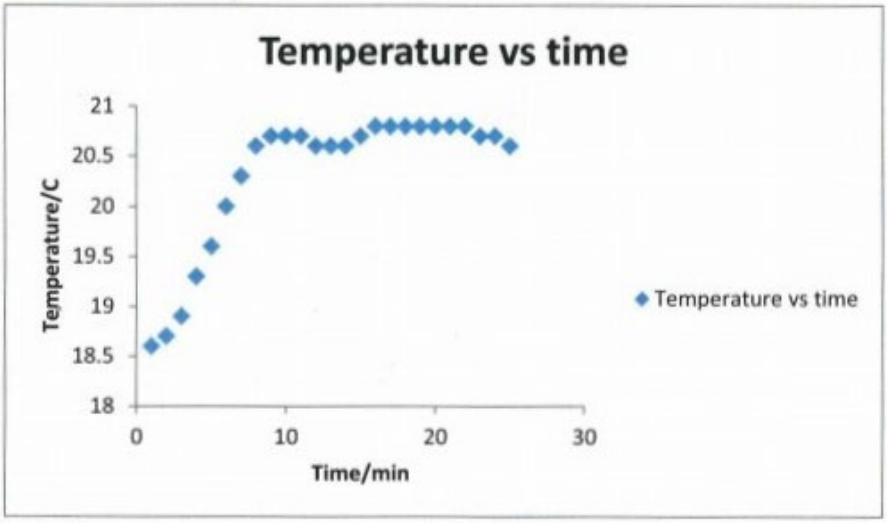

Figure 8: Temperature evolution during experiment described in table 7.

The fuel cell was able to use almost 47% of the hydrogen produced to generate electricity. The typical limit is 50%, with the remaining energy producing heat. Other sources of waste include fuel cell bypass, other losses within the system, or waste during startup and shutdown.

Chapter 5. Prototype Design

This chapter will describe the preliminary design considerations for the prototype off-grid power supply system. Figure 9 shows a simplified system schematic highlighting the major components of the prototype system. This section will describe each subsystem, as listed in table 8.

Table 8: List of prototype subsystems.

Reactor
Liquid Storage
Liquid Dispensor
Air Inlet Heat Exchanger
Fuel Cell
Power Production
Water
Heat
Battery
Control System
Safety Equipment

The basic design assumptions are listed in the table 9. Several discussions with intelligent transportation system (ITS) users helped us decide on the various design parameter values. One of the first ideas from users was to supply power for emergency lighting. This task is currently powered by batteries or diesel generators (which can supply 10,000 Watts of power). This is an ideal long range goal, but is not realistic for our proto-type system. Another use would provide constant low-level power to measurement, recording, and transmission systems. This type of system requires approximately 10 – 100 watts of power and is currently supplied by battery systems. While the larger power supply would be very useful, it was decided that a smaller prototype system would be built for testing and development, and for creating the process control logic. It would also allow unforeseen problems to be addressed in a more safe and inexpensive system.

Table 9: Design assumptions.

Power requirements:	20 W maximum
Voltage requirements:	12 V.
Operation time:	1 week constant power (24/7).
Load variability:	Minimal variation (+/- 20% during week), and always on.

The total power generation required between weekly resupply is 3,360 W-hr/week (20 Watts * 24 hours * 7 days/week). The amount of SBH needed to provide this is:

$$Xg_{SBH} = 3.36 \text{ kW-hr} \times \frac{859.8\text{kcal}}{\text{kW-hr}} x \frac{1 molH_2}{57.7\text{kcal}} x \frac{1 \text{ eff}}{0.45} x \frac{molNaBH_4}{(0.9)4 molH_2} x \frac{37.9 gNaBH_4}{molNaBH_4} = 1{,}171 g$$

Where:

$\frac{57.7\text{kcal}}{1 mol H_2}$ is the energy produced in the fuel cell per mol of hydrogen consumed,
0.45 efficiency is the rate at which the energy produced can be converted into electricity,
0.9 efficiency is the conversion rate obtained in the reactor for producing hydrogen, and
1 molH_2/mol $NaBH_4$ is the stoichiometric limit of the reaction (equation 7).

The efficiencies listed above are the lower values obtained in our experiments. The energy production efficiency may be closer to 50%, and the reaction efficiency may approach 98.5%. However, operation in the field is likely to be worse than in the lab, so the lower values were chosen for design purposes.

The amount of water/glycol solution required is:

$$Xl_{solution} = 3.36 \text{ kW-hr x} \frac{859.8\text{kcal}}{\text{kW-hr}} x \frac{1 mol_{H_2}}{57.7\text{kcal}} x \frac{1 \text{ eff}}{0.45} x \frac{4 mol_{solution}}{(0.9)4 mol_{H_2}} x \frac{40g}{mol_{solution}} x \frac{liter}{1200g} = 4.12 liter_{solution}$$

Where:

4 mol H_2 are produced for 4 mol of solution (H_2O and Glycol),
The average molecular weight of the solution is 40 g/mol, and
The density of the solution is 1200 g/liter.

The results in the US system of units are roughly 2.5 lbs of SBH and one gallon of solution (50% water and 50% ethylene glycol) for one week of power.

Each sub-system was designed with the whole in mind. The following section provides discussion for each unit.

Reactor

The reactor is sized to minimize volume, but also to allow for the solid-liquid reactants to form the solid and gas phase products. Since one of the products is a gas (H_2) the system must be designed to accommodate changes in pressure. These changes will be periodic, with the greatest pressure just after addition of the liquid reactants, and pressure will be lowest just before their addition. The chosen equipment is capable of adding 0.5 ml of solution each time the supply valve is opened. This valve could be open longer, but that would create larger spikes in pressure. Further, we will assume the entire amount added reacts within one minute or less.

$$Xml_{H_2} = 0.5 ml_{solution} x \frac{1200g}{1000 ml_{solution}} x \frac{1 mol_{solution}}{40g} x \frac{(0.9)4 mol_{H_2}}{4 mol_{solution}} x \frac{22,400 ml_{STP}}{1 mol_{H_2}} = 302 ml_{H_2}$$

Where:

STP is standard conditions (P = 1 atm, T = 273 K)
The allowable pressure change in the reactor will be less than 2% (2 kPa, or 0.3 psi). The added gas (302 mlH_2) is the equivalent of (302/22400) = 0.0135 mol of H_2. Assuming ideal gas conditions allows us to calculate the volume of gas space required in the reactor:

Let P = .02 atm
T = 273 K
n = 0.0135 mol
R = 0.082 l atm/ mol K

$$V = \frac{nRT}{P} = \frac{(0.0135mol)\left(0.082\frac{l \cdot atm}{mol \cdot K}\right)(273K)}{0.02atm} = 15.1liter = 4gallons$$

This is the volume needed for just the additional gas in the reactor such that it does not change the pressure by more than 2 %. There must also be volume for the reactants and left over solid products. We are adding one gallon of liquid, but most of that will be consumed in the reaction. The SBH has a density similar to water (1.04 g/cm^3) and the product solid has a density of 1.73 g/cm^3. This suggests that the volume of solids will decrease as the reaction progresses; however the reaction will not go to completion, so some residual liquid will remain within the reactor. The required volume for the SBH is about 1,125 cm^3 or 1.1 liters. The volume of products and unreacted solution is expected to be about 1,100 cm^3 or 1.1 liters. Hence the required reactor volume to hold all the solid reactant and product, the unreacted liquid, and the hydrogen gas (at a no more than 2% pressure increase) is 16.2 liters, or 4.3 gallons. A low cost reactor capable of holding this pressure and volume is available in a 5 gallon size.

Liquid Storage

The liquid solution of water and ethylene glycol requires a storage volume of 4.1 liters (1.1 gallons). This container will also collect the water produced from the fuel cell, so it could be somewhat smaller if the recycled water is accounted for. The amount of liquid water that will drain back to this container is not well known at this time, so no allowance is made for reducing the total needed volume. Preliminary results showed some water produced, but not at a consistent rate. Also experiments were run for less than one hour, so steady state conditions were not observed. Therefore the liquid storage container was sized to be one and a half gallons.

Liquid Dispenser

Liquid solution will be dispensed to the reactor through a gravity feed controlled by an actuated valve. The smallest repeatable time the device could be open (to allow flow) was 0.5 seconds. This allowed 0.2 to 0.5 ml of solution to flow, depending on the liquid head in the storage container. This size aliquot was chosen as the design constraint for the reactor volume sizing.

Air Inlet Heat Exchanger

The fuel cell requires the operating conditions to be above 0°C. Colder temperatures will cause the water, which forms at the cathode, to freeze. Below freezing temperatures will stop the fuel cell reaction and could damage the fuel cell. The hydrogen feed will be generated within the reactor (described above) in an exothermic reaction. The air will be drawn in from outside where it may be as cold as -40°C. This air must be heated to above 0°C before entering the fuel cell. The excess heat in the reactor can be used to preheat the inlet air. The hydrogen will be generated at the reactor temperature and will not require any heating. We do not have any experimental data yet on the required level of heat exchange. The current design uses the heat within the environmental chamber to preheat the air. If this proves insufficient, the air will be ducted through the reactor. The reactor would need to be larger to account for the volume loss to this ducting.

Fuel Cell

The fuel cell chosen for this application is a 100W unit with built in control module. The module controls the flow of hydrogen to the fuel cell, and operates a fan to prevent water buildup on the cathode side, as well as to maintain a constant temperature within the cell. The fuel cell will produce water as part of the reaction to generate electricity. This water must be removed from the fuel cell, or it will flood the cathode. If the cathode is flooded it will prevent oxygen from reaching it, and it will stop the reaction. Conversely, if the proton exchange membrane is too dry, it will reduce the flow of protons across it, also slowing/ stopping the reaction.

The 100 W model was chosen because fuel cells are known to have much lower efficiencies at their rated power output. Typically it is most efficient to operate at 20 – 30 % of the rated value. This also allows for the system to occasionally supply greater bursts of power should the need arise. Finally, the cost difference between a 100W fuel cell and a 50W fuel cell is quite small, possibly because the 100 W cell is produced in larger volumes.

Battery

The fuel cell will be used to maintain the charge (and temperature) of a battery, which will be connected to the power load. The battery is the main power supply and the fuel cell is the secondary (or slave) power supply. This system allows the load to have a constant and steady power supply that is unaffected by the delays in the fuel cell due to load shifting. The battery will be much smaller than the battery packs required for typical off-grid supplies because it has the fuel cell to recharge it and to keep it warm. The warm temperature allows the battery to operate at its most efficient.

Control System

Controls for the system include:

- Temperature measurements of the fuel cell, of the air and hydrogen inlets, and of the interior of the environmental chamber.
- Pressure measurements inside the reactor

- Voltage and current measurement from the fuel cell to battery, and for the actual load.
- Hydrogen concentration within the environmental chamber.

Temperatures of the feeds to the fuel cell must be above freezing. The cell can withstand temperatures as high as 40 °C. The temperature of the inlet air and environmental chamber will be used to estimate the amount of air that can be preheated. The hydrogen temperature sensor will serve to monitor the reactor temperature.

Pressure is used to measure the efficiency of the reaction and to signal when an additional aliquot of liquid solution should be added to the reactor.

Hydrogen concentration is measured to prevent the interior of the environmental chamber from reaching the lower explosive limit for hydrogen. The box will not be air-tight, so a slowdown of the reaction should allow the interior to vent and remain at a safe condition.

Safety Equipment

The system is designed for safety. The possible hazards include:

- High temperatures
- Low temperatures
- Water buildup
- Hydrogen gas buildup within the environmental chamber
- Pressure buildup in the reactor
- Hydrogen buildup during handling (charging and replacement)
- Unintended damage from other factors

Heat is generated from the reaction to generate the hydrogen and from the reaction to generate electricity in the fuel cell. This heat must be removed from the unit. However, the heat will also be used to maintain the interior of the unit above freezing. The heat can be removed as excess air is returned outside, and as heat loss from the box to the surroundings. The box is insulated to minimize its heat loss (and to maintain above freezing temperatures within it).

Low temperatures would result from very cold air in the air inlet. This could cause freezing of the fuel cell, or freezing of the moisture released from the fuel cell. It is expected the heat from the two reactions will be able to keep the entire environmental chamber above the freezing point.

Water buildup will result from the water product of the fuel cell being vented into the environmental chamber and condensing or freezing onto the other components. It is anticipated that the heat from the reactions will prevent freezing and that the air vent to the outside will remove most moisture. However, in the event of water buildup (a maximum of two gallons in the worst case scenario) all equipment within the environmental chamber will be elevated and a drain will be provided in the bottom of the box.

Hydrogen gas buildup within the environmental chamber will be monitored. If the level reaches 25% of the lower explosive value, the reaction will be stopped until the excess hydrogen is

vented from the environmental chamber. The chamber will not be air-tight, so any buildup should be removed within minutes.

Pressure buildup in the reactor would happen if too much solution is added and the fuel cell is not operating. The pressure buildup will be reduced by the operating fuel cell. If the pressure buildup is too high, an internal pressure relieve valve will open and vent the reactor into the environmental chamber. This condition will also halt the addition of the liquid mixture into the reactor, to prevent the formation of additional hydrogen until the excess is used or vented.

There is some concern that there will be some residual SBH and solvent in the reactor at the end of the week. The concern is that these materials may suddenly react when the operator disconnects the reactor during recharging. The concern arises from observations that the residual materials after an experiment release hydrogen during cleanup. The sudden generation of unwanted hydrogen may create an unsafe condition for the operator. A safe operating procedure must be developed for use during handling of the equipment and materials during replacement. One possible suggestion is to have the operator inject a small volume of caustic solution to kill the reaction, rendering any residual materials unable to generate hydrogen. This concern and operating procedure have not been fully developed at this time.

Unintended damage from other factors includes problems from insect or rodents, accidental damage from roadside incidents, and mishandling during recharging. Insects and rodents could move into the environmental chamber because it will be warm. All inlets and outlets must be screened to prevent their entering. Accidental damage may result from a roadside incident such as the system being struck by a moving vehicle. Such accidents are not avoidable, so the system needs to fail in a safe way. Fortunately the reaction only generates small amounts of hydrogen, and hydrogen, once released into the air will quickly dissipate before reaching a dangerous concentration. The reactant and product materials are non-toxic and are in small quantities, so they should pose no environmental problems. Mishandling of the unit would most likely result in the unit not working. This may cause the equipment to freeze and be damaged. The operator must be trained with a standard operating procedure to make sure the system is working after recharging. This may involve installing a small LED light showing the unit is functioning as intended. This aspect of the prototype system has not yet been developed.

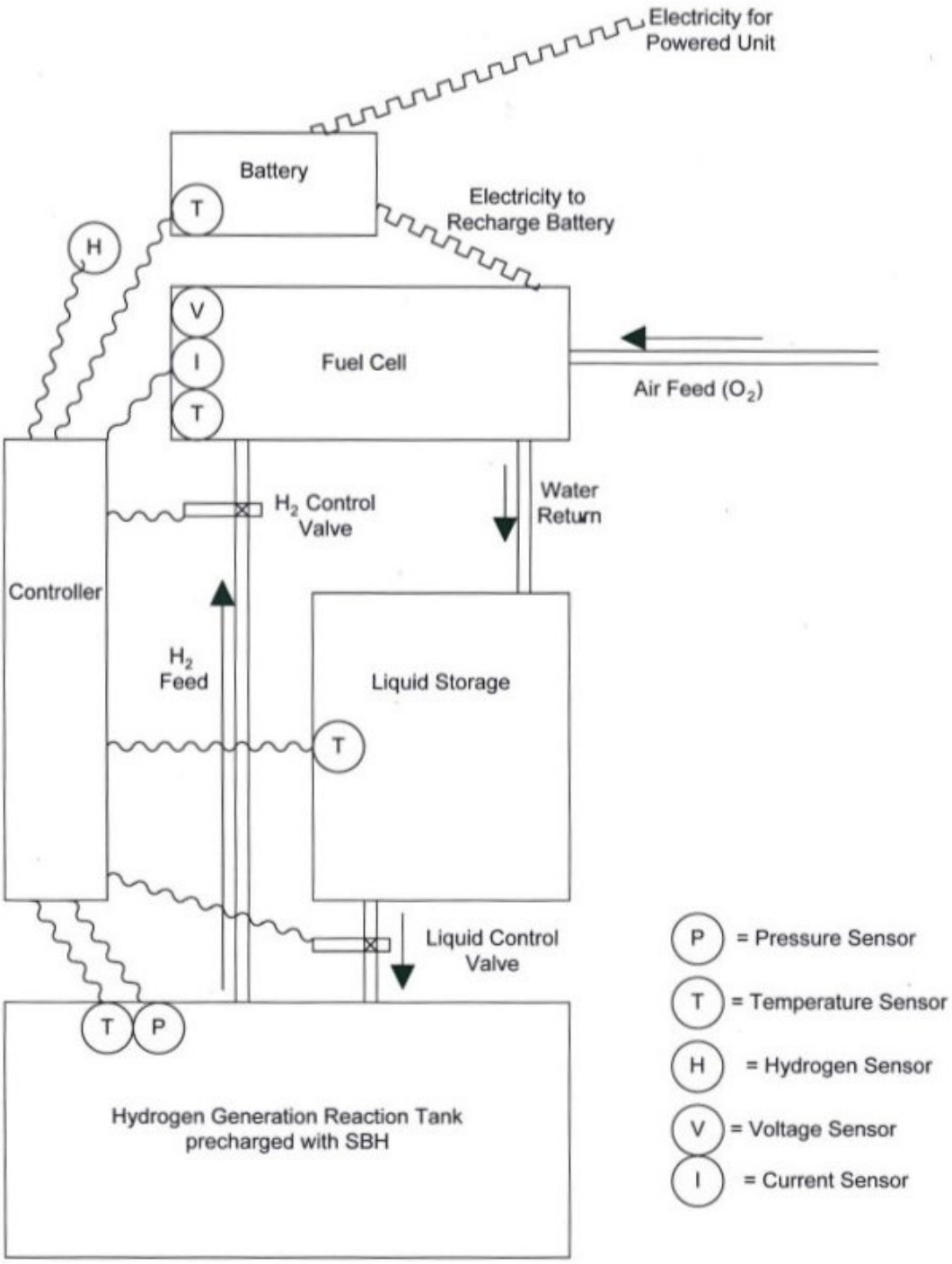

Figure 9: Prototype schematic for the generation of hydrogen for use in a fuel cell.

Chapter 6. Cost

Capital

A prototype system was constructed for collecting hydrogen generation / fuel cell operation data for cold conditions. The cost of this system was approximately $7,500. The system parts, as shown in figure 9, and cost estimates are listed below:

- 100 W Fuel Cell with hydrogen control module ($1500),
- Reaction vessel, storage tanks, tubing and wiring ($500),
- Insulated environmental chamber ($500),
- Process control ($5000)
    - Actuated valves (2)
    - Pressure sensor (1)
    - Temperature sensors (4)
    - Hydrogen concentration sensor (1)
    - Pressure relieve valves (1)
    - Logic circuit to collect sensor information and control unit (1).

Operation and Maintenance

Cost of the glycol/water, acid. and SBH would be approximately $35 / week per device.

Chapter 7. Additional Work

Near this project's conclusion some additional work was performed to explore an additional reaction for the generation of hydrogen. While this reaction is expected to have higher costs, it may also be easier to control over a greater range of temperatures.

This system used sodium borohydride ($NaBH_4$) also written as SBH, reacting with a mixture of water and tartaric acid ($C_4H_6O_6$). The tartaric acid acts as an accelerant when at high concentrations and as a catalyst at low concentrations. The implication is that the reaction is accelerated when the tartaric acid solution is initially added, but becomes catalyzed at lower concentrations.

The reaction is slower than the ethylene glycol/water reaction with SBH, which can be useful at higher temperatures (above 0°C). This reaction is not recommended for sub-zero conditions, but it much more stable above 20°C.

Testing for this reaction was performed on small batches of SBH, similar to initial work with the ethylene glycol / water system. In each experiment enough material was added to generate approximately 200 ml of H_2 gas upon completion. The experiments were analyzed to obtain the needed kinetic model equations, which would be used in designing the chemical reactor.

The experiments showed the accelerated reaction to have a rate equation of:

Eqn 11:

$$rate = 1.38x10^{-3}\frac{g-mol}{liter\cdot sec}\exp\left[-\frac{735}{T[K]}\right]$$

The experiments showed the catalyst reaction to have a rate equation of:

Eqn 12:

$$rate = 1.26\frac{g-mol}{liter\cdot sec}\exp\left[-\frac{3,220}{T[K]}\right]$$

Both of these rate equations are valid for temperature between 0°C and 32°C.

These results provide for greater flexibility in choice of materials for the reaction when higher temperatures are expected.

Chapter 8. Conclusions

The goals of this project were to choose a chemical reaction system for safe storage and generation of hydrogen; develop a prototype fuel cell powered by hydrogen that can be used in cold weather applications; and to estimate the cost of such a system. This power system is to be used to power Intelligent Transportation System (ITS) application for use in Northern Minnesota, especially during wintertime when nighttime temperature conditions can range to -30 to -40 ^{o}C. Other desirable traits for the system are that it is; independent of the power-grid, small, portable, does not need frequent recharging, can work in cold weather, is dependable, and does not create a hazard for operators or the environment.

The reaction system selected for this project was sodium borohydride combined with a 50/50 mixture of ethylene glycol/ water with a small amount of acetic acid to accelerate the reaction at the coldest temperatures.

A prototype reactor was designed and constructed, see figure 9. This system will provide a 20 watt, 12 volt load with electricity for one week using 5 pounds of sodium borohydride and one gallon of the liquid mixture. Potential problems not addressed in this report include water / ice buildup within the equipment enclosure, hydrogen release during refueling, and unintended buildup of hydrogen within the equipment enclosure due to unknown leakages.

The cost of the prototype system is approximately $7,500, where the majority of the cost is due to the process control equipment needed for safe and reliable operation. Costs of materials for operation are approximately $35 /week or about $2,000 / year.

References

Amendola, S. C., Sharp-Goldman, S. I., Saleem-Janjua, M., Spencer, N. C., Kelly, M. T., & Petillo, P. J. (2000). "A safe portable hydrogen gas generator using aqueous borohydride solution and Ru Catalyst." *Int. J. Hydrogen Energy*, pp. 969-975.

Barbir, F. (2005). *PEM Fuel Cells-Theory and Practice.* New York, NY: Elsevier Academic Press.

Breault, R. W., Larson, C., & Rolfe, J. (1999). *Hydrogen for a PEM Fuel Cell Using a Chemical Hydride Slurry.* Washington DC: U.S DOE, Hydrogen Program Review.

Demirci, U. B., & Miele, P. (2009). "Sodium borohydride versus ammonia borane, in hydrogen storage and direct fuel cell applications." *Energy & Environmental Science*, pp. 627-637.

Engineering.com. (2013). *Battery Packs*. Retrieved January 25, 2013, from Product Showcase: http://www.engineering.com/ProductShowcase/BatteryPacks.aspx.

Gervasio, D., Tasic, S., & Zenhausern, F. (2005). "Room temperature micro-hydrogen-generator." *J. Power Sources*, pp. 15-21.

Klebanoff, L. (2010). Five-Year Review of Metal Hydride Center of Excellence, Annual Progress Report, IV Hydrogen Storage. Washington, DC: U.S. Department of Energy.

Larminie, J., & Dicks, A. (2003). *Fuel Cell Systems Explained, 2nd Edition.* New York, NY: John Wiley and Sons.

Mandal, T. K. (2009). "Hydrogen storage materials: present scenarios and future directions." *Annual Reports on the Progress of Chemistry, Section A: Inorganic Chemistry, 105*, pp. 21-54.

McClaine, A. W., Breault, R. W., Larsen, C., Konduri, R., Rolfe, J., Becker, F., et al. (2000). *Hydrogen Transmission/Storage with Metal Hydride-Organic Slurry and Advanced Chemical Hydride/Hydrogen for PEMFC Vehicles.* Washington DC: US DOE Hydrogen Program Review.

Meyers, J. P. (2008). "Getting Back Into Gear: Fuel Cell Development After the Hype." *The Electrochemical Society Interface*, pp. 36-39.

Puru, J. (2011). "Materials for Hydrogen Storage: Past, Present, and Future." *Journal of Physical Chemistry Letters*, pp. 206-211.

Soloveichik, G. L. (2002). "Metal Borohydrides as Hydrogen Storage Materials." *Material Matters, 11*.

Staubitz, A., Robertson, A. P., & Manners, I. (2010). "Ammonia-Borane and Related Compounds as Dihydrogen Sources." *Chemical Reviews*, pp. 4079-4124.

V. Pe´rez-Herranz, M. P.-P. (2010). "Monitoring and control of a hydrogen production and storage system consisting of water electrolysis and metal hydride." *International J Hydrogen Energy*, pp. 912-919.

Wikicommons. (2007). *Fuel Cell*. (Wikipedia) Retrieved November 11, 2012, from http://en.wikipedia.org/wiki/File:Solid_oxide_fuel_cell.svg.

Wikipedia. (2012, November 7). *Ethylene glycol, Coolant and heat transfer agent*. Retrieved November 11, 2012, from Wikipedia: http://en.wikipedia.org/wiki/Ethylene_glycol.

Wikipedia. (2012, November 9). *Fuel cell*. Retrieved November 11, 2012, from http://en.wikipedia.org/wiki/Fuel_cell.

Wikipedia. (2013). *Diesel Engine*. Retrieved January 26, 2013, from http://en.wikipedia.org/wiki/Diesel_engine.

Wikipedia. (2013). *Solar Panel*. Retrieved January 25, 2013, from http://en.wikipedia.org/wiki/Solar_panels.

Wikipedia. (2013, January 18). *Wind Turbine*. Retrieved January 25, 2013, from http://en.wikipedia.org/wiki/Wind_turbine.

Figure A-4 Original Project Report

Appendix B: Physical Data and Applicable Graphs

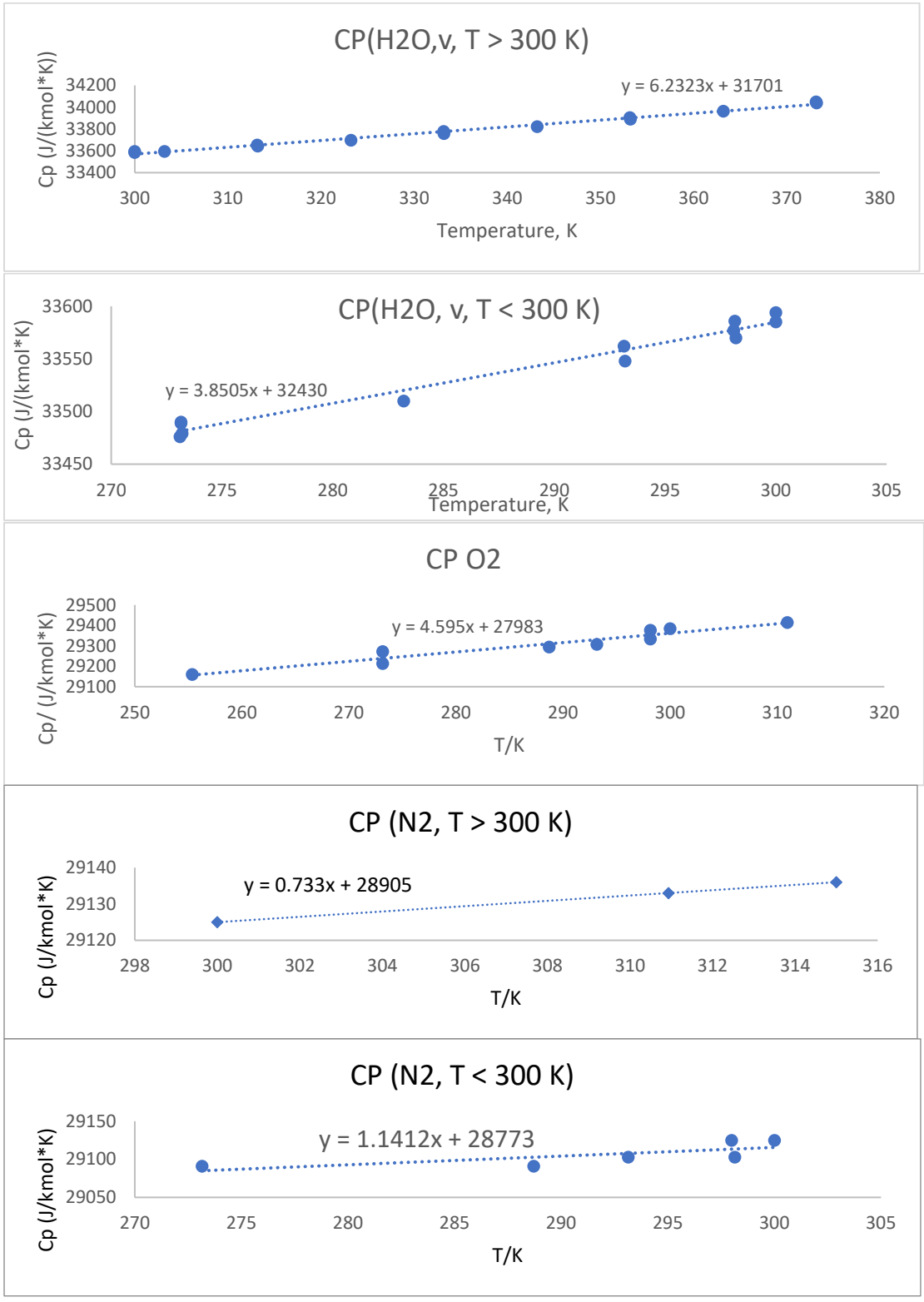

Figure B-1 Heat Capacity Graphs

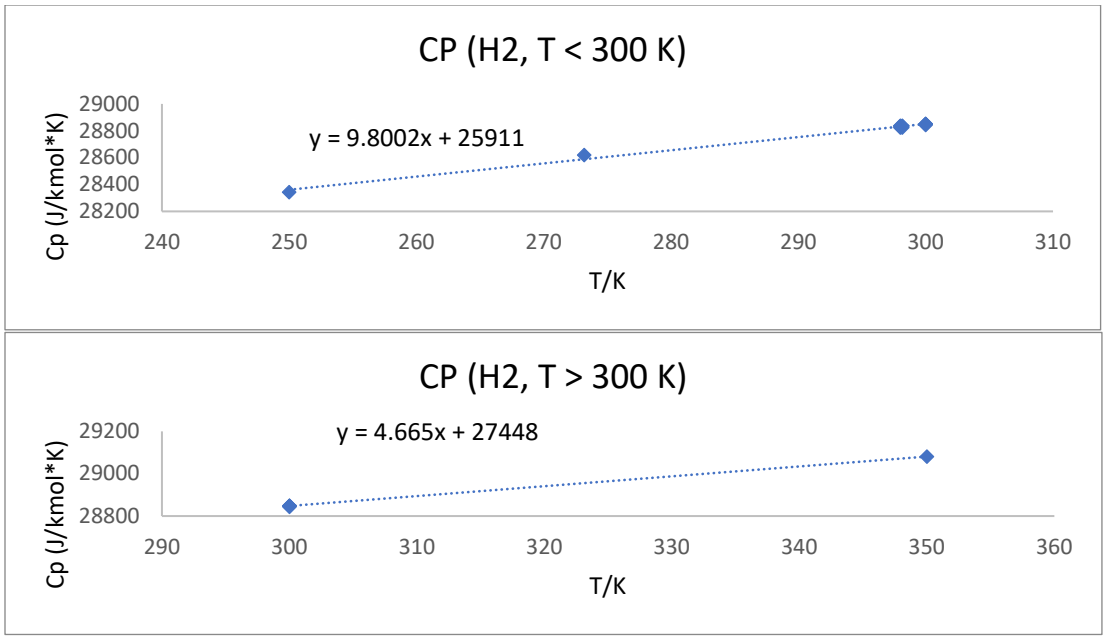

Figure B-1 Heat Capacity Graphs Continued

Table B-1 Heat Capacity Data

Oxygen		Nitrogen		Hydrogen		Water	
T (K)	Cp / (J/kmol*K)	T/K	Cp (J/kmol*K)	T (K)	Cp / (J/kmol*K)	T (K)	Cp / (J/kmol*K)
255.37	29160	273.15	29091	200	27447	273.15	33490
273.15	29213	288.71	29091	250	28344	273.15	33489
273.16	29272	293.15	29103	273.16	28620	273.2	33479
288.71	29294	298	29125	298	28836	283.2	33510
293.15	29307	298.15	29103	298	28824	293.15	33562
298.15	29376	300	29125	298	28836	293.2	33548
298.15	29334	310.93	29133	298.15	28836	298.1	33577
300	29385	315	29136	298.15	28824	298.15	33586
310.93	29414			298.15	28836	298.2	33570
366.48	29789			300	28849	300	33585
				300	28844	300	33594
				300	28849	303.2	33593
				300	28849	313.15	33652
				350	29081	313.2	33642
						323.2	33697
						333.15	33778
						333.2	33757
						343.2	33822

Table B-2 Flow Meter Calibration Data

Air Flow			Hydrogen Flow	
Setting	Flow(mL/s)	Flow (L/min)	Setting	Flow (mL/s)
2.0	34.426	2.066	50	0.736
2.0	34.375	2.063	100	1.622
2.0	32.432	1.946	150	2.496
1.75	28.125	1.688	200	3.341
1.75	27.647	1.659	250	3.974
1.75	27.160	1.630	300	4.591
1.5	24.519	1.471	350	5.626
1.5	26.000	1.560	400	6.198
1.5	25.278	1.517	450	7.020
1.25	20.769	1.246	500	7.750
1.25	21.074	1.264	550	8.578
1.25	21.121	1.267	600	9.792
1.0	17.473	1.048		
1.0	17.241	1.034		
1.0	16.827	1.010		
0.75	12.944	0.777		
0.75	12.640	0.758		
0.75	12.585	0.755		
0.75	12.981	0.779		
0.50	8.443	0.507		
0.50	8.405	0.504		
0.50	8.291	0.497		

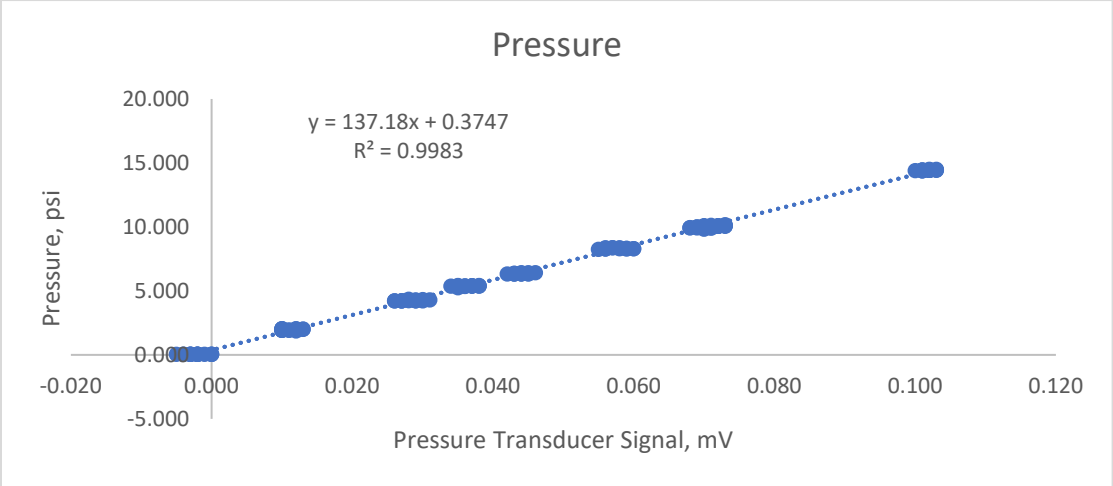

Figure B. 2 Pressure Calibration Curve

Table B-3 Pressure Calibration Curve Data

mV	P/psi	mV	P/psi	mV	P/psi	mV
-0.003	0.034	0.029	4.232	0.059	8.265	0.070
-0.004	0.034	0.028	4.242	0.056	8.277	0.071
-0.003	0.035	0.029	4.244	0.056	8.280	0.069
-0.002	0.035	0.029	4.279	0.058	8.284	0.070
-0.003	0.035	0.031	4.294	0.060	8.284	0.068
-0.004	0.035	0.030	4.302	0.060	8.294	0.068
-0.002	0.035	0.028	4.348	0.059	8.304	0.069
0.000	0.035	0.035	5.241	0.059	8.311	0.069
-0.001	0.035	0.035	5.338	0.058	8.320	0.070
0.000	0.035	0.035	5.345	0.056	8.321	0.070
-0.002	0.035	0.036	5.345	0.056	8.351	0.071
0.000	0.035	0.037	5.361	0.058	8.363	0.071
-0.002	0.035	0.038	5.366	0.057	8.369	0.071
-0.003	0.035	0.036	5.370	0.057	8.369	0.071
-0.005	0.035	0.034	5.374	0.070	9.818	0.071
-0.002	0.036	0.038	5.386	0.071	9.889	0.070
0.012	1.865	0.035	5.387	0.069	9.903	0.071
0.010	1.912	0.037	5.392	0.070	9.908	0.070
0.010	1.918	0.036	5.392	0.068	9.926	0.072
0.011	1.919	0.037	5.393	0.068	9.940	0.071
0.010	1.920	0.037	5.398	0.069	9.978	0.072
0.012	1.928	0.038	5.401	0.069	9.987	0.072
0.011	1.933	0.035	5.402	0.070	9.997	0.073
0.012	1.945	0.043	6.304	0.070	10.000	0.070
0.010	1.965	0.044	6.312	0.071	10.004	0.072
0.013	1.996	0.045	6.319	0.071	10.004	0.072
0.010	2.001	0.042	6.320	0.071	10.010	0.073
0.012	2.003	0.043	6.321	0.071	10.023	0.072
0.013	2.016	0.043	6.330	0.071	10.024	0.073
0.010	2.037	0.045	6.332	0.056	8.280	0.070
0.012	2.040	0.044	6.336	0.058	8.284	0.071
0.010	2.043	0.044	6.338	0.060	8.284	0.073
0.029	4.202	0.044	6.341	0.060	8.294	0.101
0.026	4.210	0.043	6.360	0.059	8.304	0.100
0.027	4.210	0.043	6.363	0.059	8.311	0.101
0.026	4.212	0.044	6.374	0.058	8.320	0.101
0.027	4.214	0.044	6.404	0.056	8.321	0.102
0.027	4.216	0.045	6.409	0.056	8.351	0.101
0.030	4.222	0.046	6.419	0.058	8.363	0.102
0.029	4.224	0.055	8.242	0.057	8.369	0.102
0.028	4.231	0.056	8.264	0.057	8.369	0.103

Table B-4 Mixture 10 C Reaction Data and Derivations

Time	mL H2o bur	Weight H2O	Pa/ psi	T reac	T_bur	mol H2 *10^3	mol SBH *10^2	V (mL)	C SBH Mol/L	X
0	8	11.1	15.3	285.8	300.3	0.00	2.44	5.00	4.87	0.00
100	8	11	15.5	288.0	300.2	0.0773	2.44	5.00	4.87	0.00
250	10	16.8	15.6	288.1	299.9	0.250	2.43	5.00	4.86	0.00
300	13	19.7	15.6	288.4	299.8	0.380	2.43	4.99	4.86	0.00
350	16	23.4	15.6	288.4	299.8	0.509	2.42	4.99	4.86	0.01
400	19	26.3	15.6	287.0	299.8	0.638	2.42	4.99	4.85	0.01
450	22	29.6	15.6	288.4	299.8	0.767	2.42	4.99	4.85	0.01
500	26	32.7	15.6	287.4	299.8	0.940	2.41	4.99	4.84	0.01
550	29	35.9	15.6	287.5	299.8	1.07	2.41	4.99	4.83	0.01
600	32	39	15.6	287.1	299.8	1.20	2.41	4.98	4.83	0.01
650	35	42.5	15.6	287.2	299.7	1.33	2.40	4.98	4.82	0.01
700	37	46.5	15.6	287.0	298.7	1.42	2.40	4.98	4.82	0.01
750	39.5	47.9	15.6	287.0	298.3	1.53	2.40	4.98	4.82	0.02
800	43	52.2	15.6	287.0	298.1	1.68	2.39	4.98	4.81	0.02
850	46	54.8	15.6	287.2	297.9	1.82	2.39	4.98	4.81	0.02
900	49	57.5	15.6	287.2	297.8	1.94	2.39	4.97	4.80	0.02
950	52	60.5	15.6	287.2	297.8	2.07	2.39	4.97	4.80	0.02
1000	55	63.9	15.6	287.2	297.8	2.20	2.38	4.97	4.79	0.02
1100	61	70.1	15.6	287.4	297.7	2.47	2.38	4.97	4.78	0.03
1200	67	76	15.6	287.6	297.5	2.73	2.37	4.96	4.77	0.03
1300	73	82	15.6	287.7	297.4	2.99	2.36	4.96	4.76	0.03
1700	96	105.3	15.6	286.6	296.6	4.00	2.34	4.95	4.72	0.04
1900	108	116.5	15.6	286.8	296.7	4.54	2.32	4.94	4.70	0.05
2100	120	127.4	15.6	287.0	296.7	5.05	2.31	4.93	4.68	0.05
2300	123	131.6	15.6	287.3	296.8	5.17	2.31	4.93	4.68	0.05
2750	127	135.3	15.6	287.0	296.3	5.37	2.30	4.93	4.67	0.06

Mass/g SBH 1	Mass/g SBH 2	Difference	mL input
0.9224	0.0005	0.9219	5

Table B-5 Mixture 10 C Part 2 Reaction Data and Derivations

Time	mL H2o	g H2O	Pa/ psi	T_r	T_b	Mol H_2 *10^3	Mol SBH *10^3	V mL Solxn	C SBH Mol/L	X
0	2	-0.5	15.2	289.0	296.2	0.00	25.88	5.00	5.18	0.000
10	5	10	15.3	288.8	295.9	0.47	25.76	4.99	5.16	0.005
30	11	14	15.3	288.8	295.7	0.73	25.70	4.99	5.15	0.007
50	18	21	15.3	288.8	295.6	1.03	25.62	4.99	5.14	0.010
70	24	26.4	15.3	288.8	295.6	1.29	25.56	4.98	5.13	0.012
100	31	33.6	15.3	288.8	295.6	1.59	25.48	4.98	5.12	0.015
120	36	38	15.3	288.8	295.6	1.80	25.43	4.98	5.11	0.017
140	40	42.2	15.3	288.8	295.5	1.98	25.39	4.97	5.10	0.019
160	45	47	15.3	288.8	295.5	2.19	25.33	4.97	5.10	0.021
180	48	51	15.3	288.8	295.5	2.32	25.30	4.97	5.09	0.022
200	52	53.5	15.3	288.8	295.6	2.49	25.26	4.97	5.08	0.024
220	56	57.5	15.3	288.8	295.6	2.66	25.21	4.96	5.08	0.026
240	59	61	15.3	288.8	295.6	2.79	25.18	4.96	5.07	0.027
260	62	64	15.3	288.9	295.6	2.92	25.15	4.96	5.07	0.028
280	66	67.2	15.3	288.9	295.6	3.09	25.11	4.96	5.06	0.030
300	69	70.3	15.3	288.9	295.6	3.22	25.07	4.96	5.06	0.031
320	72	73.5	15.3	288.9	295.6	3.34	25.04	4.96	5.05	0.032

360	78	79.4	15.3	288.9	295.6	3.60	24.98	4.95	5.04	0.035
400	84	85.5	15.3	288.9	295.5	3.87	24.91	4.95	5.03	0.037
440	90	90.8	15.3	288.9	295.5	4.12	24.85	4.95	5.02	0.040
480	95	96.2	15.3	288.9	295.5	4.33	24.80	4.94	5.02	0.042
520	101	101.5	15.3	288.9	295.5	4.59	24.73	4.94	5.01	0.044
560	106	106.6	15.3	288.9	295.5	4.81	24.68	4.94	5.00	0.046
600	111	111.5	15.3	288.9	295.5	5.02	24.62	4.93	4.99	0.048
640	116	116.5	15.3	288.9	295.4	5.24	24.57	4.93	4.98	0.051
680	121	121.4	15.3	289.0	295.4	5.46	24.51	4.93	4.97	0.053
740	128	128.4	15.3	289.0	295.4	5.75	24.44	4.92	4.96	0.056
760	131	130.6	15.3	289.0	295.4	5.88	24.41	4.92	4.96	0.057
800	136	135	15.3	289.0	295.4	6.10	24.36	4.92	4.95	0.059
840	140	140	15.3	289.0	295.5	6.27	24.31	4.92	4.94	0.061
880	145	144.2	15.3	289.0	295.5	6.50	24.25	4.91	4.94	0.063
920	149	148.5	15.3	289.0	295.5	6.66	24.21	4.91	4.93	0.064
960	154	152.7	15.3	289.0	295.5	6.87	24.16	4.91	4.92	0.066
1000	158	157.4	15.3	289.0	295.5	7.04	24.12	4.91	4.92	0.068
1040	162	161	15.3	289.0	295.5	7.21	24.08	4.90	4.91	0.070
1080	166	164.9	15.2	289.0	295.6	7.33	24.05	4.90	4.90	0.071
1120	170	169	15.3	289.1	295.6	7.57	23.99	4.90	4.90	0.073
1160	174	172.8	15.3	289.1	295.6	7.72	23.95	4.90	4.89	0.075
1200	178	176.4	15.3	289.1	295.6	7.91	23.90	4.90	4.88	0.076
1240	182	180.5	15.3	289.1	295.5	8.07	23.86	4.89	4.88	0.078
1280	186	184	15.3	289.1	295.6	8.24	23.82	4.89	4.87	0.080
1320	190	187.5	15.3	289.1	295.6	8.42	23.77	4.89	4.86	0.081
1360	193	191.4	15.4	289.1	295.6	8.57	23.74	4.89	4.86	0.083
1400	197	194.8	15.3	289.1	295.6	8.72	23.70	4.88	4.85	0.084
	mL input		Mass/g SBH 1		Mass/g SBH 2		Difference			
	5		0.9803		0.0013		0.979			

Table B-6 Mixture Second Room Temperature Reaction and Derivation Data

Time	mL H2o	g H2O	Pa/ psi	T_r	T_b	Mol H_2 *10^3	Mol SBH *10^3	V mL Solxn	C SBH Mol/L	X
0	-5	4.8	15.1	291.5	297.3	0.00	17.48	5.00	3.50	0.000
1100	-5	6.2	15.7	291.9	295.9	0.26	17.41	5.00	3.48	0.004
1150	0	9.2	15.7	291.9	295.9	0.57	17.33	4.99	3.47	0.008
1200	2	16.3	15.7	291.9	295.9	0.66	17.31	4.99	3.47	0.009
1250	8	22.9	15.8	291.9	295.9	0.93	17.25	4.99	3.46	0.013
1300	15	29	15.7	291.7	295.9	1.24	17.17	4.98	3.45	0.018
1350	22	35.2	15.8	291.7	295.9	1.55	17.09	4.98	3.43	0.022
1400	30	43	15.8	291.7	295.9	1.90	17.00	4.97	3.42	0.027
1450	35	48.6	15.8	291.7	295.9	2.13	16.95	4.97	3.41	0.030
1500	41	54	15.8	291.7	295.9	2.39	16.88	4.97	3.40	0.034
1550	47	60.5	15.8	291.7	295.9	2.65	16.81	4.96	3.39	0.038
1600	53	66.9	15.8	291.8	295.8	2.92	16.75	4.96	3.38	0.042
1650	60	72.6	15.8	291.8	295.9	3.23	16.67	4.96	3.36	0.046
1700	65	78.9	15.8	291.8	295.9	3.45	16.62	4.95	3.35	0.049
1750	71	84	15.8	291.8	295.9	3.71	16.55	4.95	3.34	0.053
1800	77	89.9	15.8	291.8	295.9	3.98	16.48	4.95	3.33	0.057
1850	83	95.4	15.8	291.8	295.9	4.25	16.42	4.94	3.32	0.061
1900	88	100.9	15.8	291.8	295.9	4.47	16.36	4.94	3.31	0.064
1950	94	106.3	15.8	291.8	295.9	4.73	16.29	4.94	3.30	0.068

2000	99	111.8	15.8	291.8	295.9	4.95	16.24	4.93	3.29	0.071
2050	104	117.2	15.8	291.9	295.9	5.18	16.18	4.93	3.28	0.074
2100	109	122.5	15.8	291.9	295.9	5.40	16.13	4.93	3.27	0.077
2150	115	127.3	15.8	291.9	295.9	5.67	16.06	4.92	3.26	0.081
2200	120	132.3	15.8	291.9	295.9	5.89	16.01	4.92	3.25	0.084
2250	125	137	15.8	291.9	295.9	6.12	15.95	4.92	3.24	0.088
2300	130	141.5	15.8	291.9	296.0	6.33	15.89	4.92	3.23	0.091
2350	134	146.5	15.8	291.9	296.0	6.51	15.85	4.91	3.23	0.093
2400	139	151	15.8	291.9	296.0	6.73	15.80	4.91	3.22	0.096
2450	144	155.5	15.8	291.9	296.0	6.95	15.74	4.91	3.21	0.099
2500	149	160.1	15.8	291.9	296.1	7.16	15.69	4.91	3.20	0.102
2550	153	164.5	15.8	291.9	296.1	7.34	15.64	4.90	3.19	0.105
2600	157	168.4	15.8	291.9	296.1	7.52	15.60	4.90	3.18	0.108
Mass/g SBH 1			Mass/g SBH 2			Difference			mL input	
0.6772			0.016			0.6612			5	

Table B-7 Mixture Second Room Temperature Reaction and Derivation Data

Time	mL H2o bur	Weight H2O	Pa/ psi	T_r	T_b	Mol H_2 *10^3	Mol SBH *10^3	V mL Solxn	C SBH Mol/L	X
0	0	8.8	15.5	296.7	298.8	0.00	14.02	5.00	2.80	0.000
30	1	14.5	15.7	296.8	298.6	0.48	13.89	4.99	2.78	0.009
50	8	20	15.6	296.8	298.6	0.79	13.82	4.99	2.77	0.014
70	14	26.2	15.7	296.8	298.5	1.05	13.75	4.99	2.76	0.019
90	19	31.8	15.7	296.7	298.5	1.27	13.70	4.98	2.75	0.023
110	25	38.4	15.7	296.8	298.5	1.53	13.63	4.98	2.74	0.027
130	31	42.5	15.6	296.7	298.5	1.79	13.57	4.98	2.73	0.032
150	36	48.3	15.7	296.7	298.5	2.01	13.51	4.97	2.72	0.036
170	42	53.9	15.7	296.1	298.5	2.27	13.45	4.97	2.71	0.040
190	47	58.3	15.7	298.1	298.5	2.49	13.39	4.97	2.70	0.044
210	52	64.2	15.7	298.1	298.5	2.70	13.34	4.96	2.69	0.048
230	58	68.6	15.6	298.1	298.5	2.96	13.28	4.96	2.68	0.053
250	62	73.3	15.7	298.1	298.5	3.14	13.23	4.96	2.67	0.056
270	67	78.4	15.7	298.0	298.5	3.36	13.18	4.96	2.66	0.060
290	71	82.9	15.6	298.1	298.5	3.53	13.13	4.95	2.65	0.063
310	76	87.8	15.7	298.0	298.4	3.75	13.08	4.95	2.64	0.067
330	81	92.5	15.7	298.1	298.5	3.98	13.02	4.95	2.63	0.071
350	86	96.8	15.7	298.1	298.4	4.19	12.97	4.94	2.62	0.075
370	91	101.5	15.6	298.1	298.5	4.39	12.92	4.94	2.61	0.078
390	95	105.9	15.7	298.1	298.5	4.58	12.87	4.94	2.61	0.082
410	99	111	15.7	298.0	298.5	4.75	12.83	4.94	2.60	0.085
430	103	114.9	15.7	298.0	298.5	4.92	12.78	4.93	2.59	0.088
450	108	119.3	15.7	298.0	298.5	5.15	12.73	4.93	2.58	0.092
470	111	123.5	15.7	298.1	298.5	5.27	12.70	4.93	2.58	0.094
490	116	127.2	15.7	298.1	298.5	5.49	12.64	4.93	2.57	0.098
510	120	131.3	15.6	298.0	298.5	5.66	12.60	4.93	2.56	0.101
530	124	135.5	15.7	298.0	298.5	5.85	12.55	4.92	2.55	0.104
550	128	139.3	15.7	298.0	298.5	6.03	12.51	4.92	2.54	0.108
570	132	143.2	15.6	298.0	298.6	6.18	12.47	4.92	2.54	0.110
590	136	147.3	15.7	298.0	298.6	6.36	12.42	4.92	2.53	0.113
610	140	151	15.6	298.0	298.6	6.52	12.38	4.91	2.52	0.116
630	144	154.5	15.7	298.0	298.6	6.71	12.34	4.91	2.51	0.120
650	147	158.4	15.6	298.0	298.6	6.83	12.31	4.91	2.51	0.122
670	151	161.9	15.6	298.0	298.6	7.00	12.26	4.91	2.50	0.125

690	155	165.8	15.6	298.0	298.6	7.18	12.22	4.91	2.49	0.128
710	158	169.4	15.6	298.0	298.6	7.31	12.19	4.90	2.49	0.130
730	162	172.7	15.7	298.0	298.6	7.48	12.14	4.90	2.48	0.134
750	166	176	15.7	298.0	298.6	7.66	12.10	4.90	2.47	0.137
770	169	179.5	15.6	298.0	298.5	7.78	12.07	4.90	2.46	0.139
790	172	183	15.7	298.0	298.6	7.92	12.04	4.90	2.46	0.141
810	175	186.4	15.6	298.0	298.6	8.04	12.01	4.89	2.45	0.143
830	179	189.6	15.6	298.0	298.6	8.22	11.96	4.89	2.45	0.147
850	182	192.7	15.6	298.0	298.6	8.35	11.93	4.89	2.44	0.149
870	186	196.3	15.7	297.9	298.6	8.53	11.88	4.89	2.43	0.152
890	189	199	15.7	298.0	298.6	8.66	11.85	4.89	2.43	0.154
910	192	202.4	15.6	298.0	298.6	8.78	11.82	4.88	2.42	0.157
930	194	205	15.7	298.0	298.6	8.87	11.80	4.88	2.42	0.158
950	197	207.5	15.6	297.9	298.6	8.99	11.77	4.88	2.41	0.160
970	200	210	15.7	297.9	298.6	9.14	11.73	4.88	2.40	0.163
990	203	212.5	15.7	298.0	298.6	9.27	11.70	4.88	2.40	0.165
1010	206	215.3	15.6	298.0	298.6	9.38	11.67	4.88	2.39	0.167
1050	210	220	15.6	297.9	298.7	9.56	11.63	4.87	2.39	0.170
1070	212	222.5	15.6	297.9	298.7	9.63	11.61	4.87	2.38	0.172
1100	216	226	15.7	297.9	298.7	9.83	11.56	4.87	2.37	0.175
1200	227	237	15.7	297.9	298.7	10.32	11.44	4.86	2.35	0.184
1250	233	242.4	15.6	297.9	298.7	10.54	11.38	4.86	2.34	0.188
1300	237	247.3	15.6	297.9	298.7	10.73	11.33	4.86	2.33	0.191
1350	242	252	15.7	297.8	298.7	10.96	11.28	4.85	2.32	0.195

Mass/g SBH 1	Mass/g SBH 2	Difference	mL input
0.5349	0.0047	0.5302	5

Table B-8 Mixture 10 C Reaction Model Data

t	x	V	Ca	rA		a1	a0
0.0	0.0000	0.0050	4.874	-8.67E-05	Coefficients	1.73E-05	0.000204
68	0.0012	0.0050	4.870	-8.66E-05	Std.dev.s	1.11E-08	1.78E-05
90	0.0016	0.0050	4.868	-8.66E-05	R2, SE (y)	0.99996	8.8E-05
112	0.0020	0.0050	4.867	-8.65E-05	95% conf. int.	2.17E-08	3.49E-05
156	0.0028	0.0050	4.864	-8.65E-05	Variance	7.74E-09	
178	0.0032	0.0050	4.862	-8.65E-05	SS	7.59E-07	
200	0.0036	0.0050	4.861	-8.64E-05			
232	0.0041	0.0050	4.859	-8.64E-05	Model	x = a1 * t + a0	
254	0.0045	0.0050	4.858	-8.64E-05			
279	0.0050	0.0050	4.856	-8.64E-05			
303	0.0054	0.0050	4.854	-8.63E-05			
342	0.0061	0.0050	4.852	-8.63E-05			
376	0.0067	0.0050	4.850	-8.62E-05			
398	0.0070	0.0050	4.848	-8.62E-05			
426	0.0075	0.0050	4.847	-8.62E-05			
448	0.0079	0.0050	4.845	-8.62E-05			
470	0.0083	0.0050	4.844	-8.61E-05			
498	0.0088	0.0050	4.842	-8.61E-05			
529	0.0094	0.0050	4.840	-8.61E-05			
551	0.0097	0.0050	4.839	-8.61E-05			
582	0.0103	0.0050	4.837	-8.60E-05			
607	0.0107	0.0050	4.835	-8.60E-05			

651	0.0115	0.0050	4.832	-8.59E-05
672	0.0119	0.0050	4.831	-8.59E-05
692	0.0122	0.0050	4.830	-8.59E-05
727	0.0128	0.0050	4.827	-8.58E-05
749	0.0132	0.0050	4.826	-8.58E-05
777	0.0137	0.0050	4.824	-8.58E-05
799	0.0141	0.0050	4.823	-8.58E-05
844	0.0149	0.0050	4.820	-8.57E-05
862	0.0152	0.0050	4.819	-8.57E-05
882	0.0156	0.0050	4.817	-8.57E-05
908	0.0160	0.0050	4.816	-8.56E-05
935	0.0165	0.0050	4.814	-8.56E-05
967	0.0171	0.0050	4.812	-8.56E-05
1005	0.0177	0.0050	4.810	-8.55E-05
1025	0.0181	0.0050	4.808	-8.55E-05
1046	0.0184	0.0050	4.807	-8.55E-05
1082	0.0191	0.0050	4.805	-8.54E-05
1103	0.0194	0.0050	4.803	-8.54E-05
1132	0.0199	0.0050	4.802	-8.54E-05
1155	0.0203	0.0050	4.800	-8.54E-05
1199	0.0211	0.0050	4.797	-8.53E-05
1218	0.0214	0.0050	4.796	-8.53E-05
1238	0.0218	0.0050	4.795	-8.53E-05
1273	0.0224	0.0050	4.793	-8.52E-05
1313	0.0231	0.0050	4.790	-8.52E-05
1324	0.0233	0.0050	4.789	-8.52E-05
1362	0.0239	0.0050	4.787	-8.51E-05
1383	0.0243	0.0050	4.786	-8.51E-05
1404	0.0247	0.0050	4.784	-8.51E-05
1439	0.0253	0.0050	4.782	-8.50E-05
1461	0.0256	0.0050	4.781	-8.50E-05
1490	0.0262	0.0050	4.779	-8.50E-05
1513	0.0265	0.0050	4.777	-8.50E-05
1558	0.0273	0.0050	4.775	-8.49E-05
1577	0.0276	0.0050	4.773	-8.49E-05
1597	0.0280	0.0050	4.772	-8.49E-05
1623	0.0284	0.0050	4.770	-8.48E-05
1651	0.0289	0.0050	4.769	-8.48E-05
1684	0.0295	0.0050	4.767	-8.48E-05
1722	0.0302	0.0050	4.764	-8.47E-05
1743	0.0305	0.0050	4.763	-8.47E-05
1764	0.0309	0.0050	4.761	-8.47E-05
1800	0.0315	0.0050	4.759	-8.46E-05
1822	0.0319	0.0050	4.758	-8.46E-05
1852	0.0324	0.0050	4.756	-8.46E-05
1874	0.0328	0.0050	4.755	-8.46E-05
1898	0.0332	0.0050	4.753	-8.45E-05
1927	0.0337	0.0050	4.751	-8.45E-05
1960	0.0342	0.0050	4.749	-8.45E-05
1980	0.0346	0.0050	4.748	-8.44E-05
2014	0.0352	0.0050	4.746	-8.44E-05
2036	0.0356	0.0050	4.744	-8.44E-05
2063	0.0360	0.0050	4.743	-8.43E-05

2093	0.0365	0.0050	4.741	-8.43E-05
2128	0.0371	0.0050	4.738	-8.43E-05
2145	0.0374	0.0050	4.737	-8.43E-05
2186	0.0381	0.0050	4.735	-8.42E-05
2217	0.0387	0.0049	4.733	-8.42E-05
2239	0.0390	0.0049	4.732	-8.41E-05
2263	0.0395	0.0049	4.730	-8.41E-05
2285	0.0398	0.0049	4.729	-8.41E-05
2325	0.0405	0.0049	4.726	-8.40E-05
2340	0.0408	0.0049	4.725	-8.40E-05
2381	0.0415	0.0049	4.723	-8.40E-05
2409	0.0419	0.0049	4.721	-8.40E-05
2431	0.0423	0.0049	4.719	-8.39E-05
2453	0.0427	0.0049	4.718	-8.39E-05
2475	0.0431	0.0049	4.717	-8.39E-05
2512	0.0437	0.0049	4.714	-8.38E-05
2533	0.0440	0.0049	4.713	-8.38E-05
2564	0.0446	0.0049	4.711	-8.38E-05
2586	0.0449	0.0049	4.710	-8.38E-05
2633	0.0457	0.0049	4.707	-8.37E-05
2640	0.0459	0.0049	4.706	-8.37E-05
2674	0.0464	0.0049	4.704	-8.37E-05
2708	0.0470	0.0049	4.702	-8.36E-05
2730	0.0474	0.0049	4.701	-8.36E-05
2750	0.0477	0.0049	4.699	-8.36E-05

Table B-9 Mixture 10 C Second Reaction Model Data

t	x	V mL	Ca	rA		a1	a0
0	0	5.00	5.176	-1.16E-04	**Coefficients**	2.2E-05	8.45E-05
36	8.01E-04	5.00	5.173	-1.16E-04	**Std.dev.s**	8.98E-09	7.35E-06
47	1.05E-03	5.00	5.172	-1.16E-04	**R2, SE (y)**	0.999984	3.63E-05
58	1.30E-03	5.00	5.171	-1.16E-04	**95% conf. int.**	1.76E-08	1.44E-05
81	1.80E-03	5.00	5.169	-1.16E-04	**Variance**	1.32E-09	
92	2.05E-03	5.00	5.168	-1.16E-04	**SS**	1.29E-07	
103	2.30E-03	5.00	5.167	-1.16E-04			
114	2.55E-03	5.00	5.166	-1.16E-04	Model	x = a1 * t + a0	
137	3.05E-03	5.00	5.164	-1.16E-04			
143	3.20E-03	5.00	5.164	-1.16E-04			
162	3.61E-03	5.00	5.162	-1.15E-04			
172	3.85E-03	4.99	5.161	-1.15E-04			
184	4.10E-03	4.99	5.160	-1.15E-04			
205	4.58E-03	4.99	5.159	-1.15E-04			
215	4.79E-03	4.99	5.158	-1.15E-04			
235	5.24E-03	4.99	5.156	-1.15E-04			
238	5.31E-03	4.99	5.156	-1.15E-04			
262	5.84E-03	4.99	5.154	-1.15E-04			
272	6.06E-03	4.99	5.153	-1.15E-04			
285	6.35E-03	4.99	5.152	-1.15E-04			
295	6.59E-03	4.99	5.151	-1.15E-04			
308	6.86E-03	4.99	5.150	-1.15E-04			
327	7.28E-03	4.99	5.148	-1.15E-04			

338	7.52E-03	4.99	5.148	-1.15E-04
355	7.91E-03	4.99	5.146	-1.15E-04
366	8.16E-03	4.99	5.145	-1.15E-04
381	8.48E-03	4.99	5.144	-1.15E-04
402	8.95E-03	4.99	5.142	-1.15E-04
407	9.06E-03	4.99	5.142	-1.15E-04
424	9.44E-03	4.99	5.140	-1.15E-04
435	9.68E-03	4.99	5.139	-1.15E-04
454	1.01E-02	4.99	5.138	-1.15E-04
465	1.03E-02	4.99	5.137	-1.15E-04
481	1.07E-02	4.99	5.136	-1.15E-04
492	1.09E-02	4.98	5.135	-1.15E-04
505	1.12E-02	4.98	5.134	-1.15E-04
526	1.17E-02	4.98	5.132	-1.15E-04
537	1.19E-02	4.98	5.131	-1.15E-04
547	1.22E-02	4.98	5.130	-1.15E-04
568	1.26E-02	4.98	5.128	-1.15E-04
577	1.28E-02	4.98	5.128	-1.15E-04
597	1.33E-02	4.98	5.126	-1.15E-04
604	1.34E-02	4.98	5.125	-1.15E-04
623	1.38E-02	4.98	5.124	-1.15E-04
633	1.41E-02	4.98	5.123	-1.15E-04
645	1.43E-02	4.98	5.122	-1.15E-04
666	1.48E-02	4.98	5.120	-1.15E-04
676	1.50E-02	4.98	5.119	-1.15E-04
697	1.55E-02	4.98	5.118	-1.14E-04
700	1.55E-02	4.98	5.117	-1.14E-04
724	1.61E-02	4.98	5.115	-1.14E-04
730	1.62E-02	4.98	5.115	-1.14E-04
748	1.66E-02	4.98	5.113	-1.14E-04
759	1.68E-02	4.98	5.112	-1.14E-04
780	1.73E-02	4.98	5.111	-1.14E-04
791	1.75E-02	4.98	5.110	-1.14E-04
800	1.77E-02	4.98	5.109	-1.14E-04
820	1.82E-02	4.98	5.107	-1.14E-04
827	1.83E-02	4.97	5.107	-1.14E-04
846	1.87E-02	4.97	5.105	-1.14E-04
856	1.90E-02	4.97	5.104	-1.14E-04
868	1.92E-02	4.97	5.103	-1.14E-04
889	1.97E-02	4.97	5.101	-1.14E-04
899	1.99E-02	4.97	5.101	-1.14E-04
920	2.04E-02	4.97	5.099	-1.14E-04
928	2.05E-02	4.97	5.098	-1.14E-04
948	2.10E-02	4.97	5.097	-1.14E-04
954	2.11E-02	4.97	5.096	-1.14E-04
972	2.15E-02	4.97	5.095	-1.14E-04
983	2.17E-02	4.97	5.094	-1.14E-04
1004	2.22E-02	4.97	5.092	-1.14E-04
1015	2.24E-02	4.97	5.091	-1.14E-04
1024	2.26E-02	4.97	5.090	-1.14E-04
1044	2.31E-02	4.97	5.089	-1.14E-04
1051	2.32E-02	4.97	5.088	-1.14E-04
1070	2.36E-02	4.97	5.086	-1.14E-04

1080	2.39E-02	4.97	5.086	-1.14E-04
1093	2.41E-02	4.97	5.085	-1.14E-04
1114	2.46E-02	4.97	5.083	-1.14E-04
1124	2.48E-02	4.97	5.082	-1.14E-04
1145	2.53E-02	4.97	5.080	-1.14E-04
1148	2.54E-02	4.97	5.080	-1.14E-04
1173	2.59E-02	4.96	5.078	-1.14E-04
1179	2.60E-02	4.96	5.077	-1.14E-04
1197	2.64E-02	4.96	5.076	-1.14E-04
1208	2.67E-02	4.96	5.075	-1.14E-04
1219	2.69E-02	4.96	5.074	-1.14E-04
1240	2.74E-02	4.96	5.072	-1.13E-04
1249	2.76E-02	4.96	5.072	-1.13E-04
1270	2.80E-02	4.96	5.070	-1.13E-04
1277	2.82E-02	4.96	5.069	-1.13E-04
1296	2.86E-02	4.96	5.068	-1.13E-04
1306	2.88E-02	4.96	5.067	-1.13E-04
1319	2.91E-02	4.96	5.066	-1.13E-04
1340	2.95E-02	4.96	5.064	-1.13E-04
1345	2.96E-02	4.96	5.064	-1.13E-04
1360	3.00E-02	4.96	5.062	-1.13E-04
1372	3.02E-02	4.96	5.061	-1.13E-04
1388	3.06E-02	4.96	5.060	-1.13E-04
1400	3.08E-02	4.96	5.059	-1.13E-04

Table B-10 Mixture Room Temperature Reaction Model Data

t	x	V	Ca	rA		a1	a0
0	0.00E+00	5.00E-03	3.496	-1.93E-04	**Coefficients**	5.12E-05	0.001687
65	3.55E-03	5.00E-03	3.486	-1.92E-04	**Std.dev.s**	9.59E-08	0.000146
85	4.69E-03	5.00E-03	3.482	-1.92E-04	**R2, SE (y)**	0.999657	0.000721
106	5.83E-03	4.99E-03	3.479	-1.92E-04	**95% conf. int.**	1.88E-07	0.000286
148	8.11E-03	4.99E-03	3.473	-1.91E-04	**Variance**	5.2E-07	
169	9.25E-03	4.99E-03	3.469	-1.91E-04	**SS**	5.09E-05	
189	1.04E-02	4.99E-03	3.466	-1.91E-04			
210	1.15E-02	4.99E-03	3.463	-1.91E-04	Model	x = a1 * t + a0	
238	1.30E-02	4.99E-03	3.458	-1.91E-04			
260	1.42E-02	4.99E-03	3.455	-1.90E-04			
302	1.65E-02	4.98E-03	3.449	-1.90E-04			
319	1.74E-02	4.98E-03	3.446	-1.90E-04			
338	1.85E-02	4.98E-03	3.443	-1.90E-04			
372	2.03E-02	4.98E-03	3.438	-1.89E-04			
410	2.23E-02	4.98E-03	3.432	-1.89E-04			
420	2.29E-02	4.98E-03	3.430	-1.89E-04			
455	2.48E-02	4.98E-03	3.425	-1.89E-04			
475	2.58E-02	4.98E-03	3.422	-1.88E-04			
495	2.69E-02	4.98E-03	3.419	-1.88E-04			
529	2.87E-02	4.97E-03	3.413	-1.88E-04			
549	2.98E-02	4.97E-03	3.410	-1.88E-04			
578	3.13E-02	4.97E-03	3.406	-1.88E-04			
598	3.24E-02	4.97E-03	3.403	-1.87E-04			
641	3.47E-02	4.97E-03	3.396	-1.87E-04			

659	3.57E-02	4.97E-03	3.393	-1.87E-04
679	3.67E-02	4.97E-03	3.391	-1.87E-04
703	3.80E-02	4.96E-03	3.387	-1.87E-04
730	3.94E-02	4.96E-03	3.383	-1.86E-04
761	4.10E-02	4.96E-03	3.378	-1.86E-04
796	4.29E-02	4.96E-03	3.372	-1.86E-04
817	4.40E-02	4.96E-03	3.369	-1.86E-04
837	4.50E-02	4.96E-03	3.366	-1.85E-04
871	4.68E-02	4.96E-03	3.361	-1.85E-04
891	4.79E-02	4.96E-03	3.358	-1.85E-04
920	4.94E-02	4.95E-03	3.354	-1.85E-04
941	5.05E-02	4.95E-03	3.351	-1.85E-04
964	5.17E-02	4.95E-03	3.347	-1.84E-04
991	5.31E-02	4.95E-03	3.343	-1.84E-04
1022	5.47E-02	4.95E-03	3.338	-1.84E-04
1042	5.58E-02	4.95E-03	3.335	-1.84E-04
1073	5.74E-02	4.95E-03	3.331	-1.83E-04
1094	5.85E-02	4.95E-03	3.327	-1.83E-04
1120	5.98E-02	4.94E-03	3.323	-1.83E-04
1149	6.13E-02	4.94E-03	3.319	-1.83E-04
1182	6.30E-02	4.94E-03	3.314	-1.83E-04
1198	6.38E-02	4.94E-03	3.312	-1.82E-04
1237	6.58E-02	4.94E-03	3.306	-1.82E-04
1249	6.65E-02	4.94E-03	3.304	-1.82E-04
1286	6.84E-02	4.94E-03	3.298	-1.82E-04
1310	6.96E-02	4.94E-03	3.295	-1.82E-04
1330	7.06E-02	4.93E-03	3.292	-1.81E-04
1368	7.26E-02	4.93E-03	3.286	-1.81E-04
1388	7.36E-02	4.93E-03	3.283	-1.81E-04
1420	7.52E-02	4.93E-03	3.278	-1.81E-04
1441	7.63E-02	4.93E-03	3.275	-1.80E-04
1467	7.76E-02	4.93E-03	3.271	-1.80E-04
1488	7.87E-02	4.93E-03	3.268	-1.80E-04
1509	7.98E-02	4.93E-03	3.265	-1.80E-04
1535	8.11E-02	4.92E-03	3.261	-1.80E-04
1565	8.26E-02	4.92E-03	3.257	-1.79E-04
1586	8.36E-02	4.92E-03	3.254	-1.79E-04
1614	8.51E-02	4.92E-03	3.250	-1.79E-04
1638	8.63E-02	4.92E-03	3.246	-1.79E-04
1680	8.83E-02	4.92E-03	3.240	-1.78E-04
1699	8.93E-02	4.92E-03	3.237	-1.78E-04
1718	9.03E-02	4.92E-03	3.234	-1.78E-04
1743	9.15E-02	4.92E-03	3.231	-1.78E-04
1770	9.29E-02	4.91E-03	3.227	-1.78E-04
1794	9.41E-02	4.91E-03	3.223	-1.78E-04
1838	9.63E-02	4.91E-03	3.217	-1.77E-04
1847	9.67E-02	4.91E-03	3.215	-1.77E-04
1880	9.84E-02	4.91E-03	3.210	-1.77E-04
1916	1.00E-01	4.91E-03	3.205	-1.77E-04
1936	1.01E-01	4.91E-03	3.202	-1.76E-04
1966	1.03E-01	4.90E-03	3.198	-1.76E-04
1987	1.04E-01	4.90E-03	3.195	-1.76E-04
2011	1.05E-01	4.90E-03	3.191	-1.76E-04

2032	1.06E-01	4.90E-03	3.188	-1.76E-04
2071	1.08E-01	4.90E-03	3.183	-1.75E-04
2086	1.09E-01	4.90E-03	3.180	-1.75E-04
2124	1.10E-01	4.90E-03	3.175	-1.75E-04
2136	1.11E-01	4.90E-03	3.173	-1.75E-04
2172	1.13E-01	4.90E-03	3.168	-1.75E-04
2194	1.14E-01	4.89E-03	3.165	-1.74E-04
2215	1.15E-01	4.89E-03	3.162	-1.74E-04
2251	1.17E-01	4.89E-03	3.156	-1.74E-04
2271	1.18E-01	4.89E-03	3.154	-1.74E-04
2301	1.19E-01	4.89E-03	3.149	-1.73E-04
2322	1.20E-01	4.89E-03	3.146	-1.73E-04
2347	1.21E-01	4.89E-03	3.143	-1.73E-04
2368	1.22E-01	4.89E-03	3.140	-1.73E-04
2407	1.24E-01	4.88E-03	3.134	-1.73E-04
2422	1.25E-01	4.88E-03	3.132	-1.73E-04
2461	1.27E-01	4.88E-03	3.126	-1.72E-04
2473	1.27E-01	4.88E-03	3.124	-1.72E-04
2510	1.29E-01	4.88E-03	3.119	-1.72E-04
2532	1.30E-01	4.88E-03	3.116	-1.72E-04
2552	1.31E-01	4.88E-03	3.113	-1.71E-04
2589	1.33E-01	4.88E-03	3.108	-1.71E-04
2600	1.33E-01	4.88E-03	3.106	-1.71E-04

Table B-11 Mixture Room Temperature Second Reaction Model Data

t	x	V	Ca	rA		a1	a0
0	0.00E+00	5.00E-03	2.803	-5.12E-04	**Coefficients**	0.000162	0.004809
35	6.31E-03	5.00E-03	2.788	-5.10E-04	**Std.dev.s**	5.19E-07	0.000409
45	8.27E-03	4.99E-03	2.783	-5.09E-04	**R2, SE (y)**	0.998991	0.00202
56	1.02E-02	4.99E-03	2.779	-5.08E-04	**95% conf. int.**	1.02E-06	0.000801
78	1.41E-02	4.99E-03	2.769	-5.06E-04	**Variance**	4.08E-06	
89	1.61E-02	4.99E-03	2.765	-5.05E-04	**SS**	0.0004	
99	1.80E-02	4.99E-03	2.760	-5.05E-04			
110	1.99E-02	4.99E-03	2.755	-5.04E-04	Model	x = a1 * t + a0	
132	2.38E-02	4.98E-03	2.746	-5.02E-04			
135	2.44E-02	4.98E-03	2.745	-5.02E-04			
159	2.86E-02	4.98E-03	2.735	-5.00E-04			
165	2.97E-02	4.98E-03	2.732	-4.99E-04			
183	3.29E-02	4.98E-03	2.724	-4.98E-04			
193	3.47E-02	4.97E-03	2.720	-4.97E-04			
204	3.66E-02	4.97E-03	2.715	-4.96E-04			
224	4.02E-02	4.97E-03	2.707	-4.95E-04			
233	4.17E-02	4.97E-03	2.703	-4.94E-04			
253	4.52E-02	4.97E-03	2.695	-4.93E-04			
260	4.64E-02	4.97E-03	2.692	-4.92E-04			
278	4.96E-02	4.96E-03	2.684	-4.91E-04			
288	5.13E-02	4.96E-03	2.680	-4.90E-04			
300	5.34E-02	4.96E-03	2.675	-4.89E-04			
311	5.52E-02	4.96E-03	2.670	-4.88E-04			
325	5.77E-02	4.96E-03	2.664	-4.87E-04			
340	6.03E-02	4.96E-03	2.658	-4.86E-04			

351	6.22E-02	4.95E-03	2.653	-4.85E-04
367	6.49E-02	4.95E-03	2.647	-4.84E-04
378	6.68E-02	4.95E-03	2.642	-4.83E-04
392	6.91E-02	4.95E-03	2.636	-4.82E-04
412	7.26E-02	4.95E-03	2.628	-4.80E-04
424	7.45E-02	4.94E-03	2.623	-4.80E-04
433	7.61E-02	4.94E-03	2.619	-4.79E-04
446	7.82E-02	4.94E-03	2.614	-4.78E-04
462	8.10E-02	4.94E-03	2.608	-4.77E-04
473	8.28E-02	4.94E-03	2.603	-4.76E-04
488	8.53E-02	4.94E-03	2.597	-4.75E-04
508	8.87E-02	4.93E-03	2.589	-4.73E-04
514	8.96E-02	4.93E-03	2.586	-4.73E-04
531	9.24E-02	4.93E-03	2.579	-4.72E-04
541	9.42E-02	4.93E-03	2.575	-4.71E-04
561	9.74E-02	4.93E-03	2.567	-4.69E-04
571	9.92E-02	4.93E-03	2.563	-4.68E-04
588	1.02E-01	4.92E-03	2.556	-4.67E-04
599	1.04E-01	4.92E-03	2.552	-4.66E-04
613	1.06E-01	4.92E-03	2.546	-4.65E-04
623	1.08E-01	4.92E-03	2.542	-4.65E-04
635	1.10E-01	4.92E-03	2.537	-4.64E-04
654	1.13E-01	4.92E-03	2.530	-4.62E-04
665	1.14E-01	4.91E-03	2.525	-4.62E-04
683	1.17E-01	4.91E-03	2.518	-4.60E-04
694	1.19E-01	4.91E-03	2.514	-4.60E-04
709	1.22E-01	4.91E-03	2.508	-4.58E-04
720	1.23E-01	4.91E-03	2.503	-4.58E-04
730	1.25E-01	4.91E-03	2.500	-4.57E-04
752	1.28E-01	4.90E-03	2.491	-4.55E-04
763	1.30E-01	4.90E-03	2.487	-4.55E-04
773	1.32E-01	4.90E-03	2.482	-4.54E-04
793	1.35E-01	4.90E-03	2.475	-4.52E-04
797	1.36E-01	4.90E-03	2.473	-4.52E-04
810	1.38E-01	4.90E-03	2.468	-4.51E-04
824	1.40E-01	4.90E-03	2.463	-4.50E-04
845	1.43E-01	4.89E-03	2.454	-4.49E-04
855	1.45E-01	4.89E-03	2.450	-4.48E-04
867	1.47E-01	4.89E-03	2.446	-4.47E-04
887	1.50E-01	4.89E-03	2.438	-4.46E-04
891	1.50E-01	4.89E-03	2.436	-4.45E-04
906	1.53E-01	4.89E-03	2.431	-4.44E-04
918	1.54E-01	4.89E-03	2.426	-4.43E-04
932	1.57E-01	4.88E-03	2.420	-4.42E-04
952	1.60E-01	4.88E-03	2.413	-4.41E-04
965	1.62E-01	4.88E-03	2.408	-4.40E-04
976	1.63E-01	4.88E-03	2.404	-4.39E-04
986	1.65E-01	4.88E-03	2.400	-4.39E-04
1006	1.68E-01	4.87E-03	2.392	-4.37E-04
1017	1.70E-01	4.87E-03	2.388	-4.37E-04
1034	1.72E-01	4.87E-03	2.382	-4.35E-04
1044	1.74E-01	4.87E-03	2.377	-4.35E-04
1059	1.76E-01	4.87E-03	2.372	-4.34E-04

1069	1.78E-01	4.87E-03	2.368	-4.33E-04
1080	1.79E-01	4.87E-03	2.364	-4.32E-04
1101	1.82E-01	4.86E-03	2.356	-4.31E-04
1111	1.84E-01	4.86E-03	2.352	-4.30E-04
1121	1.85E-01	4.86E-03	2.349	-4.29E-04
1141	1.88E-01	4.86E-03	2.341	-4.28E-04
1149	1.89E-01	4.86E-03	2.338	-4.27E-04
1167	1.92E-01	4.86E-03	2.331	-4.26E-04
1177	1.94E-01	4.86E-03	2.328	-4.25E-04
1190	1.95E-01	4.85E-03	2.323	-4.25E-04
1210	1.98E-01	4.85E-03	2.315	-4.23E-04
1215	1.99E-01	4.85E-03	2.313	-4.23E-04
1231	2.01E-01	4.85E-03	2.308	-4.22E-04
1242	2.03E-01	4.85E-03	2.303	-4.21E-04
1259	2.06E-01	4.85E-03	2.297	-4.20E-04
1269	2.07E-01	4.85E-03	2.293	-4.19E-04
1284	2.09E-01	4.84E-03	2.288	-4.18E-04
1304	2.12E-01	4.84E-03	2.281	-4.17E-04
1310	2.13E-01	4.84E-03	2.279	-4.17E-04
1326	2.15E-01	4.84E-03	2.272	-4.15E-04
1337	2.17E-01	4.84E-03	2.269	-4.15E-04
1350	2.19E-01	4.84E-03	2.264	-4.14E-04

Table B-12 Average Efficiency Data and Modeling Results

Avg I	Avg V	Avg P	Avg Eff	Model	SS		
0	0	0	0	0	0	**a**	**b**
0.50092	2.163895	1.083938	0.264454	0.299792	0.001249	**1.376055**	**0.981597**
0.508782	2.330195	1.185561	0.289244	0.302539	0.000177		
0.99892	2.068625	2.066391	0.424233	0.42396	7.45E-08	**SS**	**0.040286**
1.007732	2.1846	2.201491	0.452059	0.42551	0.000705		
1.49969	2.100118	3.149526	0.492165	0.492468	9.19E-08	**y=x/(a*x^2+b)**	
1.50796	2.128794	3.210136	0.510159	0.49334	0.000283		
2.000987	2.075659	4.153367	0.528706	0.53573	4.93E-05		
2.007544	2.096261	4.208336	0.563155	0.53619	0.000727		
2.497668	1.958256	4.891073	0.622939	0.565272	0.003325		
2.69733	1.831209	4.939375	0.54883	0.574723	0.00067		
2.7969	1.742249	4.872896	0.541464	0.579034	0.001412		
3.000885	1.946362	5.840809	0.584079	0.587145	9.4E-06		
3.008017	1.935809	5.822946	0.582295	0.587412	2.62E-05		
3.493498	1.792552	6.262277	0.532497	0.603488	0.00504		
3.500976	1.84081	6.444632	0.548018	0.603707	0.003101		
5.002087	1.868611	9.346955	0.710309	0.636014	0.00552		
5.008544	1.87808	9.406446	0.717346	0.636116	0.006598		
5.018004	1.884257	9.455209	0.719332	0.636266	0.0069		
8.003156	1.609173	12.87846	0.662814	0.667242	1.96E-05		
8.008919	1.602072	12.83086	0.660363	0.667282	4.79E-05		

8.015895	1.584295	12.69954	0.653865	0.667329	0.000181
10.01182	1.46352	14.6525	0.629944	0.678381	0.002346
10.01812	1.473938	14.76609	0.634828	0.678409	0.001899

Appendix C: Programs, Functions, and Associated Items

```
Public Function gasmoles(P_gas, l_start, l_end, l_tube_start, l_tube_end, T)
    'P brought in as psia, changing to atm
    P = P_gas / 14.6959
    inner_radius = 0.75 / 2 / 100  'changing ID to inner radius, then cm to m
    tube_CA = WorksheetFunction.Pi() * (inner_radius ^ 2)
    m_per_mL = 1.5 / 11 / 100 'measured as 1.5 cm per 11 mL, so divide by 100 to
    vol_tube = m_per_mL * tube_CA * (l_tube_end - l_tube_start) * 1000 'Accountin
    If l_end > l_start Then 'If the gas has reached the burette, add the 2 mL tha
        vol_tube = vol_tube + 0.002
    End If
    vol_bur = (l_end - l_start) / 1000 'changing the mL read in to L
    tot_vol = vol_bur + vol_tube '[=]L

'pv=nrt
Rg = 0.08206 'L*atm/mol*K
n = P * tot_vol / (Rg * T)
gasmoles = n

End Function
```

```
Public Function EG_Dens(T_EG)
'molar density in mol/L if T is given in K
'valid from 260.15 to 719 K

A_EG = 1.3717
B_EG = 0.25663
C_EG = 719
D_EG = 0.22173
B_EXP = 1 + ((1 - T_EG / C_EG) ^ D_EG)
'A-D constants from DIPPR
EG_Dens = A_EG / (B_EG ^ B_EXP)
'Max uncertainty of .2%

End Function
```

```
Public Function H2O_Dens(T_H2O)
'molar density in mol/L if T is given in K
'valid from 273.16-353.15

A_H2O = -13.851
B_H2O = 0.64038
C_H2O = -0.0019124
D_H2O = 1.8211 * 10 ^ -6

'A-D constants from DIPPR
H2O_Dens = A_H2O + B_H2O * T_H2O + C_H2O * T_H2O ^ 2 + D_H2O * T_H2O ^ 3

'Max uncertainty of .2%
End Function
```

```
Public Function test_tube(P_gas, l_start, l_end, l_tube_start, l_tube_end, T)
    'P brought in as psia, changing to atm
    P = P_gas / 14.6959
    inner_radius = 0.75 / 2 / 100  'changing ID to inner radius, then cm to m
    tube_CA = WorksheetFunction.Pi() * (inner_radius ^ 2)
    m_per_mL = 1.5 / 11 / 100 'measured as 1.5 cm per 11 mL, so divide by 100 to
    vol_tube = m_per_mL * tube_CA * (l_tube_end - l_tube_start) * 1000 'Accounti
    If l_end > l_start Then 'If the gas has reached the burette, add the 2 mL th
        vol_tube = vol_tube + 0.002
    End If
    vol_bur = (l_end - l_start) / 1000 'changing the mL read in to L
    tot_vol = vol_bur + vol_tube '[=]L

'pv=nrt
Rg = 0.08206 'L*atm/mol*K
n = P * tot_vol / (Rg * T)
test_tube = vol_tube

End Function
```

Figure C- 1 VBA User Defined Functions for Reaction Rate Mole Calculations

```
Public Function Air_Set(V_new, T_new, P_new)
V_L = V_new / 1000 * 60
sl = 0.9759
int_er = 0.0317
T_cal = 292.43 '/k
P_cal = 750.623 / 1.0125 '/mmHg
V_cal = T_cal / T_new * P_new / P_cal * V_L 'using the volume that reflects initial se
                                            'flow meter was calibrated
Air_Set = ((V_cal - int_er) / sl)  'setting that should be approximately used

End Function
```

```
Public Function Air_Vol(sett_, T_cur, P_cur)

sl = 0.9759
int_er = 0.0317
T_cal = 292.43 '/k
P_cal = 750.623 / 1.0125 '/mmHg
V_cali = (sl * sett_ + int_er) * 1000 / 60 'mL/s from L/min

Air_Vol = T_cur / T_cal * P_cal / P_cur * V_cali

End Function
```

```
Public Function H2_Set(V_n, T_n, P_n)

m = 0.0157
b = 0.0274
T_1 = 291.65 '/k
P_1 = 743.623 / 1.0125 '/mmHg
V = T_1 / T_n * P_n / P_1 * V_n 'using the volume that reflects initial settings when
                               'flow meter was calibrated
H2_Set = (V - b) / m 'setting that should be approximately used

End Function
```

```
Public Function H2_Vol(sett, T, P)

m = 0.0157
b = 0.0274
T_1 = 291.65 '/k
P_1 = 743.623 / 1.0125 '/mmHg
V_1 = m * sett + b 'mL
P_2 = P
T_2 = T
H2_Vol = T_2 / T_1 * P_1 / P_2 * V_1

End Function
```

Figure C-2 VBA User Defined Functions for Flow Setting Derivations

1	**Feed H2 Desired**	6.0E-05	mol/s	757.174				
2	**% Excess Desired**	48						
3	**Pressure**	760	mmHg					
4	**Temperature**	71.4	°F					
5	**rel humidity**	**26**						
6	V_H2	1.45	mL/s					
7	V_air	5.15	mL/s					
8	H2 SetNeed	93						
9	H2Set	12.5						
10	V_H2 act	0.2	mL/s					
11	Air SetNeed	0.29						
12	AirSet	0.9						
13	V_Air act	14.9	mL/s					
14	Expected Energy	2.18	J					
15	Feed H2 Actual	9.03E-06	Accommodating the accuracy of the flow meter					
16	Feed Air Actual	6.17E-04	Accommodating the accuracy of the flow meter					
17	Temperature	295	K					
18	Temperature	22.0	C					
19	gas constant	0.08206	L*atm/mol*K					
20	vap_press	19.827	mmHg					
21	y_H2O in	0.0068	=p*/P					
22	y_O2 in	0.2086	=(1-yH2O)/(1+79/21)					
23	y_N2 in	0.7846	=79/21*yO2					
24	fract check	1.000	making sure sum of fractions is = 1					
25	nf_air desired	2.13E-04	=(1+excess)*nf_H2/(2*yO2)					
26	n_N2	4.84E-04	=nair*yN2					
27	extent	4.52E-06	=nf_H2/2 because H2 is assumed to achieve 100% conversion					
28	n_out_O2	1.24E-04	=nf_air*y_O2in-extent					
29	n_out_H2O	1.32E-05	=nf_air*yH2O in+2*extent					
30	y_H2O out	0.021	=n_out_H2O/(n_out_H2O+n_out_O2+n_N2)					

Figure C-3 VBA Excel User Interface for Flow and Expected Energy Calculations

```
Public Function E_a(TR, TP, exc, y_H2O)
If TP < 305 Then
    m_H2 = 9.8002 * 10 ^ -3
    'm and b for CP=mx+b where x = temperature
    b_H2 = 25.911
    m_N2 = 1.1412 * 10 ^ -3
    b_N2 = 28.733
    m_H2O = 3.8505 * 10 ^ -3
    b_H2O = 32.43
Else
    m_H2 = 4.665 * 10 ^ -3
    'm and b for CP=mx+b where x = temperature
    b_H2 = 27.448
    m_N2 = 0.733 * 10 ^ -3
    b_N2 = 28.905
    m_H2O = 6.2323 * 10 ^ -3
    b_H2O = 31.701
End If
m_O2 = 4.595 * 10 ^ -3
b_O2 = 27.983
lamb = (1 + exc / 100) / 2
'this gives ratio of mol O2/mol H2 by combining excess and stoich
wat_con = lamb * y_H2O / 0.21

a_R = m_H2 + m_O2 * lamb + m_N2 * 0.79 / 0.21 * lamb + m_H2O * wat_con
'everything has to be in terms of J/mol H2*K
b_R = b_H2 + b_O2 * lamb + b_N2 * 0.79 / 0.21 * lamb + b_H2O * wat_con

H_R = a_R * (TR ^ 2 - TP ^ 2) + b_R * (TR - TP)
SR = a_R * (TR - TP) + b_R * Log(TR / TP)
hf_H2O = -285830 'J/mol
HP = hf_H2O
SP = -44.405 'J/mol/K
W = H_R - HP + TP * (SP) - (TR * SR)
E = (m_H2 + 0.5 * m_O2) * (TR ^ 2 - TP ^ 2) + (b_H2 + 0.5 * b_O2) * (TR - TP) - hf_H2O
E_a = W / E
End Function
```

```
Public Function S_(TR, TP, exc, y_H2O)
If TP < 305 Then
    m_H2 = 9.8002 * 10 ^ -3 'm and b for CP=mx+b where x = temperature
    b_H2 = 25.911
    m_N2 = 1.1412 * 10 ^ -3
    b_N2 = 28.733
    m_H2O = 3.8505 * 10 ^ -3
    b_H2O = 32.43
Else
    m_H2 = 4.665 * 10 ^ -3  'm and b for CP=mx+b where x = temperature
    b_H2 = 27.448
    m_N2 = 0.733 * 10 ^ -3
    b_N2 = 28.905
    m_H2O = 6.2323 * 10 ^ -3
    b_H2O = 31.701
End If

m_O2 = 4.595 * 10 ^ -3
b_O2 = 27.983

lamb = (1 + exc / 100) / 2
'this gives ratio of mol O2/mol H2 by combining excess and stoich
wat_con = lamb * y_H2O / 0.21

a_R = m_H2 + m_O2 * lamb + m_N2 * 0.79 / 0.21 * lamb + m_H2O * wat_con
'everything has to be in terms of J/mol H2*K
b_R = b_H2 + b_O2 * lamb + b_N2 * 0.79 / 0.21 * lamb + b_H2O * wat_con

SR = a_R * (TR - TP) + b_R * Log(TR / TP)

SP = -44.405 'J/mol/K
S_term = TP * (SP) - (TR * SR)
S_ = S_term / TP

End Function
```

```
Public Function H_(TR, TP, exc, y_H2O)
If TP < 305 Then
    m_H2 = 9.8002 * 10 ^ -3
    'm and b for CP=mx+b where x = temperature
    b_H2 = 25.911
    m_N2 = 1.1412 * 10 ^ -3
    b_N2 = 28.733
    m_H2O = 3.8505 * 10 ^ -3
    b_H2O = 32.43
Else
    m_H2 = 4.665 * 10 ^ -3
    'm and b for CP=mx+b where x = temperature
    b_H2 = 27.448
    m_N2 = 0.733 * 10 ^ -3
    b_N2 = 28.905
    m_H2O = 6.2323 * 10 ^ -3
    b_H2O = 31.701
End If

m_O2 = 4.595 * 10 ^ -3
b_O2 = 27.983

lamb = (1 + exc / 100) / 2
'this gives ratio of mol O2/mol H2 by combining  excess and stoich
wat_con = lamb * y_H2O / 0.21

a_R = m_H2 + m_O2 * lamb + m_N2 * 0.79 / 0.21 * lamb + m_H2O * wat_con
'everything has to be in terms of J/mol H2*K
b_R = b_H2 + b_O2 * lamb + b_N2 * 0.79 / 0.21 * lamb + b_H2O * wat_con

H_R = a_R * (TR ^ 2 - TP ^ 2) + b_R * (TR - TP)
hf_H2O = -285830 'J/mol
HP = hf_H2O
H_ = H_R - HP

End Function
```

```
Public Function G_(TR, TP, exc, y_H2O)

If TP < 305 Then
    m_H2 = 9.8002 * 10 ^ -3 'm and b for CP=mx+b where x = temperature
    b_H2 = 25.911
    m_N2 = 1.1412 * 10 ^ -3
    b_N2 = 28.733
    m_H2O = 3.8505 * 10 ^ -3
    b_H2O = 32.43
Else
    m_H2 = 4.665 * 10 ^ -3  'm and b for CP=mx+b where x = temperature
    b_H2 = 27.448
    m_N2 = 0.733 * 10 ^ -3
    b_N2 = 28.905
    m_H2O = 6.2323 * 10 ^ -3
    b_H2O = 31.701
End If

m_O2 = 4.595 * 10 ^ -3
b_O2 = 27.983

lamb = (1 + exc / 100) / 2
'this gives ratio of mol O2/mol H2 by combining  excess and stoich
wat_con = lamb * y_H2O / 0.21

a_R = m_H2 + m_O2 * lamb + m_N2 * 0.79 / 0.21 * lamb + m_H2O * wat_con
'everything has to be in terms of J/mol H2*K
b_R = b_H2 + b_O2 * lamb + b_N2 * 0.79 / 0.21 * lamb + b_H2O * wat_con

H_R = a_R * (TR ^ 2 - TP ^ 2) + b_R * (TR - TP)
SR = a_R * (TR - TP) + b_R * Log(TR / TP)
hf_H2O = -285830 'J/mol
HP = hf_H2O
SP = -44.405 'J/mol/K
G_ = H_R - HP + TP * (SP) - (TR * SR)
End Function
```

Figure C-4 VBA User Defined Functions for Theoretical Efficiency Model Calculations